RioTinto

Kennecott Utah Copper LLC
P.O. Box 6001
12000 West 2100 South
Magna, Utah 84044
USA
T 801-569-7427
F 801-569-6408

Chris Kaiser
Principal Advisor
Environmental Operations Support
Kennecott Utah Copper

Ms. Dana Dean, Associate Director - Mining
Division of Oil, Gas & Mining
Utah Department of Natural Resources
P.O. Box 145801
Salt Lake City, Utah 84114 - 5801

March 9, 2010

Attn: Paul Baker & Leslie Heppler, Minerals Regulatory Program

Re: M/035/002 – Bingham Canyon Mine
      May 12, 2008 Order Vacating NOV #N2007-58-01
      Submittal of Final Clean Waste Rock Stability Study Documents

Dear Ms. Dean:

Pursuant to your letter dated February 9, 2010 and received by Kennecott Utah
Copper (KUC) February 15, 2010, please find attached two (2) clean copies of the
following documents included in the final Waste Rock Stability Study accepted by the
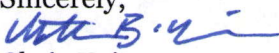Division:

- FILE02Rev2009-10WasteRockDumpsSummaryReportCLEAN20100309
- FILE03-Rev2009-10AppendixA-FoundationConditions(South)CLEAN20100309
- FILE04-Rev2009-10AppendixB-WasteRockMaterialPropertiesCLEAN20100309
- FILE05-Rev2009-10AppendixC-StabilitySouthernWasteRockCLEAN20100309
- FILE06-Rev2009-10AppendixD-ConstructionSouthWasteRockDumpsOverTimeCLEAN20100309
- FILE08-Rev2009-10AppendixF-DebrisFlowAnalysisReportCLEAN20100309
- FILE09Rev2009-10AppendixG-SouthDumpStabilityCLEAN20100309

Please note that the following was previously submitted to the Division in hard copy:

- FILE07-Rev2009-10AppendixE-SouthEndHydrologicReportCompleteURS20090224

It is KUCs understanding that a stamped copy will be retained by the Division and a
stamped copy will be returned to Kennecott for our records.

Please contact me or Zeb Kenyon at 801-569-6035, should you have any questions
concerning this submittal.

Sincerely,

Chris Kaiser
Principal Advisor
Environmental Operations Support

RECEIVED

MAR 1 0 2010

DIV. OF OIL, GAS & MINING

RioTinto

| Project Code | 12094 | **Report Number** | 12094-02 | **Version** | 1.0 |

Technology and Innovation

Kennecott Utah Copper LLC

South Waste Rock Dumps Summary Report

October 20, 2009

Prepared for		**Author/s**	Joergen Pilz
Distribution			
Project Manager		**Reviewer**	
	Joergen Pilz		Z.M. Zavodni

Section 1 - Executive summary

This report entitled *Kennecott Utah Copper South Waste Rock Dumps Summary Report October 2009* has been prepared to fulfil the requirement identified at Page 3, Item c. of the Order Vacating Notice of Violation N2007-58-01 for an off site excursion that occurred in July 2007. Specifically, Item c. states: "Undertake additional modelling and prepare a slope stability study to supplement the existing August 16, 2004 study, and update the 2003 Plan accordingly, as detailed in Attachment 3 to the March 20th letter.

As noted above, Attachment 3 (Additional Slope Stability for Waste Rock Within the South End Drainages) to the March 20th (2008) letter incorporates many specific aspects but has been summarized as follows: *"The proposed scope of work will further investigate the risk and mechanism for large-scale deep seated failures and well as surface slumping and debris flows. The overall goal of the study will be to investigate the long-term stability of the KUC South End waste rock dumps. In this context, the study will assimilate the available historical data and begin quantifying the aspects of surface water infiltration, geochemistry and geotechnical conditions that contribute to waste rock dump stability."*

Please note that some information provided in the technical appendices may apply to the northern dumps and also to other dumps surrounding the pit. All provided and/or referenced appendices and technical attachments should be considered "work in progress" which may change or be added to throughout mine operations. As such, only certain technical attachments are provided with this Summary Report.

Rio Tinto is independently developing internal standards (Waste Rock Dump Management Standard) and guidance documents to provide consistency within its operations, including Kennecott Utah Copper, in regards to planning, design and construction of waste rock disposal facilities. The technical appendices referenced in the *Kennecott Utah Copper South Waste Rock Dumps Summary Report October 2009*, which are historic data comprising field and laboratory investigations, geochemistry, surface water infiltration, waste rock material properties, foundation soil and bedrock information and observations regarding surface erosion, are also being utilized to complete the ongoing development of a KUC Dump Management Plan (DMP).

Available geologic, geotechnical data and soils maps were compiled into a Geographic Information Systems (ArcGIS) database. These data were then used to estimate the foundation soil and bedrock conditions below the dumps and develop dump geometries for screening level stability analysis.

Dump stability assessment requires site characterization: including bedrock geology, foundation soil, groundwater, construction methods and dump material strength. Available dump stability background information has been assembled within the attached report and appendices. The report establishes the mapped foundation geology, bedrock outcrops, drainage locations and soil types below and in proximity to the toe of the dumps, and dump

material strength range. Preliminary cross sections intended for screening level stability analysis were also developed. Parametric stability analyses found that the foundation soil / bedrock conditions are the most crucial characteristics required to quantify the stability of the inactive dumps. The report also includes studies regarding the surface water hydrology and infiltration rate through the dumps.

Performance of the existing KUCC waste dumps over the past 25 to 85+ years suggests that the dumps are stable when advanced under controlled conditions. Secondly, "old" waste dumps (greater than 50 yrs. old) have cemented with iron oxide compounds, thereby gaining strength and improving stability over time. The majority of the dump materials are quartzite and calc-silicates (limestone in the south dumps), which are not expected to weather to clay over time as the intrusive material would. This observation suggests that there will be little to no shear strength degradation that could lead to deep seated dump instability over time. The cementation is well corroborated by leaching studies of the dumps, which indicated that active leaching tended to seal the dump surface. For example, some of the north / northwest Bingham Canyon mine pit slopes are being excavated at slope angles of 50+ degrees through historic dumps that border the mine. These dumps experience both production blasting and seepage and have exhibited good stability within the pit.

Contents page

List of figures

List of tables

Section 2 - Major Findings and Actions

Introduction

This report summarizes a study investigating the long-term stability of the KUC waste rock (WR) dumps. The study goal assimilates the available historical data and begins quantifying the aspects of surface water infiltration, geochemistry and geotechnical conditions that contribute to WR dump stability. This report summarizes primarily information relating to the South End drainages, whose names are shown on Figure 1.

Figure 1 - Locations and drainage names for South End Dumps

The *Kennecott Utah Copper Waste Rock Dumps Summary Report October 2009 utilizes* technical appendices, as follows:

- Appendix A - Foundation Conditions - Summarizes the available foundation geology and subsurface soil information. The available data were compiled into an ArcGIS database containing the maps from original investigations which were superimposed on published surface and subsurface geology maps.

- Appendix B - Waste Rock Dump Materials – Summarizes the available investigations and data regarding the waste rock dump materials. Much of this information was developed in conjunction with investigations evaluating the ability to leach the dumps and improve metal recovery from the leached dumps.

- Appendix C - Summarizes geochemical conditions in a report by Geochemica, Inc. The appendix also contains information relating to the history of leaching and similar information relating to dump geochemistry.

- Appendix D - Dump Progression – Summarizes a review of historic aerial photographs showing how the dumps were placed and developed over time. This information is useful to obtain some idea of the types of materials incorporated into the dumps. Current observations of the various dump areas are also included herein.

- Appendix E - Hydrology – Contains two technical reports: 1) a study by O'Kane Consultants evaluating the infiltration rate of the dumps and 2) a study by URS Corporation summarizing the surface water hydrology along the south dumps. It also contains spreadsheets summarizing East Side drain flows, meteorological data from snow and precipitation stations and other precipitation information.

- Appendix F – Debris Flows –Summarizes information regarding surface erosion processes and, in particular, development of debris flows from the dumps. The appendix contains debris flow modeling using the software program Dan-W.

- Appendix G – Dump Stability – Contains preliminary screening level stability analysis of critical sections developed along the dumps. The analyses were based on generalized conditions developed along the dumps and are intended to identify areas where further investigations are warranted.

The following summarize the key findings in each discipline and area of study.

Major findings

A. Foundation Conditions

Appendix A summarizes the information that is available regarding the soil and bedrock geologic conditions below the dumps. In most cases, these historic investigations were completed for purposes other than assessment of dump stability, yet yield useful data are available regarding the conditions below the footprint of the dumps. The foundation soils and bedrock below the dumps are now largely inaccessible even when using the most advanced Sonic drilling methods[1].

In general, the surface and bedrock geology underlying the Eastside Waste dumps is well understood and has been mapped in detail. Subsoil conditions beyond the toe of the dump have also been mapped by a number of investigators, including private consultants, internal KUCC studies and the UGS (Utah Geologic Survey). Due to the historic nature of the dumps,

---

[1] To T&I knowledge, the deepest borings advanced through dumps is on the order of 600 feet using the sonic drilling method. Other methods have largely proven to be unsuccessful.

conditions below the exact footprint of the dumps must be extrapolated from the historic investigations and geologic maps. However, complete surface geology mapping is available below the southern dumps. Soils underlying the dumps are expected to consist of colluvium and residual soils derived from the underlying bedrock materials. Drainages have alluvial materials derived from the underlying bedrock. Many of the ridges, particularly below the south dumps, consist of bedrock ridges and outcrops, whose location is identified on historic maps.

In general, foundation conditions underlying the south dumps can be characterized as primarily silty to clayey gravel soils with some layers of sandy clay with gravel underlain by bedrock consisting of sedimentary calcareous quartzites and limestone that dip at a high angle towards the Bingham pit. Numerous bedrock outcrops are present below the south end dumps. Soils derived from these deposits consist of silty, sandy to clayey gravels. The combination of more granular soils and bedrock outcrops provide much stronger foundation conditions than those found to the North of the Burma Road. There have been no foundation-related failures below the South truck waste dumps.

Appendix A also contains a compilation of the available field and laboratory data into a (excel) database of foundation soil properties. Investigation locations and the available attributes of those investigations were also compiled into an ArcGIS shapefile[2] to develop a database of investigations and materials encountered in those investigations.

The original historical documents, as summarized in Table 1, have been compiled as attachments to this appendix and are referenced but not included with this Summary Report.

Table 1 – Summary of historic and supplemental foundation information

Attachment in Appendix A – Foundation Conditions	Description
Attachment A – UGS and USGS Geology Maps	2007 Utah Geologic Survey (UGS) map of soils extending beyond the toe of present day dumps. USGS Bedrock Geology map of the Bingham Canyon quadrangle
Attachment B – Historical studies	Investigations for original leach collection dams not included.
Summers, 1981, Hydrogeology and Effects of Mine Dump Expansion on Ground Water Quality	The BLM reports summarizing the site conditions below the South end dumps.
The Hydrologic Effects of Increased Mine Dumps Expansion on the "Nevada" tract in Butterfield Canyon, Utah	A report by Battelle summarizing the hydrology of Butterfield Canyon related to the proposed dump expansion into this area.
Attachment C Bear Creek Mining Company (BCMC, also Kennecott Exploration) 1964 surface geology	Select scanned images (obtained from KUCC Geology and NAE) summarizing surface geology

---

[2] A shapefile contains the locations of the investigations and an associated database file containing the identification, depth of investigation, materials encountered for each point in the file, which are collectively termed "attributes."

Attachment in Appendix A – Foundation Conditions	Description
mapping below East Side Dumps	mapping below the southern east side dumps (South Dumps and Keystone)
Attachment D NAE (North American Exploration) – AutoCad drawings and cross sections	AutoCad drawings completed during the installation of the East Side Collection system cut off wall showing exploration locations and summarizing investigation data.
Attachment E – 2007 Investigations	Map of 2007 Test Pit locations Copies of Test Pit Logs by NAE Summary of laboratory classification, index property and shear strength tests.
Attachment F – 2008 AMEC	Pipe berm road and desilting basin investigations

As summarized in Appendix A- Attachment D, detailed mapping of the soils is available along the location of the Eastside Surface Water Collection System cut off walls. These barrier walls were essentially constructed where the depth to bedrock was reasonably accessible along the toe of the dumps. Conditions upslope of these cut off walls are expected to exhibit less soil thickness, while down slope of the walls the bedrock depth increases rapidly. Many of the soils present below the cut off walls were excavated and utilized in the construction of the Eastside Surface Water Collection System, therefore many areas adjacent to the cut off walls presently represent disturbed areas not suitable for supplemental investigations.

Although a considerable number of investigations had historically been completed beyond the toe of the dumps, there was an absence of laboratory test data classifying the soils and evaluating the foundation shear strength. Secondly, the historic (1975, 1977) rail dump leach collection dam studies focused primarily on the clay soil deposits, which tended to bias the available strength information towards the weakest soil deposits. To improve our understanding of the overall soil conditions, fourteen supplemental test pits were completed in 2007 to obtain samples for laboratory index property, classification of bulk samples and shear strength testing. These investigations are summarized in Attachment E and found few undisturbed areas, as expected. However, the investigations did find that most soils are gravelly, classifying as clayey gravels to gravelly clays north of the Burma Road. South of the Burma Road the soils were predominantly silty to clayey gravels with some sandy gravels. A description of the soil types encountered within the South End drainages is provided in Appendix A, Table A-2. In general, materials within the drainages vary from clayey to silty gravel with sand to gravelly, sandy clay. For characterization purposes, materials described as clayey gravel are expected to be clast supported and are assigned the strength properties of the gravel constituents. Materials described as gravelly clay are expected to be matrix supported and are assigned the strength properties of the clay matrix.

As part of the 2007 study, six direct shear strength tests were completed on suitable Shelby tube samples of the clayey soils to estimate the drained shear strength parameters. Results indicate that the clays classify into either low plasticity (CL) and high plasticity (CH and MH) soils. The low plasticity soils possess an average friction angle of 24 degrees and cohesion of 1725 pounds per square foot (psf) for the low plasticity clayey soils. A lower bound value with a friction angle of 20 degrees and cohesion of 1400 psf was used in stability analysis.

Where gravel content exceeds about 60 percent, the shear strength begins to be governed by the larger particle sizes (clasts) interlocking and is subsequently higher. A friction angle of 35 degrees and cohesion of 500 psf was used to represent these soils. Utilizing the strength test data for the soil matrix in stability analysis is therefore conservative. The high plasticity clays / silts are of limited extent and exhibited a friction angle of 11 degrees and cohesion of 1490 psf. Such soils are not extensive below the South dumps, therefore these values were not assigned in the screening level stability calculations.

B. Waste Rock Material Properties

The WR material properties are summarized in the following appendices:

- Appendix B summarizes the (types, density, moisture content, shear strength) characteristics of the WR materials,

- Appendix C describes the geochemistry affecting the WR materials, and

- Appendix D summarizes the sequence of dump construction

- Appendix F summarizes surface erosion processes and dump construction

A graph of the total waste tonnage developed over the life of the mine is depicted in Figure 2 Waste Tonnage. The early mine waste that was generated was placed on the hill slopes above the mine on the north and west sides. The total waste produced from early in the mine life to the mid-1990's was on the order of 140 Billion tons with the majority of the waste being placed after the 1940's on the east side of the mine. After 1995, the waste was placed above the Markham dumps, Dry Fork and within Bingham Canyon with a small amount of waste placed above the Yosemite dumps and above the uppermost East side dumps.
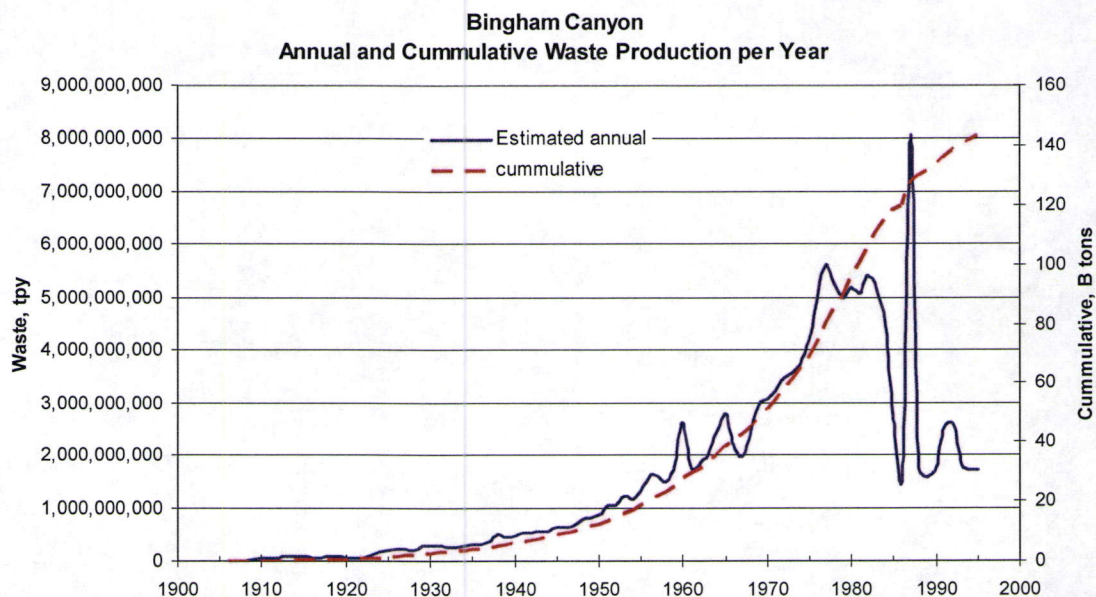
Bingham Canyon
Annual and Cummulative Waste Production per Year

Figure 2 - Estimated waste placed at Bingham Canyon from beginning of open pit mining to the mid-1990's
(estimated from ore production and stripping ratio)

In general, the dump materials are generally very coarse-grained with the following percentages of particles.

Table 2 – Summary of Bingham 1980 to present estimated ore and waste distribution

Type	Ore %	Waste %	Size Distribution, inches (percent)			
			- 1 inch	1 to 5 inch	5 to 10 inch	+ 10 inch
Intrusive	68%	32%	30	50	16	+4
Quartzite	24%	62%	41	34	21	+4
Limestone (south WR)	8%	6%	35	28	14	+23
Overall waste size distribution		100%	37	39	19	+5
Source: KUCC Internal data						

Based on investigations completed within the dumps, the available gradation data indicate that the majority of the dump materials have relatively low fines content[3], generally less than 20 percent. The majority of the particles sizes are gravel size or larger, ranging to very large boulder size at the base of the dump due to particle segregation during placement. Larger size particles have not been adequately sampled at depth, due to restrictions in the drill core diameter. However, surface observation clearly indicates the particle segregation that occurs down a dump face and tends to concentrate the larger particles at the toe of the dumps.

Field density data suggest that the surface of the dumps have a total density between 125 to 130 pcf (pounds per cubic feet). Kennecott mine data suggest an increasing density with depth. The dumps are generally considered to be permeable at depth, although the dump surface may exhibit very low permeability and infiltration. Surface areas of the dump have been subject to cementation and "plugging" when leached, as indicated by the lower permeability values of 10^{-6} to 10^{-8} cm/sec A discussion of near surface infiltration and permeability is provided in the O'kane report presented in Appendix E.1. The surface cementation was an ongoing problem during dump leaching operations where barren, acidic solution had a difficult time penetrating the dumps. The lower surface permeability of the dumps was also attributed to "plug dumping" and the nearly horizontal layering caused by dumping materials on the surface and then spreading the material by dozer into near horizontal lifts. Available permeability test data below the dump surface are summarized in Table B-3 and indicate generally permeable conditions are present below the upper dump surface.

There is little information suggesting that the dump materials degrade in strength over time due to geochemical decomposition. During end dump placement, it is observed that the larger rock particles bounce and break apart as they roll down the end dump slope. This process tends to break the rocks apart along natural planes of weakness into their stronger constituents. Secondly, waste rock materials are generated by mine blasting, which also breaks the rock apart along any in-situ bedding, joint or fractures. These observations indicate that the rock materials that end up along the base of the dump are the most competent overburden materials from the mine.

It is expected that under the very high dumps, the stresses result in particle crushing which reduces the shear strength with depth. A generalized non-linear shear strength range was developed as part of this study. The shear strength envelopes were developed based on the angularity of the particles, the high stresses and published correlations between stress and shear strength. The non-linear envelope is based on the average material characteristics (quartzites, sedimentary deposits, etc.) using the Barton rockfill interlock criteria (2008) and the Leps (1970) chart. The best estimate envelope of the waste rock strength based on using a variety of methods to assess the range in dump material strengths (described in Appendix B) is shown on Figure 3.

---

[3]   Technically, the fines content should be the percent passing the no. 200 sieve; but sometimes, the term "slimes" have been used in the available references. Slimes may be particles sizes down to the no. 325 sieve.
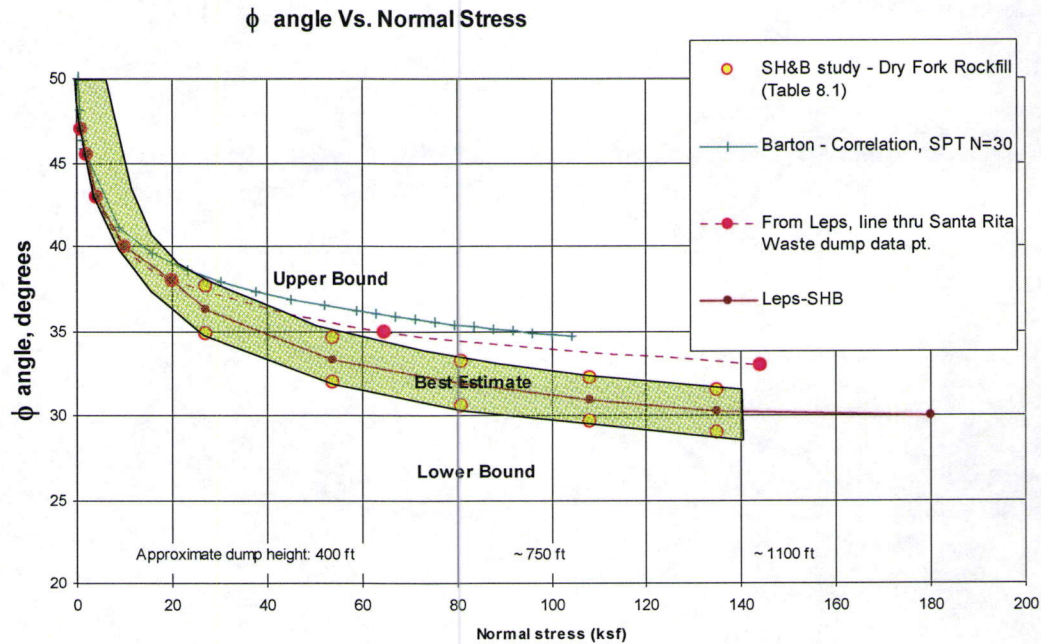
φ angle Vs. Normal Stress

Legend:
- ○ SH&B study - Dry Fork Rockfill (Table 8.1)
- —+— Barton - Correlation, SPT N=30
- – ● – From Leps, line thru Santa Rita Waste dump data pt.
- —● Leps-SHB

Upper Bound

Best Estimate

Lower Bound

Approximate dump height: 400 ft ~ 750 ft ~ 1100 ft

φ angle, degrees

Normal stress (ksf)

Figure 3 - Shear strength of rock fill based on Leps chart correlating rock fill shear strength to confining stress

C. Geochemistry

Geochimica Inc. was retained to evaluate the geochemistry of the dumps. They participated in field investigations and split samples with O'Kane Consultants (OKC) to complete laboratory chemical tests of the waste materials. Laboratory work was performed at the Kennecott Environmental Laboratory (KEL). Geochimica reviewed the relevant geochemical information from Kennecott and other technical studies, synthesized the historic and recent data to the extent practicable, supervised acid-base accounting and mineralogical studies on the near surface test pit samples obtained, and interpreted the geochemical results in terms of impact on shear strength. The major findings by Geochimica include:

- In the Castro pile, cap-rock and test pits containing predominantly intrusive rock have low pH and elevated conductivities. However, one test pit, (TP06) was excavated into predominantly calc-silicate rock. Below the intrusive cap, the pH of this material remains circum-neutral (pH 6.88-7.6), and the conductivity values fall toward the low end (near 2,000 μS/cm) for all samples tested.

- The finer fraction (silt and smaller-size) of the samples has lower pH and generally somewhat higher conductivity, as compared to the coarse fraction.

- The bulk-sample paste-pH values measured immediately after excavation tend to have distinctly lower paste-pH and paste-conductivity values than those measured several weeks later. The reasons for these trends are not known at this time. Perhaps, there has been some precipitation of low-solubility phases that incorporate

some of the labile acidity, as, for instance, hydronium (H_3O^+) ion in jarosites that do not re-dissolve in the paste procedure.

- Although moisture contents below the very-near-surface of the piles were low and the system was entirely unsaturated, in a number of areas there is moist, warm to hot air venting upward through coarse layers in the dump. Some vents reach the dump surface, where they appear as water-vapor "fumaroles" on cool days.

- Static acid-base accounting data have been reported for the samples obtained. Portions of the Castro pile that contain calc-silicate clasts have sufficient Neutralization Potential present, despite the presence of pyrite, to have positive NNP values. Measured values of carbonate-carbon in these samples indicate that the initial NP is present as calcite and can be relied on in such rocks to provide available, not just potential, NP. No samples from Keystone or Midas contained any measurable carbonate-carbon.

In the northern dump surface samples, essentially all the rock clasts sampled were quartzite. In two of three Keystone samples, intrusives (monzonite) predominate the clasts, whereas in TP-03, there is abundant quartzite. In contrast, the sample from Castro includes not only quartzite and intrusive, but also a significant fraction of carbonate-bearing calc-silicate.

From a mineralogical perspective, the following were found:

- The only secondary minerals that appear as coatings and cements are jarosite [(K, H_3O^+)$Fe^{III}(SO_4)_2(OH)_6$) and gypsum ($CaSO_4 \cdot 2H_2O$). Although very tiny amounts can be identified in SEM-EDS investigations, the effective absence of goethite (FeOH) or its predecessor, ferrihydrite ($Fe(OH)_3$) is noticeable. There is no significant chemical or mineralogical difference between the jarosites in the leached sample from Code 51 and the jarosite in the unleached samples from Keystone and Castro.

- In the Northern dump samples, there are few to no carbonates present, but limestone remains inside partially skarnified clasts in a Castro sample. This is consistent with the Neutralization Potentials for Northern dumps which are close to zero for all samples with paste pH < 4.5. At Castro, where the samples contain the calc-silicate clasts, the paste-pH values are all close to pH 7.

- There are no identifiable examples of either newly-formed clay minerals or secondary, amorphous silica. There are rare clay minerals in some of the intrusive fragments, but these appear to be hypogene hydrothermal minerals that do not reflect clay generation in the pile after mining. The only silicate mineral that shows alteration is biotite.

In summary, the following conclusions were made regarding the geochemistry of the Southern Eastside WR dumps:

- There is no evidence from the new or old Kennecott mineralogy reports that feldspars and other alumino-silicates are being converted to clay minerals at rates that lead to observable amounts of clay minerals (in periods of several decades).

- There is active precipitation of secondary, cementing minerals, largely jarosite [$KFe(SO_4)_2(OH)_6$] and lesser amounts of gypsum ($CaSO_4.2H_2O$), in both leached (Code 51) and non-leached (Keystone and Castro) dumps.

- The mineralogy of the cements does not depend on the lithology of the local clasts. The cements relate more to the presence of pyrite.

- The amount of cementation is presently greater in the leach dumps than in the non-leach dumps because a significantly higher flux of Fe^{3+} and SO_4^{2-} has passed through the leached dumps.

- There is no reason to expect that the ferric minerals precipitated in the waste-rock dumps would become chemically unstable and dissolve. Over time, they may convert to a more goethite-like ferric hydroxide (FeOOH), but this is expected to occur over centuries or even longer and would leave the dumps still iron-cemented. Gypsum in very shallow zones may be subject to dissolution and re-precipitation cycles during shallow infiltration events, but this is unlikely to be important more than a very few meters below the ground surface.

- Because the geochemical processes are identical, the non-leach dumps will evolve toward conditions such as those seen in the leach dumps [i.e., increasing cementation (cohesion) over time]. However, because the rates of cementation are controlled by iron and sulfate fluxes, it would take a long time for the degree of cementation seen in old leach dumps to occur in non-leached dumps, and the full extent seen in the leach dumps is unlikely because there is not enough iron in the waste rock to achieve the amount of cementation formed in the leach dumps.

- Geochemically, dissolution of particles as a mechanism for grain-size reduction, break down of particles and accelerated weathering does not appear to be occurring at a significant, measurable rate. Such weathering in the dumps would occur over very long time periods.

- Oxidation of pyrite within the dumps precipitates jarosite, gypsum and other compounds. Over time, such precipitation could fill up to about 25 percent of the WR void space. If this extent of cementation actually occurs, such precipitates would cement the particles and could produce perched water table conditions (or significantly increase the degree of saturation at these locations) in dumps that are currently drained.

Based on the lack of neutralization potential or other arresting physical conditions, the waste rock piles are currently active and expected to remain geochemically active well into the future. Conditions are therefore likely to remain similar to current conditions into the future. Future meteoric infiltration will be much slower due to the neutral water and lower percentage of the water that infiltrates the waste rock dumps.

In conclusion, the tendency for the dumps will be to cement and increase in shear strength over time. There are little to no data supporting a break down of the particles to clay materials or a reduction in shear strength. However, the precipitation of jarosite and other compounds could, if advanced sufficiently, create "perched water tables", and/or increased saturation conditions within the dumps. The net result of weathering and the geochemical reactions is an increase in cementation (and corresponding decrease in permeability) over time.

D. Dump Progression

To gain an understanding of how the dumps were advanced over time and in general where the overburden materials were placed within the dumps, historic aerial photographs were reviewed to determine the extent of dumps at approximate 10 year intervals. The construction of the all the dumps is described in Appendix D. The extent of dumping is shown on Figure 3 and summarized on Table 3.

Table 3 - Summaries of the areas where materials were placed over time:

Date Range	Location of Primary Waste Dumps	Color on Figure 3 and D-2 through D-6
Prior to 1940's (>70 yr old)	Markham (north) and west wall of pit [Note: some of these materials were subsequently re-mined.]	violet
1940 to 1950 (60-70 yr old)	Along south slope of Bingham Canyon via rail	Purple
1950 to 1960's (50 – 60 yr old)	Extending outward from Bingham Canyon and around the East side via rail	Blue
1960's to 1970's (40 – 50 yr old)	Extending out from Yosemite notch and extending further south along the East side (rail and truck). Some waste being placed in Dry Fork	Green
Mid 1970's (~45 yr old)	Extending further out along North half of East Side	Light green˚
1980's (20 - 30 yr old)	High truck waste dumps established late in the 1970's immediately north of Yosemite Notch. Toe of East side rail dumps was extended. South dumps were established.	Yellow
1990's (10-20 yr old)	Material placed in Dry Fork Canyon and in South dumps	Orange
2000	Bingham Canyon dumps developed	Not shown in color

The Yosemite and Saint's Rest (south) dumps were initiated in the late 1960's with waste from the south pit slope. In the late 1970's to early 1980's, most waste was hauled through Copper and Yosemite notch. The south dumps were a major deposition area.
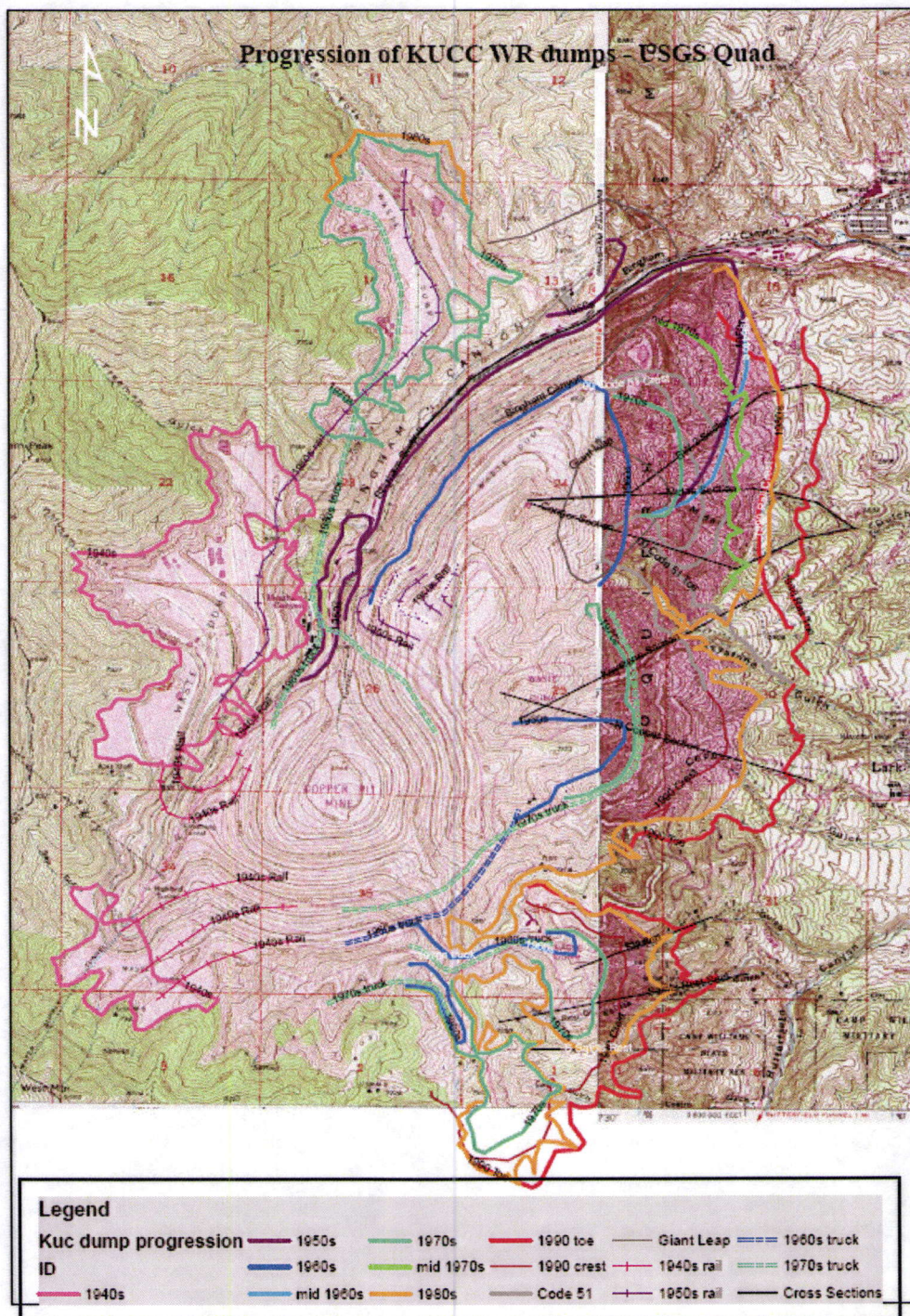
Figure 4 - Extent of dumping at approximately 10 year increments in time.

E. Hydrology

A summary of the available hydrology studies regarding the WR dumps reviewed in the preparation of this summary report include:

- E.1 A study by O'Kane Consultants (OKC, 2006) evaluating surface water infiltration into the East Side Dumps.

- E.2   A study by URS Corporation (February 2009) evaluating the surface water hydrology of the Yosemite drainage and the South End dumps

- E.3   Spreadsheets summarizing the annual Snow Water Equivalent data, the East Side Collection System flows and Water Balance.

- E.4   Ground water monitoring well and surface water data.

E1. Surface Water Infiltration

OKC was retained to evaluate the moisture infiltration characteristics of the waste rock dumps. To accomplish this task, OKC sampled eight test pits on the Castro, Keystone and Code 51 (Eastside Rail) dumps. Gradation and index property testing was completed on 34 bulk samples of the surficial waste rock materials. OKC supervised the installation of PVC access tubes to a maximum depth of 16.5 feet to measure changes in near surface waste rock moisture content with a portable moisture probe. Lastly, OKC completed field permeability tests on the near surface waste rock materials. The analytical phase of OKC's work included soil-atmosphere numerical modeling to evaluate the overall influx of surface moisture to the dumps.

OKC found a relatively consistent surface layer extending across most of the dump surfaces. The surface layer appears to be associated with construction of roadways and surfacing of the dumps, which is consistent with information from KUCC operations personnel. The surface layer is relatively well graded, ranging from rock to sand to silt and clay size particles. These layer(s) help to reduce net infiltration because of lower permeability and increased moisture retention, which leads to higher rates of actual evaporation during summer months. Field-saturated hydraulic conductivity values for surface material tested on the Keystone and Castro dumps ranged from 1.4×10^{-6} cm/sec to 1.0×10^{-3} cm/sec.

Soil-atmosphere (infiltration) modeling results were based on 20 years of climate data measured at the Salt Lake City National Weather Service Field Office (NWSFO) and estimated hydraulic properties for the waste rock materials (i.e., saturated hydraulic conductivity and moisture retention). The preliminary modelling also focused on a 12 m thick, one-dimensional waste rock profile, with a 0.3 m thick surface layer (as described above) and a 11.7 m thick layer of intermediately graded waste rock (indicative of the average material found on the Keystone dump). It is important to note that the models at this stage are one-dimensional and, as such, surface runoff to topographic lows is not accounted for as yet. In reality, surface runoff to local topographic lows will occur, and if any cracks, fissures, or "day-lighting" of coarse zones occurs in this area, then net surface infiltration could be significantly higher in these localized zones as a result of the accumulated surface runoff.

Based on their sampling and analysis, OKC found that the average net infiltration value into the dumps was on the order of 15 to 20 percent of the annual precipitation. The maximum infiltration rate was estimated to be 30 percent. There are variations in the infiltration value throughout the year, so the values cited by OKC should be considered as a range of net infiltration. In addition, this value will range from year to year, depending on the time and form of precipitation, and in relation to potential evaporation conditions. Precipitation as snow and rainfall that occurs during low evaporation conditions, most likely results in higher

infiltration. However, precipitation as summer rainfall is stored near the surface and is subsequently evaporated from the profile, resulting in essentially no percolation to deeper waste rock. Hence, generally, infiltration to the deeper waste rock profile for any given year is a function of the volume and intensity of winter precipitation. Fumaroles on the dump surface also vent moisture from within the dumps from unknown depths and release some of the infiltration moisture. Leach collection flow monitoring shows seasonal variations in the water emanating from the dumps, suggesting that the dumps drain that water that has infiltrated in accord with prior KUCC studies. Soil moisture tubes installed during this study and monitored from April to November 2007 suggest very limited soil moisture changes below the upper 10 inches of the surface.

E2. Surface Water Hydrology (2009 URS report)

URS Corporation (URS) evaluated the hydrology of the 2008 configuration of the South End Waste Rock Piles. URS included analyses of the hydrology that comprises a 10-year, 24 hour storm event, and a specific event that occurred in July 2007 that led to sediment that traveled beyond the property boundary.

URS summarized various events based on the National Oceanic and Atmospheric Association (NOAA) precipitation frequency atlas of the maps for the western United States. Table 4 shows selected few return intervals along with the rainfall depth to be expected given specific storm duration:

Table 4 - Precipitation Frequency Estimate NOAA Atlas 14 (inches)

Annual Exceedence Probability	15 min	30 min	1 hour	2 hour	24 hour
2 years	0.28	0.38	0.47	0.59	1.39
10 years	0.53	0.71	0.88	1.02	2.09
25 years	0.70	0.94	1.16	1.32	2.44
100 years	1.0	1.39	1.72	1.91	2.98

The South End drainage system consists of seven individual drainage basins. These basins, from north to south are: Yosemite, Saints Rest, South Saints Rest, Castro, Butterfield, Olsen and Queen. In all, the South End drainage system covers approximately 1,213 acres of disturbed and natural areas. The tributary areas consist of three very distinct topographic features,

- the disturbed areas of the waste rock pile flat upper surface areas
- the disturbed waste rock pile slopes, and

- the undisturbed areas forming the natural canyons of each basin.

An estimate was made of the sediment contributed by the dumps to the collection systems at the dump toe. The SEDCAD™4 (Civil Software Design, LLC) model software (Warner, et. al., 2006) was used to evaluate runoff. SEDCAD4 stands for "Sediment, Erosion, Discharge by Computer Aided Design". SEDCAD4 is a key core software component in the U.S. Department of the Interior, Office of Surface Mining's Technical Innovation and Professional Services (TIPS) program and is often used for permitting and design of control systems for abandoned mine lands. The SEDCAD output is described in detail in Attachment E.2.

The highest reaches of the basins consist of approximately 327 of the acres of disturbed land that occurs above the crest of the waste rock piles. These 327 acres consists of relatively flat land that is divided into three sub-basins. During larger storms, these three sub-basins potentially contribute flows to the Yosemite, Castro, and Olsen basins.

On the steeper sections of the waste rock piles, runoff is rapidly channelized and directed to rock check dams, meandering channels, stilling ponds, and storm water sedimentation ponds; from there, water is conveyed to cement cut-off walls where it is transported via gravity pipeline eventually discharging into the storm water collection system, where it flows to a treatment plant or lined reservoir. The system as a whole is referred to as the East Side Collection System.

Table 5 provides the areas contributing flows to each basin and the sedimentation pond storage volumes. The runoff coefficients used in this analysis are considered to be on the conservative end of the input criteria, meaning that water is calculated to report more rapidly to the basins than it may in the field.

Table 5 Contributing Areas and Sedimentation Basins Volumes (after URS, 2008)

Basin	Yosemite	Saints Rest	South Saints Rest	Castro 1	Castro 2	Butterfield	Olsen	Queen
Areas Above Cut-Off Wall (Acres)								
Disturbed (Top of Waste Rock Pile)	222.8	None	None	12.6		None	91.6	None
Disturbed (Sloped areas)	52.5	61.4	20.8	50.1	12.8	16.2	37.5	9.6
Undisturbed (Sloped Areas)	92.2	48.4	79.9	32.7	19.7	21.3	25.5	216.8
Total Area (Above Cut-off Wall and below the Top of the waste pile)	144.7	109.9	100.6	82.8	32.5	37.5	63.0	226.4
Areas Beyond Cut-Off Wall (Acres)								
Total Area (Below Cut-off Wall)	59.4	14.7	15.7	89.4		54.7	55.5	35.2
Total Area (Above and Below Cut-off Wall)	204.1	124.6	116.4	204.6		92.2	118.5	261.6
Sediment Basin Volumes (CY)								
Sediment Basin (Above Cut-off Wall)	1579.3	10455.4	None	1952.8		1477.5	2513.5	None
Sediment Basin (At Cut-off Wall)	789.7	44.5	303.3	227.5	77.3	238.4	136.6	
Sediment Basin (Below Cut-off Wall)	80241.2	50154.1	23481.2	170.5		1361.4	1635.1	
Total Sediment Basin	82610.2	60654.1	23784.5	2350.8	77.3	3077.3	4285.2	

Table 6 summarizes the hydroCadd and SedCadd modeling results.

Table 6 Summary of HydroCAD and SEDCAD Models Results (after URS, 2008)

	Yosemite	Saints Rest	So. Saints Rest	Castro**	Butterfield	Olsen	Queen
10 yr/ 24 hr storm peak inflow (cfs) *	9.9	2.4	16.3	11.6	2.1	7.2	14.5
Capacity Excceded?	No	No	No	No	No	No	No
10 yr / 24 hr Sediment Load (tons)	1144	1172	278	1583	220	1130	143
Capacity Exceedent Storm (24 hr)	25 yr	100 yr	25 yr	25 yr	100 yr	25 yr	50 yr
CES peak inflow (cfs)	30.5	9.9	23.5	21.3	8.9	11.7	38.2
Overtopping Flow (cfs)	15.1	2.4	3.4	0.3	2.2	2.3	5.3

Note: * at cutoff wall

** Upper Castro Cutoff Wall

It was found that the existing drainage collection facilities in all seven watersheds are sufficiently sized to convey the 10 yr./ 24 hr. storm event. Saints Rest and Butterfield have capacities just short of a 100 yr./ 24 hr. event. Queen has capacity just short of a 50 yr/ 24 hr event. The capacities of the collection system for Yosemite, South Saints Rest and Castro basins are exceeded by a 25 yr./ 24 hr. event.   A discussion of the time of concentration values used to generate these results is described in the URS report contained in Appendix E.

E3. Water Balance and Flows

A plot of the East side collection system drain down from the period 1999 to 2000 following leaching is presented in Figure 5. Following the initial drain down, the annual cycles of water flow through the dumps and to the Eastside Collection System is shown on Figure 6. These plots reveal a permeable system that drains rapidly. The correlation between the Dry Fork (Snotel) data and the variation in the dump flow is shown on Figure 7 for the 2002-9 water years. These drain down flows are empirical evidence that the dumps are permeable and as a result are unlikely to support a high phreatic surface.
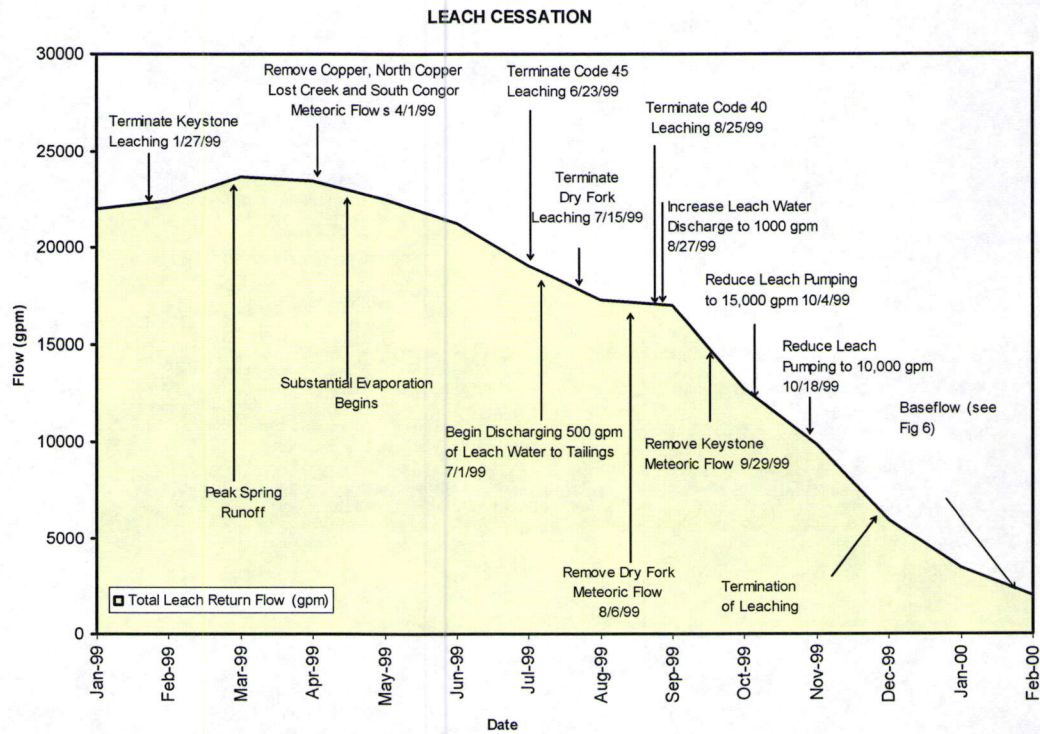
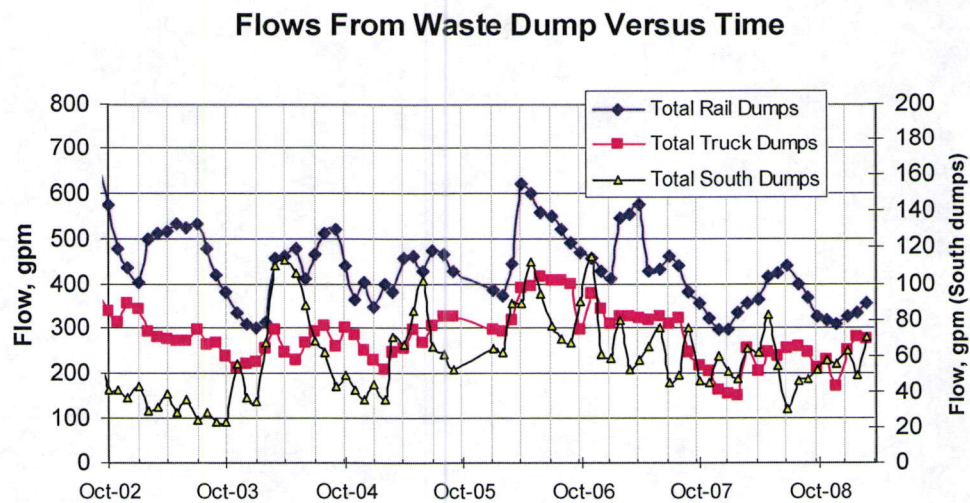Figure 5 - Drain down of the Eastside dumps following cessation of leaching.

Flows From Waste Dump Versus Time

Figure 6 - East side collection system flows following initial drain down showing annual meteoric cycles of flow.

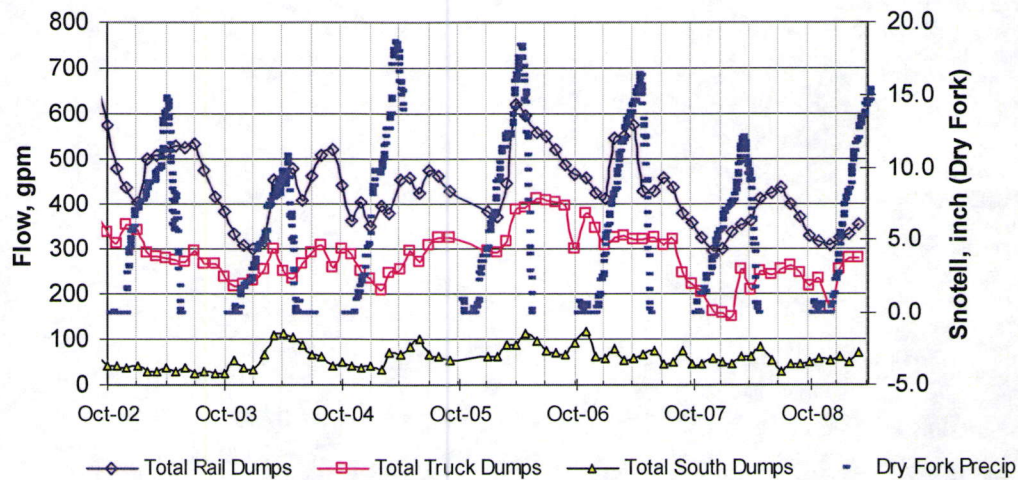## Base Flows From Waste Dump Versus Time

Figure 7 – Annual cycle of WR dump flows and precipitation after cessation of leaching

The drain down analysis and the dump construction indicate that one would expect the dumps to be well drained.

F. Debris Flow Analysis

Debris flow events are the most probable types of mass wasting that could occur in the future (as compared to deep seated slope instability). The size of potential debris flows based on historic events is described in Appendix F. The east side waste dumps have experienced a number of debris flow events over time in addition to the surface erosion or mass wasting processes described above. Erosion on the surface of the dumps is evident on aerial photographs and this erosion can be attributed to both surface erosion and periodic debris flows caused by surface water flow. The documented debris flow events that have occurred are summarized on Table 7.

Table 7 – Summary of Historic Debris Flows Documented at KUC

Date	Location	Rainfall, in/hr & duration	Maximum extent of deposits[A]	Quantity / Comment
1967	Castro		Butterfield Creek	Reportedly dammed up portion of creek
1979	Saint's Rest	Not applicable; debris flow caused by excessive dump leaching	Contained in drainage	Large failure due to excessive leaching for 30 days.
1983 – 84	Various	High spring runoff	Some deposition in Butterfield	Yellow-brown layer encountered

Date	Location	Rainfall, in/hr & duration	Maximum extent of deposits[A]	Quantity / Comment
				downstream of the Canyon mouth
June 9, 1997	Olsen drainage[A]	1.32 inches in 1 hour; 1.27 in 30 minutes	Butterfield Creek	750 yd^3 or about 1100 tons; 50% had been contained in Olsen structures
August 4, 1997	Castro Basin overtopped	Antecedent Precip: 1 inch; prior to event: 0.58 inches	Traveled along access road to Butterfield Creek & then to irrigation system	
1998	Olsen		Butterfield Creek	Plugging of pipe
Sept 3, 2005	Castro Gulch	Unknown	Butterfield	Overflow from collection pipe into Eastside Collection System
2006	Castro	Unknown	Contained on property	
July 27, 2007	Yosemite	URS 2009 report	Butterfield Creek	Filled Yosemite basin (see URS report)

Notes:

A – Most of the debris was contained on KUCC property. A 4 feet deep gully extending to the crest of the Olsen dumps was observed corresponding to an approximate volume equal to the reported release.

To evaluate whether the debris flow material will be contained on KUC property, aerial photographs were evaluated to develop input parameters, the topography was evaluated and debris flow run out analysis using the software program DAN-W were completed. The analyses found that:

- The historical review of scars showed that debris flow scars are periodically evident on the dump surface and represent slumps and / or potential sources of the debris flows.

- The size of gullies was estimated, which yielded approximate values for the erosion that may be occurring from the dumps.

- Two mechanisms for the occurrence of debris flows were developed:

  o Overtopping of the dump crest by water, which was originally the postulated cause of the debris flows.

  o Day-lighting of a perched water table near the dump crest.

- The effect of varying the geometry and grade changes along the toe of the dump was evaluated using Dan-W. The Dan-W modelling demonstrated that flattening or stair stepping the apron at the toe of the dumps would decrease debris flow velocity, causing the debris flows material to deposit prior to reaching the catch basins under most conditions. This would allow the basins to store the 10 yr 24 hour storm without

the basins filling with debris. Secondly, increasing slope steepness in the deposition area would ultimately increase the run out distance. These results were found to be valid provided that the debris flow itself does not become too fluid by incorporating water into the debris flow as it travels.

Debris flow type of events that cause the erosion and gullying observed on portions of the dumps are likely to continue unless mitigation measures are implemented. Modifications to current dump surface drainage patterns have been recommended and are being implemented at the dump crest and toe. It was recommended that the catch basins be sized to contain both a reasonable debris flow event found to be approximately 1000 yd^3 of material and the 10 yr 24 hour storm event. Debris flow run out analyses indicate that debris flows can be retained on KUC property with necessary cleaning and maintenance of the debris basins.

G. Waste Rock Dump Stability

Based on a literature review, the mapping compiled to date and screening level stability analysis, the following empirical conclusions were made:

- The waste dump materials have already been subjected to a number of factors potentially contributing to a reduction in shear strength. These factors include: acid leaching, elevated temperatures, low pH conditions, and high stress levels. The dumps exhibit few indications of movement (settlements, tension cracks, toe movement), indicating that from surface evidence, the dumps are stable.

- Periodic survey monitoring along the dump crests indicate that the dumps are settling gradually over time (less than 10 inches over 3 years[4]), but there is no indication of accelerated movements or general slope instability. The survey monitoring program is part of KUC's overall monitoring program, which includes minimum monthly inspections of the dump crest and toe.

- As long as the effect of weathering is to create a "weathering rind around the WR particles," increased temperature and weathering are unlikely to significantly modify the frictional components of the WR shear strength. Conversely, the data are suggesting that the cohesion component of shear strength is increasing, thereby increasing stability.

- The available data suggest that the majority of the dumps are well drained and do not possess an elevated phreatic surface(s). However, the South dumps are known to have had perched water table conditions. Geochemical predictions indicate that about 25% of the pore space of the dumps may eventually fill with jarosite or other precipitates in the very long term. Therefore, additional data are required regarding the phreatic surface conditions in the South dumps, as well as *in-situ* moisture conditions.

- Historically, stability of the waste dumps has been a function of foundation material types, geometry, foundation loading rates and a number of other criteria. These

---

[4] The actual measurements ranged from +2 to -10 inches, indicating possible heave of the targets or survey error.

parameters were identified as being critical to deep seated dump stability during operations. From a long term stability perspective, the range in foundation material strengths is considered to be the most critical factor to a final assessing dump stability.

- Available permeability, gradation and dump construction method information suggests that with the exception of the high limestone dumps, the dumps are well drained and do not possess an elevated phreatic surface. Dump drain down data support drainage of the dumps over time. However, perched water table conditions have been observed in the Castro dumps and this is attributed to a prior attempt to leach the high limestone dumps using acidic solution back in the 1980's. There is no plan to leach the South dumps in the future for this and other reasons.

Cross sections for stability analysis along the principal drainages were developed based on 10 feet contour spacing, except for the South dumps where 2 feet contours were available. Screening level stability analyses were completed to assess the likely factors of safety for deep seated slip surfaces. Because exact conditions are not known below the dumps, the stability analyses were completed using a range in foundation and waste rock material strengths versus site specific values. The stability analyses assumed the following:

- Shear strength of waste rock materials is reasonably modelled by the non-linear shear strength envelope developed herein. The waste rock strength was characterized by an upper bound, lower bound and average range. The average value was set to coincide with the Leps (1970) values. Strength properties for the primarily quartzite materials represent the upper bound envelope, while the lower bound estimate is represented by the sedimentary units. The non-linear envelope is shown on Figure 3.

- The foundation shear strength is based on testing a limited number of samples obtained from beyond the toe of the dump. The foundation was characterized as either having an intermediate silty clay foundation or a sandy, silty, clayey gravel foundation. It was conservatively assumed that the foundation soils were at least 10 ft thick below the entire footprint of the dump. The clay strength range is described in Appendix A.

- In general, T&I have assumed that the dumps are relatively well drained and do not support a high phreatic surface. The stability analyses assume the base of the dump is saturated, and that the phreatic surface extends 5 feet uniformly above the dump / foundation interface. This should be a reasonably conservative assumption, but actual data supporting a relatively low phreatic surface would be useful. The exception is the Yosemite dump analysis, where an elevated phreatic surface has been conservatively assumed.

The following matrix of assumptions was used to complete a probabilistic, screening level stability assessment of the waste dumps. In comparison to traditional deterministic stability assessment, this approach should be considered a non-traditional method.

Table 8 – Matrix of Waste Rock and Foundation shear strength parameters

Dump	Foundation Conditions / Strength	Upper bound Waste Rock	Average Waste Rock Strength	Lower Bound Waste rock

	Parameters	Strength		strength
South Dumps				
Yosemite and Saint's Rest	Lean Clay / ϕ = 20 deg Coh = 1400 psf	X	X	X
	Clayey, Sandy Gravel w/ ϕ = 35 deg Coh = 500 psf	X	X	X

The above matrix of WR and foundation material properties required six stability calculations per cross sections. Assuming that the upper and lower bound estimates for the WR and foundation soils represented values one standard deviation from the mean (actual) value for the WR dumps, the probability of failure was statistically calculated using a "point estimate method" (Harr). The point estimate method assumes that the lower WR/lower foundation, lower WR/upper foundation, upper WR/upper foundation, upper WR/upper foundation, average WR/lower foundation and average WR/upper foundation strengths statistically identify the range (assuming +/- one standard deviation) of possible factors of safety for the dumps. The probability that the factor of safety lies within a given range can be calculated. These calculations can therefore be used to screen which areas require further field investigation to quantify the actual stability where it is in question. Likewise, where the statistical range in stability meets or exceeds accepted criteria for WR dump stability, no further analyses are warranted.

Results of the probabilistic stability calculations are summarized in Appendix G and Table 9.

Table 9 – Summary of KUCC Waste Rock Dump Stability Analysis

Cross Section	WR shear strength	lean clay	gravel
Saint's Rest	Lower bound	1.15	1.3
	best - Leps	1.45	2.4
	Upper bound	2.0	2.7
Yosemite	Lower bound	1.0	1.1
	best - Leps	1.4	1.7
	Upper bound	2.45	2.45
	Satisfactory; FS ≥ 1.2		
	Marginal: 1.0 < FS < 1.2		
	More Data Needed: FS ≤ 1.0 (based on assumptions)		

Details of the stability analysis and findings are summarized in Appendix G. It is noted that for the parametric, screening level stability analyses a factor of safety of about 1.0 was calculated for the lower bound Yosemite dump, which currently exhibits good stability. This observation is attributed to the conservatism in the parametric input assumptions, the elevated phreatic surface used and is only an indication of conservatism in the input parameters versus being a reflection of instability. Because there is uncertainty in the continuity of the soil conditions, the calculations found that the stability of the Yosemite dump could be low. However, because a factor of safety of 1.0 was calculated, it is certain that the parametric input assumptions are conservative and the actual factor of safety is higher, as there are no indications of instability noted on the dump surface. Based on the underlying geology, a more site specific cross section was evaluated and a phreatic surface sensitivity was completed. For one case, the clay soil was assumed only where volcanic bedrock underlies the dump and gravel soils were assumed above the quartzite bedrock. For the second case, a continuous low plastic clay was assumed as before, however the phreatic surface was reduced to 5 feet above the foundation. These analyses are presented in Appendix G and indicate the lower bound deterministic factor of safety is 1.2.

Using the best estimate value on the lower bound foundation strength, the traditional factors of safety for Saints Rest and Yosemite dumps are 1.45 and 1.4, which are both above the target factor of safety of 1.2.

Conclusions

Based on these findings, data obtained to date and screening level stability analyses indicate the dumps are currently stable and are expected to remain so into the future. However, quantification of the degree of stability is challenging and to improve our understanding of long term stability, additional field and laboratory testing is warranted should additional

materials be placed in those areas identified by the screening level analysis as having potentially marginal stability.

RioTinto

| Project code | 12094 | Report number | 12094-02 | Version | 1.0 |

Technology and Innovation

Appendix A - Foundation Conditions (South Dumps)

10 Oct 2009

Prepared for	Chris Kaiser	**Author/s**	J Pilz
Distribution	Z. Kenyon, C. Kaiser, K. Payne, M. Robothym		
Project manager		**Reviewer**	
	J Pilz		Z.M. Zavodni

Section A-1 - Executive summary

Project purpose

This appendix summarizes a literature review of the information available regarding soil and bedrock foundation conditions below the KUCC East Side Waste Rock Dumps. Although information from early work below the Northern dumps is referenced where necessary, the data presented is primarily below the South Dumps.

Major findings

Evident from inspection of the bedrock geology map and the surficial geology map is that the foundation conditions underlying the north and south dumps can generally be characterized as follows:

- North of the Burma Road[1], the underlying bedrock geology is predominated by Tertiary age volcanic deposits. Above these Tertiary deposits is a mantle of colluvium derived from sedimentary units. At some locations there are residual clay soils derived from the bedrock units. The clayey weathered bedrock and soils are most prevalent below the northernmost rail dumps and isolated areas of clayey soils are present below the Keystone truck dumps.

- South of the Burma Road, the bedrock geology consists of sedimentary calcareous quartzites and limestones that dip at a high angle. These geologic units form many outcrops and present significantly more competent foundation conditions than below the north dumps. Soils present below the south dumps are considerably more granular and classify as silty to clayey gravels and sands.

---

[1] The Burma road is the former (now abandoned) access roadway to the Yosemite truck shops and is readily evident because no waste rock materials are present along this area. The current Lark access gate is situated at the eastern end of this roadway.

Contents page

List of figures

List of tables

Appendix A – Foundation Conditions

Soils below the WR dumps are largely residual soils developed from the underlying geologic materials. Some of these soils have been transported down to the drainages by mass wasting and fluvial processes.

A.1 FOUNDATION BEDROCK GEOLOGY

Detailed petrographic descriptions of the geologic units in the vicinity of the Bingham Pit can be found in the <u>Guidebook of the Bingham Mining District</u> (1975). More recently, the geology in the Copperton Quadrangle has been mapped by the Utah Geologic Survey, (Biek, et al 2007). The Bingham bedrock geology of the area is shown on Figure A-1 and the surficial geology is shown on Figure A-2.
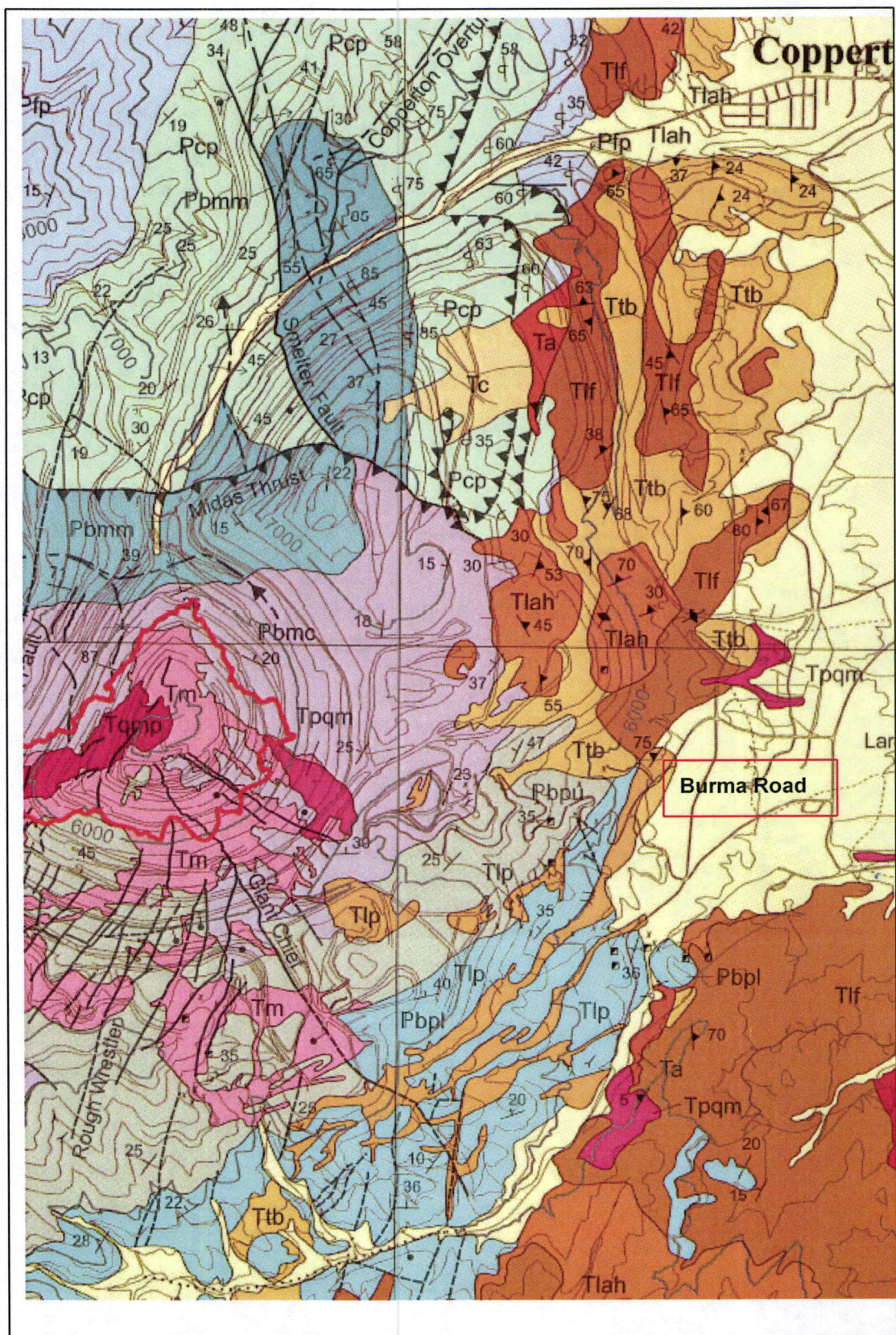
Based on descriptions contained in Babcock (1997), the geologic units are described as follows:

Sedimentary Units: Pennsylvanian and Permian Systems Oquirrh Group

Pobp, Butterfield Peaks Formation

This unit is the most abundant rock type in the southern portion of the dump area and extends southward from the high (keystone) truck waste dumps. The units include calc-quartzites, limestones and fossil-bearing limestone. The upper portion of the formation is primarily a calcareous quartzite. The unit exhibits a moderate to steep northwesterly dip from Butterfield Canyon towards the Bingham open pit at angles from 25 to 65 degrees.

Intrusive Rocks: – Tertiary Units

Volcanic units underlie the majority of the Eastside Rail dumps and most of the Truck waste dumps. Alluvial units derived from quartzites upslope of the Tertiary age rocks are also present in the drainages. Latite porphyry dikes and sills outcrop below the South dumps and trend in a northeast – southwest orientation. The volcanic units include the following:

TiLp, Latite Porphyry

This porphyry is exposed in a small area immediately adjacent to and east of the town of Lark. The unit is typically a medium to light gray biotitic, hornblende latite with an aphanitic groundmass and approximately 40 percent phenocrysts. The unit is generally found occurring as sills paralleling the bedding of Butterfield Peaks formation discussed above.

Tvb, Latite Breccia with Interbedded Tuff, Sands and Gravels

The rock unit was mapped by W.H. Smith (1961) as a dacite-andesite agglomerate, pyroclastic, tuff breccia. The primary rock type consists of gray and black lithic fragments, set in a gray lithic tuff matrix. Only small, localized outcrops occur.

Til, Latite

Latite occurs in the Bear Gulch intrusive breccia underlying a portion of the Yosemite dump. Unaltered samples of this rock are not available. The altered samples are white to light gray in color due to the intense alteration of the original constituents to clay minerals. Samples from under ground workings contain quartz grains, which make up 10 percent of the rock— this indicates the fine-grained nature of the igneous groundmass. Fresh pyrite is present as disseminated grains and some veinlets.

Tim, Quartz Monzonite

Quartz monzonite (formerly called Bingham granite or dark porphyry) makes up 32 percent of the Bingham Pit exposures. It occupies a large portion of the central area of the Bingham mine and extends to the south where it underlies a portion of the Castro-Olsen dump. The quartz monzonite is a medium gray, equigranular rock composed essentially of feldspar with interstitial quartz grains. Quartz veins, sulfide minerals, apatite, zircon, and rutile are also

present. The mineralogy is highly dependent upon location and the degree of hydrothermal alteration. This unit also underlies the western portions of the eastside waste dumps.

A.2 FOUNDATION SOILS

Due to the historic nature of the dumps, few investigations were completed below the current dump footprint. Foundation materials below the dumps must therefore be evaluated based on the soil conditions beyond the toe of the dump (Biek, 2007) and combining this information with historic surface geology mapping below the dump footprint. Figure A-2 shows both the surficial geology, consisting of bedrock and soils, extending beyond the toe of the dumps. An electronic version of the surficial geology map shown on Figure A-2 is included in Attachment A.

Figure A-2 - Surficial Geology Beyond the toe of the Eastside dumps (Biek, 2007) – see Attachment A map for detail.
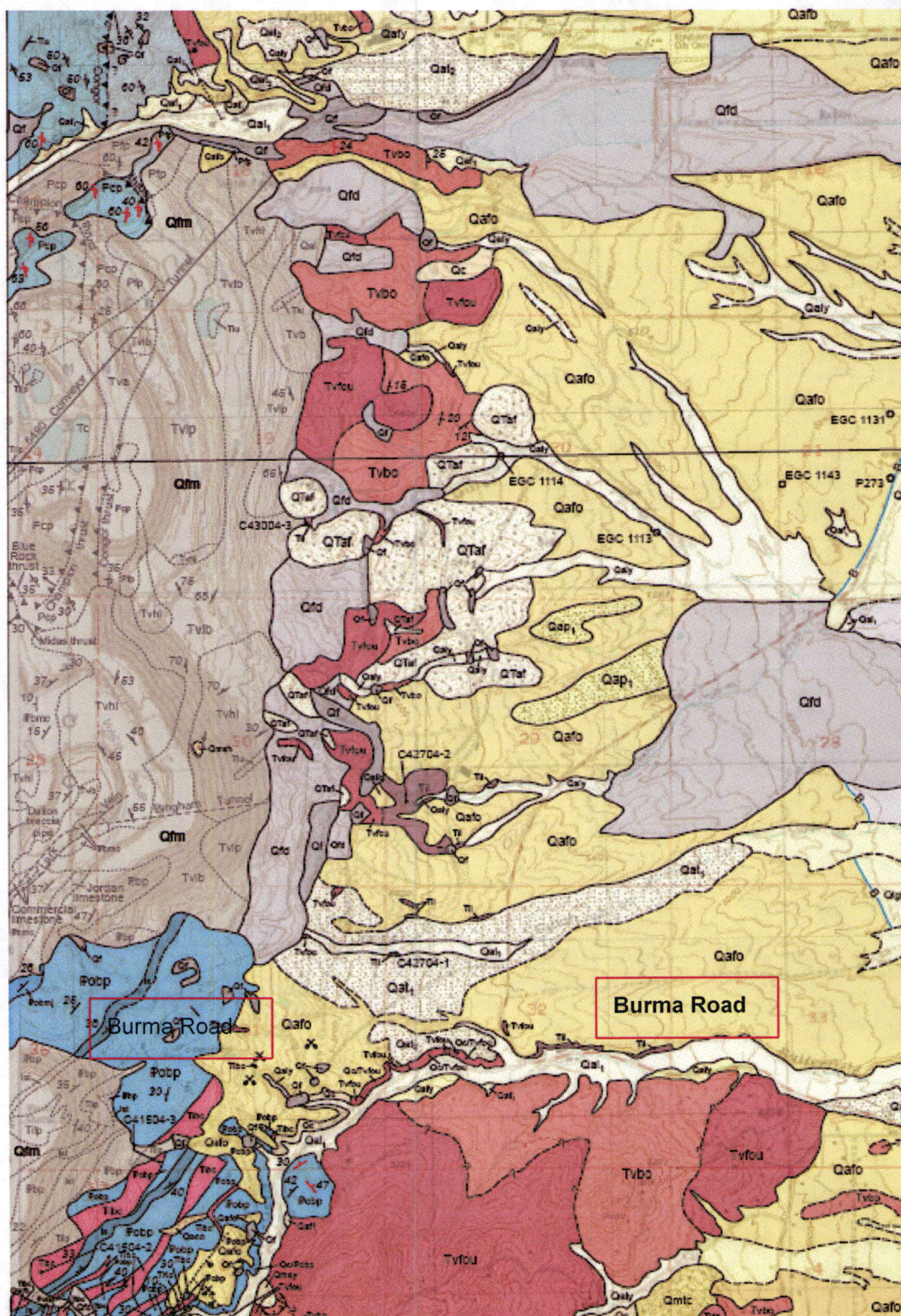
Most of the detailed investigations along the dump toe were associated with investigation for the Eastside collection system cut off walls and associated borrow investigations. The seepage cut off walls were largely located where depth to bedrock was reasonably close to the surface. Secondly, topography and historic geologic maps indicate that the soil thickness is less upslope of the cutoff walls and that the soil cover is relatively thin along the ridges. In short, the distribution of the soil types can be inferred by combining the available topography, geology maps and the mapped soil boundaries based on the following reports:

- Internal reports below the East Side rail dumps (Attachment B – not included).

- Mapping completed by Bear Creek Mining Company (BCMC in conjunction with KCC-UCD geology department mapping by Wilson), summarized as scanned images in Attachment C.

- Investigations along the cut off wall (seepage collection system) by the KUCC plant project group and NAE (North American Exploration) summarized in a series of AutoCadd drawings and summarized in Attachment D.

Review of the geology and available soils mapping indicates that foundation soil conditions can be divided into clayey soils derived from volcanic bedrock (Latite flows, Latite Breccia, Quartz Monzonite Intrusives and Tuff Breccias) north of the former Burma access road and gravelly to silty soils south of the Burma Road. South of the Burma road, Paleozoic sedimentary sequences including the Bingham Mine formation, sandstones and limestones predominate the bedrock conditions.

NRCS Soil Mapping

An initial interpretation of the near surface soils and their distribution, down to depths of approximately 5-feet, can be obtained from the National Resources Conservation Service (NRCS) soil maps. The following table summarizes the correlation between the soil types, agricultural soil series name and inferred Unified Soil Classification System (USCS).

Table A-1 – NRCS Soils Map Correlations

Soil Series Abbreviation	Description / Name	Inferred USCS Classification
DPE	Dry Creek – Copperton	Silty to Cobbly Gravel (GM), 10% other soil
HDF	Harkers – Dry Creek	Silty Gravel (GM) with cobbles.
DPD	Dry Creek – Copperton	Silts and Gravelly Silts (ML) on

Soil Series Abbreviation	Description / Name	Inferred USCS Classification
		alluvial fans
HHF	Harkers soil	GM to ML, possibly CL
WAG	Wallsburg Cobbly loam	GM to ML
GEG	Gappmeyer cobble loam	Cobble Gravels-north facing slopes (GP-GM)
GGG	Gappmeyer – very steep	Residual, Angular Gravels (GM)
BEG	Bradshaw-Agassiz Association	Silty Gravel (GM) with cobbles- south facing slopes
Note: Soil series described north to south		

Review of the NRCS data suggests that the majority of the ridge top and ridge slope soils are angular, cobbly gravels with a silt and clay matrix. Lower strength clayey soils are principally limited to the drainages. However, the NRCS mapping is rather general due to the limited agricultural usage of the ridge areas.

Foundation Conditions

The northern dumps generally extend above residual, clayey soils derived from volcanic bedrock. The clay soils range from low (CL, CL-ML) to high (CH, MH) plasticity. The MH (plastic silt) classification is rather unusual and is based on the volcanic source material of the soils. Based on investigations performed at the cut off wall, the soil deposits extend from a few feet in thickness along ridges up to 70-feet in thickness along the drainage bottoms.

In addition to the Tertiary volcanic bedrock materials, there are overlying alluvial and colluvial materials, such as wash sands and gravels present within the drainages, that were derived from upslope sedimentary units. These are generally competent materials.

It is also noted that a few of the plasticity tests were completed on the matrix of clayey gravels and sands even though the majority of the soils are angular, clayey to silty gravels. Table A-2 summarizes the general soil types below the dumps by drainage. The available drill hole information is generally summarized in the AMEC (2009) report, which included borings generally advanced through the debris basin embankments. In addition, test pits had been excavated and soil exposures logged by NAE in 2007.

Table A-2 – Summary of Foundation Soil Types below South End Drainages

Location	Soil types	Borings	Reference
Yosemite	CL – Gravelly Clay with Sand & Cobbles, GC -GM – Clayey Gravel with Sand; Poorly Graded Gravel – GP; Sandy Silt with Gravel – ML – to GM; Stiff, fat Clay with Gravel – CH to GC; Limestone bedrock	AMEC Y-3	2007 NAE test pits and 2008 AMEC Investigations
Saint's Rest	layer of Sandy Clay – CL; Silty to Sandy Gravel – GM – GP; Quartzite bedrock.	AMEC SR-2, SR-1	
South Saint's Rest	Sandy to Gravelly Clay – CL to GC; Clayey Sand – SC to Clayey Gravel – GC; Quartzite bedrock.	AMEC SSR-1	
Castro	; Silty to Clayey Gravel w/ Sand – GM to GC, Sandy Silt – ML; Clayey Sand – SC; Dacite to Latite Porphyry bedrock	AMEC C-2	
Butterfield	Clayey Gravel with Sand – GC; Gravel with Sand & Clay – GP – GC; Sandy Clay with Gravel – CL; Dacite Porphyry bedrock.	AMEC B-1	
Olsen	Gravelly, Sandy Clay – SC; Clayey Gravel – GC; Silty Sand – SM, Limestone bedrock.	AMEC O-1	
Note: See Attachment F for detailed logs of AMEC and NAE investigations.			

Kennecott Plant Projects Group (also NAE) completed extensive detail logging of exposures and trenches along the eastside collection system during the late 1980's to early 1990's. These cross sections are presented on various reports and maps developed during the period of 1991 to 1997 as summarized in Table A-3.

Table A-3 - Summary of NAE (North American Exploration) Investigations – Attachment D

Date / Drawing Number	Title	Information	Boring / Series
April 1992 / 451-T-	Eastside Collection Cutoff	Copper & Yosemite	NCU, CU

Date / Drawing Number	Title	Information	Boring / Series
2053, 451-T-2054	Wall Trenching – Yosemite, Copper, North Copper and Lost Creek/South Keystone Drainages	Cross Sections & photos of logs	trenches
Sept 1991	Clay Borrow Source Investigation – Yosemite Area	Logs of trenches	YT – test pits
April 1992	Eastside Collection – Cutoff Wall and Dam site Investigation- Queens, Olsen, and Butterfield 1 Drainages	Detailed logs of trenches and plan map below toe. Some logs have cross sections	F, OL test pits
April 22, 1991	Proposed Crapo Repository – Trenching and Sampling Program	Plan map and logs of the repository above the cut off trench	CKT
August 1992	Calcium Carbonate Investigations of In-place soils for use in stabilizing sludge from the Large Reservoir	Numerous logs with gravel, silt, clay descriptions	CA
Dec 1992	Calcium Carbonate Investigations of In-place soils for use in stabilizing sludge from the Large Reservoir – North Keystone to Copper	Numerous logs, plan map identifying areas of clay and CaCO3 for neutralization of acid sludges.	CA
1992/451-T-2051	Bingham Canyon Water Management East Side Collection Cut off wall sections, Midas 1, midas 11 and Bluewater 111	Detailed cross sections of soil type and thickness, mostly covers drainages	M, BW, KCC-TP, varies
1992/451-T-2052	Bingham Canyon Water Management East Side Collection Cut off wall sections, Midas 1, Congor 1 and Congor 11	Detailed cross sections of soil type and thickness, mostly covers drainages	M, CG, varies
1992/451-T-2053	Bingham Canyon Water Management East Side	Detailed cross sections of soil type and thickness, mostly covers	CU, varies

Date / Drawing Number	Title	Information	Boring / Series
	Collection Copper Drainages	drainages	
1992/451-T-2055	Bingham Canyon Water Management East Side Collection Cross Sections, North Copper Lost Creek / South Keystone	Detailed cross sections of soil type and thickness, mostly covers drainages	NCU, NNCU

The locations referenced above are shown on a series of AutoCadd drawings in attachment D. The information on these drawings was extracted into an ArcGIS shape file. This shape file has the location of explorations and includes the attributes of the investigations, such as bore hole ID, depth, soil type encountered, clay thickness and depth to bedrock. A summary of the investigations that were completed superimposed on the bedrock geology are shown on Figure A-3[2].

---
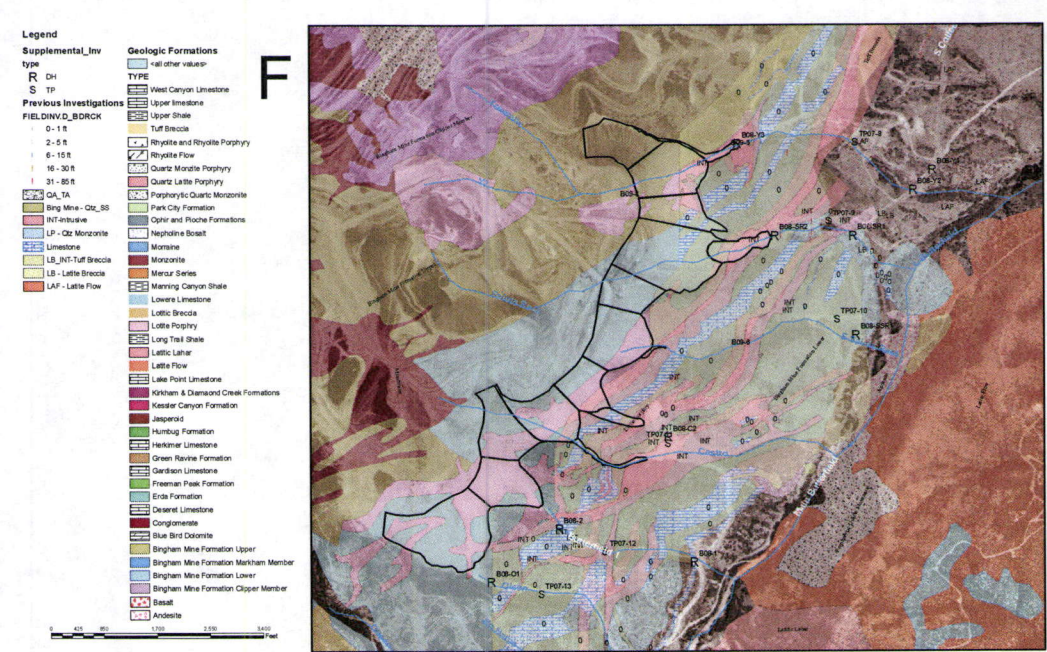
[2]   These figures are relatively large scale and significant greater detail is available in the electronic GIS format (ArcGIS) from which the figures were developed.

Date 10/20/2009   ©2008 Technological Resources Pty Limited

Estimates of the soil thickness are available along the toe of the dump and, in particular, at the cut off dams. The cut off dam locations were generally selected to be as far beyond the toe of the dumps, while still maintaining reasonable distances to bedrock for constructability. In short, these locations are likely to represent the thickest sequence of soils in the vicinity of the dump toe.

Based on these explorations, NAE developed a series of geologic cross sections along the seepage collection system and summarized these sections on Cadd drawings. The cross sections were drawn both parallel to the dump toe (across the drainages) and perpendicular to the dump toe (down the drainages). Typical cross sections through the drainages proceeding from north to south are presented in Attachment D, which contains the NAE autocadd drawings showing dump cross sections. (Note: refer to original AutoCadd drawings for lithology, descriptions and section locations.)
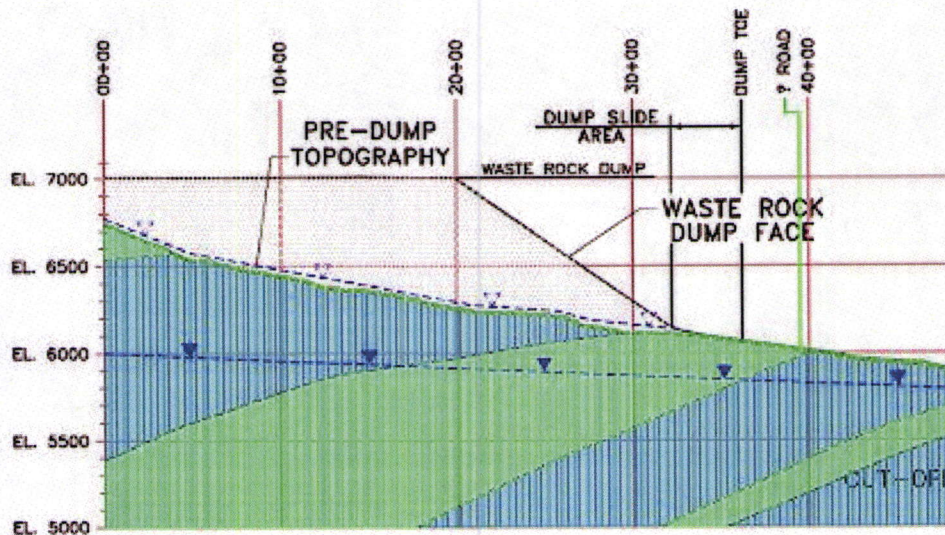

Figure A-4 - NAE cross section through Yosemite dump showing sedimentary deposits

The foundation conditions below the south dumps were initially investigated as part of the land exchange between Kennecott and the BLM (Bureau of Land Management) in the early 1980's. The reports for Butterfield Canyon and the mine dumps south of Yosemite were however based largely on the NRCS maps. However, review of the mapping indicates that the soil type descriptions are relatively uninformative from an engineering standpoint. The dumps themselves extend primarily onto the ridges and comprise areas of either bedrock

and/or very shallow soil cover, both of which are favorable to dump stability. This area has been mapped in detail by BCMC (Bear Creek Mining Company, the former exploratory subsidiary to Kennecott Copper Corporation) as part of mineral explorations. Scanned images of those maps are included in Attachment C.

The primary foundation soil types below the South dumps are referenced on Table A-4.

Table A-4 – Principal Soil Types below South Dumps

Location	Soil types and Depths	Reference
Olsen Gulch	GC-SC – Clayey sand and gravel, 0 to 42-feet CH – Plastic Clay	Summers: Hydrogeology and Effects of Mine Dump Expansion on Groundwater Quality, Butterfield Canyon, BLM.
Yosemite	GC-SC – Clayey Gravel and Sand; with SC sandy clay	AMEC, 2009
Saints Rest	GM-GC – Silty to Clayey Gravel, 0 to 15-feet; some CL, Silty Clay	As above-based on NRCS soils maps and available borings.
Castro	GC-SC – Clayey Gravel and Sand; with SC-CL mudflow material	
East Castro	GM-GC – Silty to Clayey Gravel, 0 to 15-feet; some CL, Silty Clay	
West Castro	GM-GC – Silty to Clayey Gravel, 0 to 15-feet; some CL, Silty Clay	
See also Table A-2 for soil types encountered in drainages.		

Soil Development below South Dumps

Due to the lack of site-specific field data, Rio Tinto T&I requested supplemental investigations be completed along the toe of the south waste dumps. Access along the dump toe was limited to existing roadways, which also contained numerous cuts and exposures of the soils developed along the slopes and drainages, as described below.

Soil development varies significantly from drainage to drainage and also on the north versus south facing slopes. The larger drainages contain significantly more colluvium / alluvium that have washed down from higher elevations. Some of these drainages are also more deeply incised. Source rock for much of the alluvium consists of the Paleozoic sediments versus volcanic sediments.

In general, soil horizons are more well-developed on the north facing slopes, which corresponds to the greater amount of vegetation present on these slopes. South facing slopes along the drainages tend to have poorly developed, thin soil horizons and primarily grass versus scrub oak vegetation. Exceptions occur in the larger drainages. A photograph of a road cut leading to the Castro drainage which shows the difference in north and south facing soil development is shown on Figures A-5 and A-6.

Figure A-5 – Soil development along the north facing Castro drainage. Note shallow bedrock is still present and considerable float occurs.

Figure A-6 – Transition area from thin soil layers (east facing) to thicker soil layers (north facing) near the Olsen drainage

The rounded hill tops (foot hills) present along the toe of the dumps tend to consist of thick sequences of gravel (alluvial fan) soils or comprise bedrock.

Supplemental investigations

Supplemental test pit investigations were completed in 2007 to obtain samples for laboratory testing. The investigations were extended from below the northern rail dumps to below the south dumps. Bulk samples were obtained within the test pits for engineering index property testing and direct shear strength testing. The locations of the investigations are shown on Figure A-7 and included some areas below the North dumps also.

Attachment F presents the supplemental test pits by NAE and also contains logs of borings completed in 2008 by AMEC (2009) to evaluate the debris basin embankments at the toe of the South dumps. Many of the AMEC borings extended through the embankments and into the underlying soils.
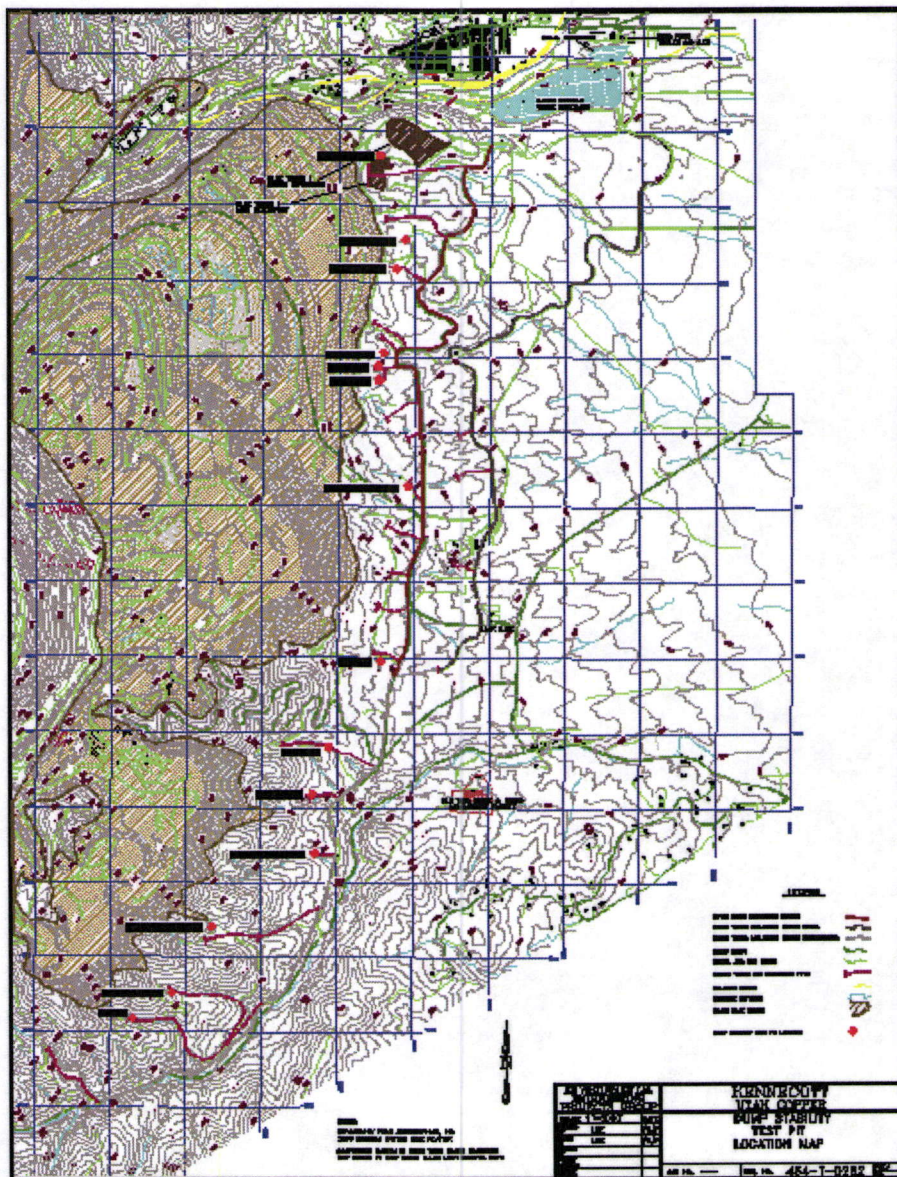
Figure A-7 - Locations of Test Pits completed by NAE (see attachment E for original map).

Laboratory test results

Gradation, plasticity and direct shear strength tests were completed on the 2007 samples. Results are presented in a detailed attachment of direct shear test results (IGES laboratory test results). The supplemental plasticity test results agreed well with previous test work and are shown on Figure A-8.
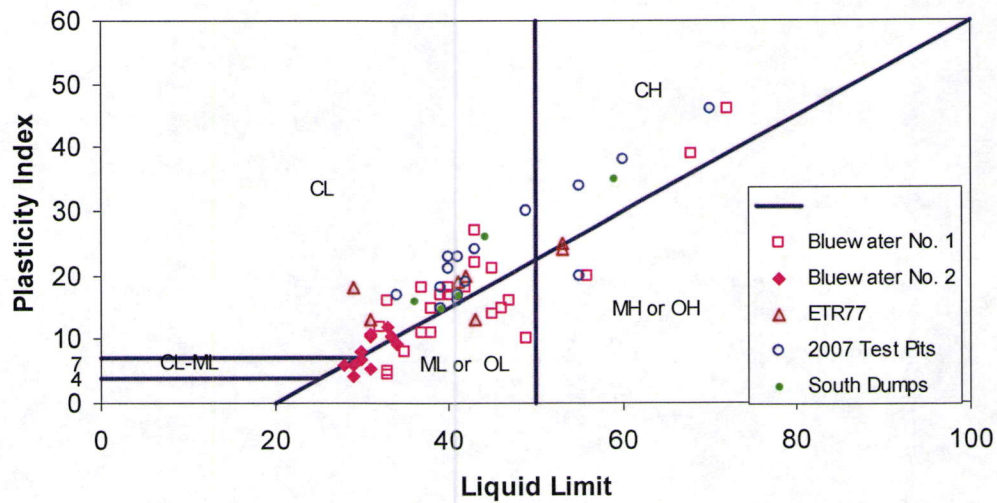
Plasticity Vs. Liquid Limit

Figure A-8 - Atterberg limit tests showing correlation of 2007 and 2008 samples with previous test work (South Dumps are 2008 tests).

A summary of the previous laboratory gradation analysis compared to the supplemental test work is presented on Table A-5. Samples are grouped by soil type.

Table A-5 – Summary of Foundation soil gradation analysis

Sample		% Gravel	% Sand	% clay/silt	Laboratory
Bluewater 2-1-2	MH	0	57	43	IGES
Butterfield 1-1-1	CH	0	13	87	IGES
Butterfield 1-1-2	CH	28	25	47	IGES
		average	32	59	**Sandy Clay**
Bluewater 3-1-2	CL	0	7	93	IGES
Congor .5-1-2	CL	2	28	71	IGES
Congor .5-1-3	CL				IGES
Congor 2-1-1	CL		13	88	IGES
Congor 2-1-2	CL				IGES
Copper 1-2	CL	3	15	83	IGES
North Keystone 1-1	CL		8	93	IGES
ETR77	CL				RBG
ETR77	CL-SM				RBG
		average	14	85	Slightly Sandy Clay
Yosemite 1-2	GC	46	15	39	IGES
Congor 1-1-2	GC-CL	37	25	38	IGES
Butterfield 1-1-3	GC-SC	26	40	34	IGES
Olsen 1-2	GM	44	35	21	IGES
RBG-1&2, Dec 1975	GM	53	26	20	RBG
RBG-1&2, Dec	GM	73	13	15	RBG

1975					
RBG-1&2, Dec 1975	GM	47	29	24	RBG
RBG-1&2, Dec 1975	GM	41	38	21	RBG
Yosemite 1-4	GP	82	10	8	IGES
Yosemite 1-1	GW-GM	52	22	26	IGES
average		**50**	**25**	**25**	**Sandy to Clayey Gravel**
Castro 1-1	SM	0	70	30	IGES
S Saints Rest 1-2	SM	10	75	15	IGES
Saints Rest 1-1	SM		61	39	IGES
RBG-1&2, Dec 1975	SM	22	52	26	RBG
RBG-1&2, Dec 1975	SM	13	71	16	RBG
RBG-1&2, Dec 1975	SM	20	50	30	RBG
RBG-1&2, Dec 1975	SM	20	35	46	RBG
RBG-1&2, Dec 1975	SM	33	40	27	RBG
RBG-1&2, Dec 1975	SM	27	50	23	RBG
RBG-1&2, Dec 1975	SW	11	85	4	RBG
average		**17**	**59**	**26**	**Gravelly, Silty/clayey sand**

Note: Data from North Dump area included in tabulation

The highly plastic CH and CL soils are generally associated with residual soils developed from underlying weathered volcanic bedrock or transported from weathered, up slope volcanic bedrock. Below the South dumps, the volcanic bedrock is present within "bands" of sedimentary materials generally trending in a southwest to northeast orientation. In addition to previous testing, an additional six direct shear tests were completed on low plasticity CL soils and one supplemental direct shear test was completed on CH soils. These results were combined with previous two tests to develop representative drained, consolidated shear strength data on the CL and CH soils, respectively. Results of the available direct shear testing are presented on Figure A-9. Individual test results are presented in attachment E to this Appendix.

Peak Stress Vs Normal Stress

$y = 0.4546x + 1725.4$
$R^2 = 0.8756$ (24 deg)

$y = 0.1888x + 1486$
$R^2 = 0.9944$ (11 deg)

Legend: ♦ CL ■ CH — Linear (CL) – – Linear (CH)
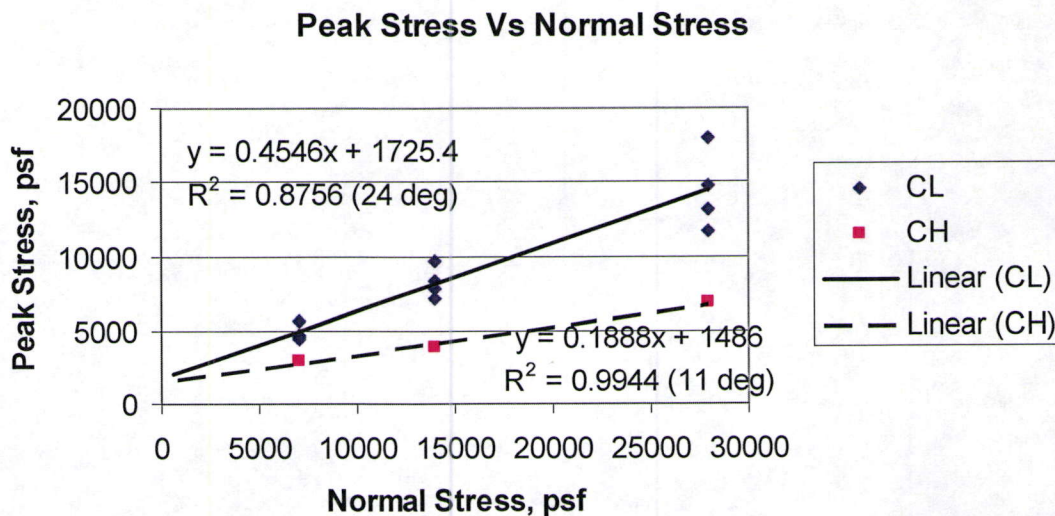
Figure A-9 - Summary of direct shear strength test results

Results indicate an average friction angle of 24 degrees and cohesion of 1725 pounds per square foot (psf) for the low plasticity clay soils. The high plasticity clays exhibited a friction angle of 11 degrees and cohesion of 1490 psf. Review of all the data available indicates that the majority of the lower plasticity clay soils posses a lower bound friction angle of 20 degrees and cohesion of 1400 psf. This lower bound value was used in stability calculations.

The shear strength of clayey to silty gravel soils (greater than 60-70 percent sand and gravel size particles) was based on the particle size distributions, clay content (Vallejo, 2000) and typical values for angular to subangular gravel and sand particles. Since many of the gravel soils possess cohesion, a small cohesion value was applied. Silty to Clayey gravel soils were therefore assigned a friction angle of 35 degrees and cohesion of 500 psf in stability analysis.

Underground Workings

Historical mining has resulted in a number of underground tunnels and adits in proximity to the dumps. KUCC has developed a plan map of the underground workings and incorporates this information 3-dimensionally into the MineSight model. A 2-dimensional portrayal of the underground workings is shown on Figure A-10. It is observed that the Saint Joe tunnel extends below the ridge between the Yosemite and Saint's Rest drainages.   The Butterfield tunnel extends along the South end of the South waste dumps and does not appear to lie below the dumps. No other tunnels are present below the South end dumps.
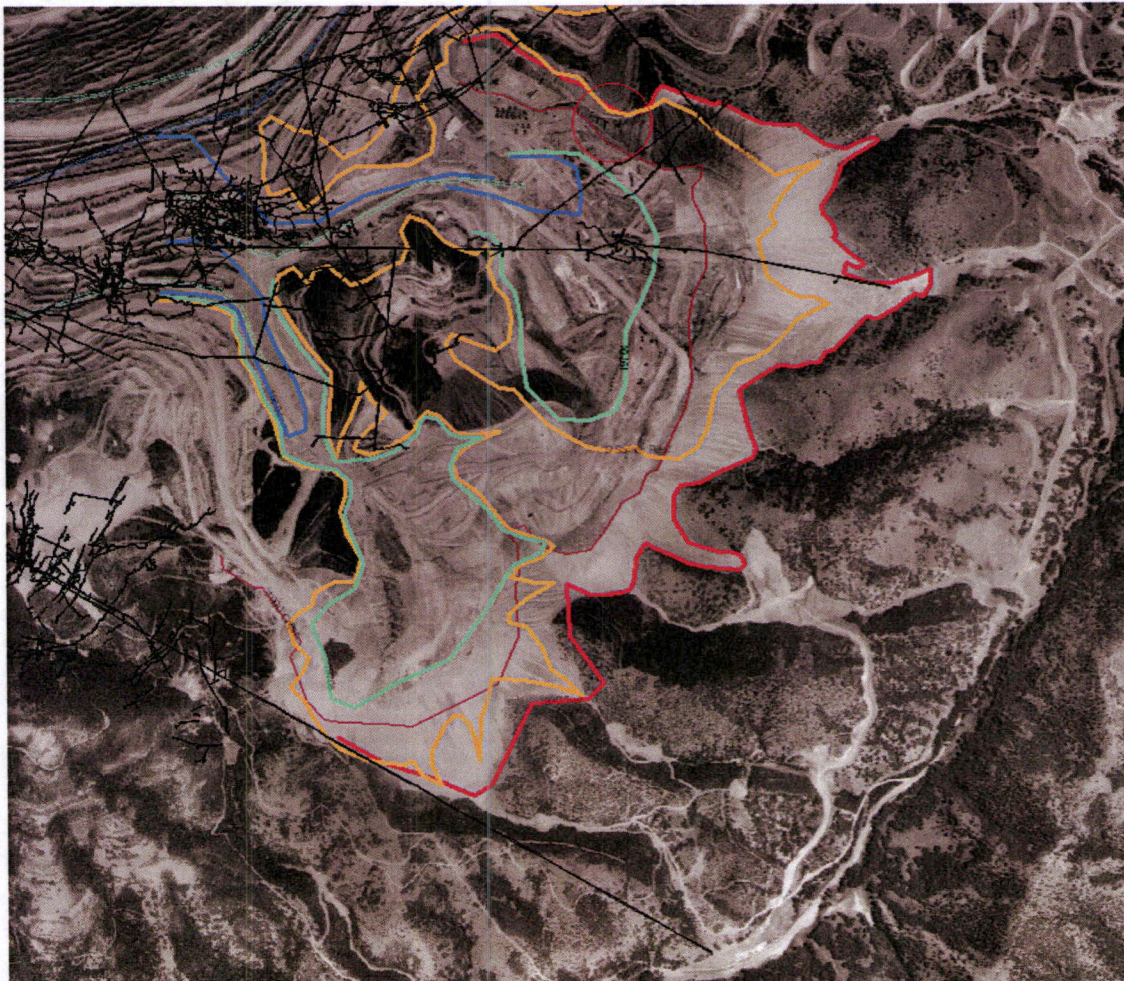
Figure A-10 - Projection of underground workings below KUCC South Dumps. The upper black line is the Saint Joe tunnel and the lower black line is the Butterfield Canyon tunnel (Red line = 1990 limits of dumps, orange line = 1980 limits, blue lines is 1970 and earlier)

A.3 REFERENCES

Babcock, R.C. Ballantyne, G.H. and Phillips, C.H., editors,. "Summary of the Geology of the Bingham Mining District." Society of Economic Geologists, Guidebook Series, Vol 29. Oct 1997.

Biek, Robert F., Solomon Barry J. Solomon, Jeffrey D. Keith, and Tracy W. Smith (2004), Interim Geological Maps of the Copperton, Magna, and Tickville Spring Quadrangles, Salt Lake and Utah Counties, Utah. Utah Geological Survey OFR 434.

Rollins, Brown and Gunnel, "Soil Investigation and Design Analysis, "Bluewater 1 ad 2 Drainages, 1975. (not included)

Summers, Paul, (1981) "Hydrogeology and effects of Mine Dump Expansion of Ground Water Quality," Butterfield Canyon, Salt Lake City, Utah.

Supplemental Assessment of the Environmental Effects of Dumping of Overburden Material in the Butterfield Canyon Area.

Doesburg, J.M., Nelson, R.W., "The hydrologic effects of Increased Mine Dumps Expansion on the Nevada Tract in Butterfield Canyon, Utah," prepared by Battale Pacific NW Laboratories, August 1981, KUCC Contract 2311204826.

Vallejo, L.E. and Iannacchione, A.T., "Shear Strength Evaluation of Clay-Rock Mixtures" in ASCE GeoDenver SP 101, Slope Stability 2000, p. 209-223.

Zavodni, Z.M., (1977), "Eastside Rail Dump Foundation Investigation," Technical Report No. ETR 77-6, Metal Mining Division, Salt Lake City, Utah. (not included)

Zavodni, Z.M., Trexler, B.D., and Pilz, J., (1981), "Waste Dump Foundations and Treatment," AIME Fall Meeting Conference, Denver, Colorado, U.S.A. (not included)

Attachment A – UGS 2007 Surface Geology Map *(provided upon request)*

Attachment B – Historic Reports *(provided upon request)*

- Rollins, Brown and Gunnel, 1975, "Soil Investigation and design analysis bluewater No 1. (not included)

- Rollins, Brown and Gunnel, 1975, "Soil Investigation and design analysis bluewater No 1. (not included)

- Zavodni, Z.M. 1977, "Eastside Rail Dump Foundation Investigation," Kennecott MMD-EC Technical report ETR 77-6. (not included)

Attachment C – Bear Creek Mining Company – Surface Geology Mapping *(provided upon request)*

Attachment D – NAE AutoCadd files of explorations *(provided upon request)*

Attachment E – 2007/8 Investigations *(provided upon request)*

Map of 2007 Test Pits

NAE boring Logs

IGES laboratory Test Results
- Summary Table of Shear strength Tests

- IGES laboratory Test Summary

- AMEC 2008 Soils Borings

RioTinto

| Project code | 12094 | Report number | 12094-02 | Version | 1.0a |

Technology and Innovation

Appendix B - Waste Rock Material Properties

20 Oct 2009

Prepared for	C. Kaiser, K. Payne, Z. Kenyon, M. Robothym	**Author/s**	J Pilz
Distribution			
Project manager		**Reviewer**	
	J Pilz		Z.M. Zavodni

Section 1 - Executive summary

Project purpose

This appendix of the KUCC waste dump report summarizes the available knowledge regarding the dump material properties, summarizes the available data, provides references to other studies and evaluates the most probable range in waste rock shear strength.

Major findings

Performance of the existing KUCC waste dumps over the past 25 to 85+ years suggests that the dumps are stable in all but times of high dump advance rates over clay foundation soils, such as was experienced in the late 1970's to early 1980's. Secondly, "old" waste dumps (greater than 50 yrs. old) have cemented with iron oxide compounds, thereby gaining strength and improving stability over time. The cementation is well corroborated by leaching studies of the dumps, which indicated that active leaching tended to seal of the dump surface under acidic conditions. Lastly, some of the north / northwest pit slopes at KUCC are being excavated at slope angles of 50+ degrees through former dumps that border the open pit mine. These dumps experience both production blasting and seepage and have exhibited good stability.

A range of waste rock shear strength failure envelopes are developed based on the angularity of the particles, stresses and published correlations between stress and shear strength. However, the effect of cementation affecting particle cohesion is not included within the shear strength envelopes developed herein, therefore the shear strengths developed are considered conservative.

Contents page

List of figures

List of tables

B WASTE ROCK DUMP MATERIAL PROPERTIES

B.1 DISTRIBUTION OF MATERIAL TYPES

The overburden materials placed into the dumps over time are described in Attachment D, Dump progression. A graph of the total waste tonnage developed over the life of the mine is depicted in Figure B-1, Waste tonnage. This graph was developed after Krahulec (1997) by multiplying the stripping ratio times the total annual ore production using 5 year increments of ore production. The total waste produced from early in the mine life to the mid-1990's was on the order of 140 Billion tons. After 1995, the majority of waste was placed above the Markham dumps, Dry Fork and within Bingham Canyon with a small amount of waste placed above the Yosemite dumps and above the uppermost East side dumps.
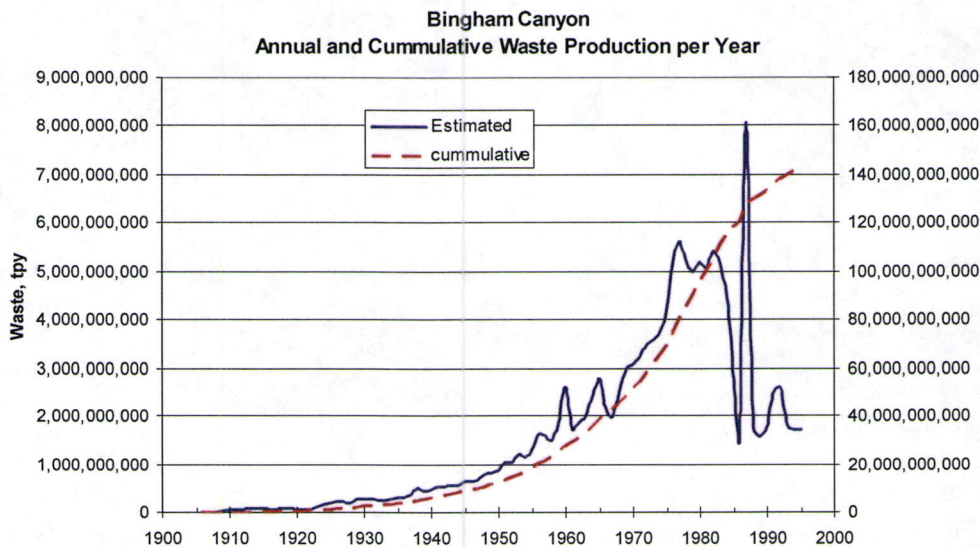

Bingham Canyon
Annual and Cummulative Waste Production per Year

Figure B-1 - Estimated Waste Placed at Bingham Canyon from beginning of open pit mining to the mid-1990's
(estimated from ore production and stripping ratio)

Records of waste and ore improved in the 1980's. The occurrence of ore and waste in different rock types was summarized in a KUCC memorandum dated May 14, 1982. Samples were based on 400 pound bulk samples.

Table B-1 – Summary of Bingham 1980 to present estimated ore and waste distribution (KUCC Internal data)

Type	Ore %	Waste %	Size Distribution, inches			
			- 1 inch	1 to 5 inch	5 to 10 inch	+ 10 inch
Intrusive	68%	32%	30	50	16	+4
Quartzite	24%	62%	41	34	21	+4
Limestone	8%	6%	35	28	14	+23
Overall waste size distribution		100%	37	39	19	+5

As observed, the majority of waste produced is quartzite with approximately 1/3 of the material being intrusive and the remainder being limestone. Most of the limestone material was placed in the South end dumps. It was found that only the meta-limestone exhibit high blocky materials with the remainder having relatively small block fragmentation size.

The above estimated size ranges should be compared to samples of the waste materials obtained from the waste dumps. Also, none of the bulk samples contained excessive amounts of fines, which is also found in the waste rock samples obtained from the dumps.

In summary, the principal drainages and dumps are as follows:

Table 2.1 – Summary of Dump Groups

Dump Group	Drainages Filled	Waste Materials Placed
North and West Pit Dumps	Markham Gulch	Primarily Quartzite with intrusives
	Cottonwood Gulch	
	Dry Fork	
	Freeman Gulch	
Bingham Canyon Dumps	Bingham Canyon	

Dump Group	Drainages Filled	Waste Materials Placed
Eastside Rail Dumps	Bluewater 1, 2 and 3	About 32 percent intrusives and 60+ percent quartzites, other minor constituents.
	Midas 1 and 2`	
	Congor 1, 2 and South Congor	
	Crapo	
Eastside Truck Waste Dumps	North Keystone and Keystone	Quartzites and intrusives
	Lost	
	North Copper and Copper	
South Dumps	Yosemite	Intrusives, quartzites and calc-silicates / limestones (these are primarily limestone dumps)
	Saints Rest and South Saints Rest	
	Castro	
	Butterfield 1	
	Olsen	
	Queen	

The mineralogy of the materials present in various waste rock dumps was studied in a number of internal memorandum by the Kennecott Metal Mining Division department in the 1970's. These studies focused on the mineralization of the waste dump materials and the ability to leach these materials for recovery of metal values. The following table summarizes the various mineralogical studies completed on the waste materials.

Table B-2 – Summary of Mineralogical Studies of the KUC Mine waste rock dumps

Abou-zied, S., (1972) "Rock Characteristics and Mineralogy of UCD Midas Dump," Metal Mining Division Kennecott Copper, Salt Lake City, Utah.

Cathles, L,M., (1973), "An Analysis of the Physics and Chemistry of Waste Dumps," Technical Report, Lexington, Massachusetts.

Gauna, M., (1975), "Permeability Testing Program at the UCD Waste Leach Dumps," Kennecott Interoffice Memorandum, Salt Lake City, Utah.

Grubaugh, P., (1976), "5960 Dye Staining Test," Interoffice Letter, Utah Copper Division, Salt Lake City, Utah.

Gupta, U.K., and Gauna, M., (1976), "UCD Waste Dump in Situ Permeability and Oxygen Temperature Investigation," Metal Mining Division, Salt Lake City, Utah.

Jueschke, A.A., (1974), "Size Analysis of Waste Rock on Blue Water No. 2 Dump," Kennecott Research Center, Salt Lake City, Utah.

Klinger, P.B. and Schlitt, W.J., (1978), "Mineralogical Study of Samples Recovered" By the Westinghouse Becker Drilling Program on UCD Dumps," Technical Report No. RTR 77-15, Kennecott Metal Mining, Salt Lake City, Utah

Logsdon, Mark, J., (2005), "Long term stability of Waste-Rock Stockpiles", draft memorandum, September 2005.

Malouf, E.E., (1972), "The Plugging of Leaching Columns by Precipitation of Basic Iron Sulfate Salts, Inter-Office Memorandum, Salt Lake City, Utah.

Ream, B.P., (1975), "Freeman Dump Staining Test," Interoffice Letter, Kennecott Mine, Salt Lake City, Utah

Stephens, J.D., (1971), "Study of Copper Mineralization in Eleven Samples of Waste From UCD Keystone Dump", Kennecott Copper Corporation, Salt Lake City, Utah.

B.2 GRADATION DATA

A number of gradation analyses of mine waste are available from surface sampling, previous studies and drill cuttings. However, the majority of the data are at shallow depth within the

mine waste pile and do not fully represent the very large (cobble to boulder size) particle distribution at depth.

The available gradation data indicate that the majority of the dump materials have relatively low fines content[1], generally less than 20 percent. The majority of the particles sizes are gravel size or larger, ranging to very large boulder size. Larger size particles have not been adequately sampled at depth, due to restrictions in the drill core diameter. Surface observation clearly indicates the particle segregation that occurs down a dump face which also tends to concentrate the larger particles at the toe of the dumps. What is less clear is whether high stresses and resulting particle crushing reduces the average particle size at depth.

Table B.2 and Figure B-2 present a summary of the WR particles size distributions obtained from previous studies.

Table B-1 – Typical Ranges in Dump Particles Sizes (KUCC data)

Location	Gravel or larger, percent	Sand, percent	Slimes or fines content, percent
Freeman	72	15	13
Run of Mine, 1980's	77	20	3
Quartz Monzonite Porphery	54	38	8
This study (plug dumped areas)			11 +/- 6 % (+/- 1 standard dev.)

---

[1] Technically the fines content should be the percent passing the no. 200 sieve, but sometimes the term "slimes have been used in the available references. Slimes may be particles sizes down to the no. 325 sieve.
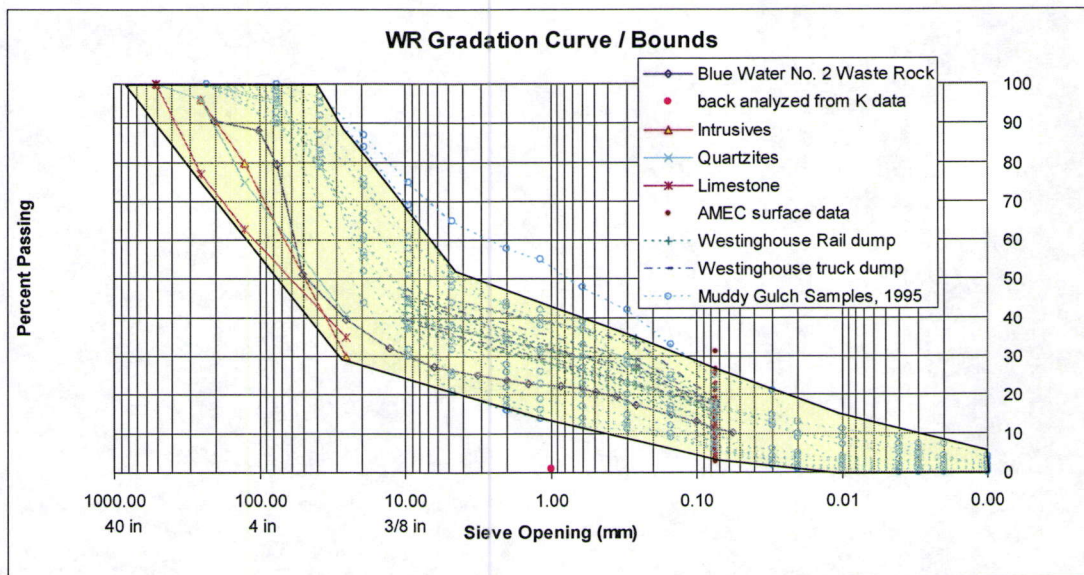
Figure B-2 - Summary of WR dump gradation data based on previous investigations (KUCC and AMEC data)

Recent advances in Sonic drilling technology have improved our ability to advance borings through waste rock dumps and obtain representative samples of the materials. Previously, borings through dumps could only be advanced using rotary circulation drill holes or a Becker hammer drill rig. Both of these methods results in poor quality, disturbed samples. Sonic drilling methods have improved both penetration rate during drilling and our ability to obtain disturbed samples of the dump materials. In 2007-2008, a piezometer installation program was completed on the west dumps above the Bingham mine using sonic drilling. Samples of the sonic core were obtained and logged at select locations. Although the Sonic rig does break down large particles for the drill steel to penetrate the dump, the sonic cores do reveal representative samples of dump materials at depth.

To evaluate the west dumps, KUCC logged the core in terms of percentage of silt and clay, sand, gravel and cobble size particles. A plot of these percentages versus depth is presented on Figure B-3. Although this figure seems to indicate a higher percentage of fines versus depth, the geologist logging the core indicated that drill penetration was slow at depth, reflecting the fact that the sonic rig was breaking down large particles. It is believed that the increase in fines content versus depth is due to particle breakage due to drill rig penetration versus actual change in fines content.
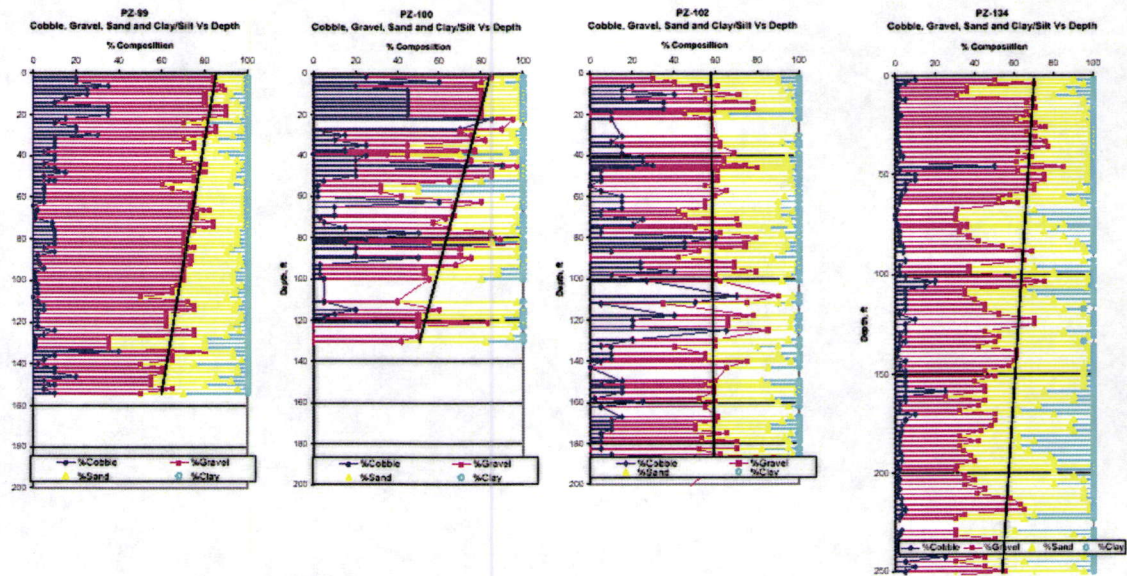
Figure B-3 – Distribution of cobble (blue), gravel (magenta), sand (yellow) and silt/clay particles sizes versus depth based on Sonic core (visual / manual method).

A photograph of a typical sonic core showing medium to fine grain size particles is provided on Figure B-4.

Figure B-4 – Typical Sonic core in plastic jacket.

A comparison between the field log and the laboratory based particle size analyses is presented on Figure B-5.
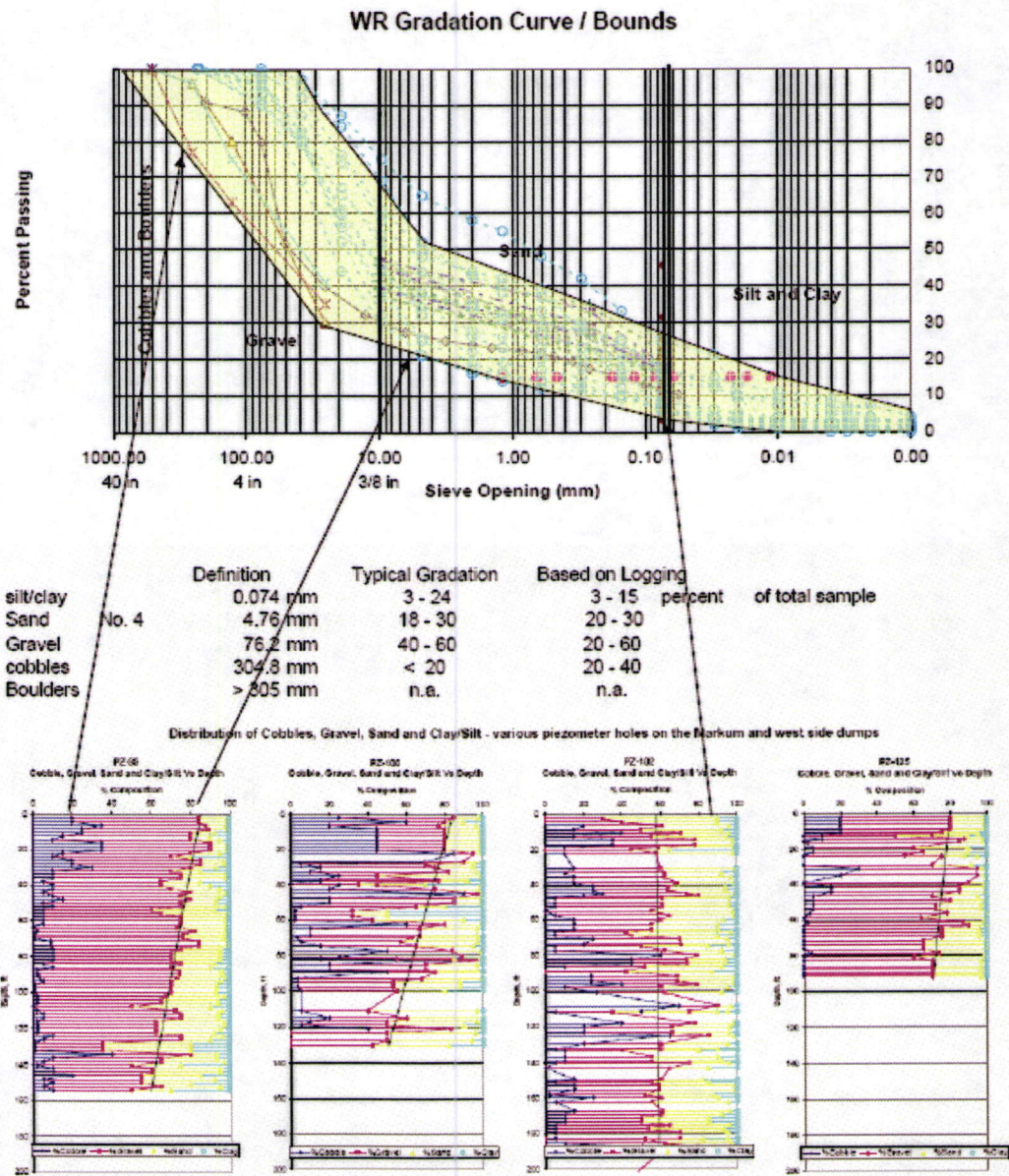
Figure B- 5 - Comparison of Laboratory Particle size and field logs

B.3 DENSITY AND MOISTURE CONTENT

Field density data suggest that the surface of the dumps have a total density between 125 to 130 pcf (pounds per cubic feet). Kennecott Mine data (Erickson, 1994) suggests an increasing density with depth, which appears logical. Select density data are plotted on Figure B-6.
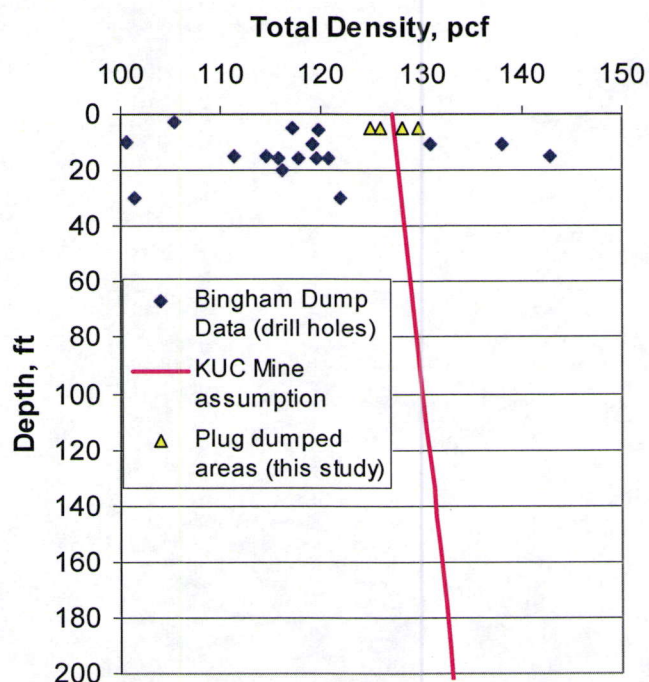
Total Density Vs Depth

Figure B-6 Density Data (KUCC data)

It is observed that the drill hole data contain considerable scatter, which is likely attributed to sample disturbance. The KUCC mine has estimated that the dump total density increased up to about 140 pounds per cubic feet with depth (at 400-feet).

Available moisture content data also indicate relatively low moisture contents, generally less than 10 to 15 percent. Density data from the 2005 O'kane field study are summarized in Table B.2.

Table B-2 – Density Data from Plug Dumped Areas (O'Kane 2005)

Date	Dry Density, pcf	Water Content, %	Total Density, pcf
31-Mar	112.7	13.7	128.1
01-Apr	113.5	10.2	125.0
02-Apr	115.4	9.0	125.8
03-Apr	116.8	11.0	129.7
	114.6	11.0	127.2

B.4 PERMEABILITY DATA

A conceptual model of the WR dumps is presented in Appendix F. This model indicates that the initial particle segregation down the dump face causes a general increase in permeability versus depth. However, the upper portion of the dump may have low permeability due to "plug dumping" and a layer of road base that was placed on the dumps for trafficability. In general, the overall low fines content appears to correlate to the relatively high permeability that has been measured in the dumps, which are summarized in Table B.3.

Table B-3 – Summary of Select Dump Permeability Data

	date test	Permeability, darcies		Permeability, cm/sec	
		Min	Max	Min	Max
Cathles, L.M.	1973	140	11700	1.4E-01	11.7
	1973	500		5.0E-01	
	1974	150		1.5E-01	
	1974	5		5.0E-03	
	1974	74		7.4E-02	
	1974	2		2.0E-03	
	1974	10		1.0E-02	
	1974	11		1.1E-02	
Dames and Moore	1970	2.1		2.1E-03	
	1970	0.18		1.8E-04	
	1970	0.045		4.5E-05	
	1971	0.0012		1.2E-06	

	1971	0.00034		3.4E-07	
	1971	0.000094		9.4E-08	
Hoyt	1968	2.4		2.4E-03	
Shehata	1069	4700		4.7E+00	
	1974	1.3		1.3E-03	
Jueshcke, A.A.	1974	0.1	0.45	1.0E-04	4.5E-04
			Average	3.1E-01	

Surface areas of the dump have been subject to cementation and "plugging," as indicated by the lower permeability values 10^{-6} to 10^{-8} cm/sec, above. The surface cementation was an ongoing issue during dump leaching operations where barren, acidic solution had a difficult time penetrating the dumps. The lower surface permeability of the dumps was also attributed to "plug dumping" and the nearly horizontal layering caused by dumping materials on the surface following by grading the material by dozer. The "plug dumping" was necessary to maintain a constant elevation as the dump settled following initial placement.

B.5 RANGE IN ROCKFILL AND MINE WASTE STRENGTH

Background on Frictional Shear Strength

In general, the frictional shear strength of cohesionless materials is a function of (A) the mineral to mineral contact frictional properties and (B) a component termed "interlocking." The interlocking component has three sub-components: B1) the frictional resistance at point contacts, B2) particle rearrangements and B3) dilation. The total frictional resistance is a combination of the mineral on mineral friction angle and the interlocking component. For quartz on quartz, measured values of mineral to mineral friction, ϕ_u are shown on Figure B-7 (after Mitchell, 1976).

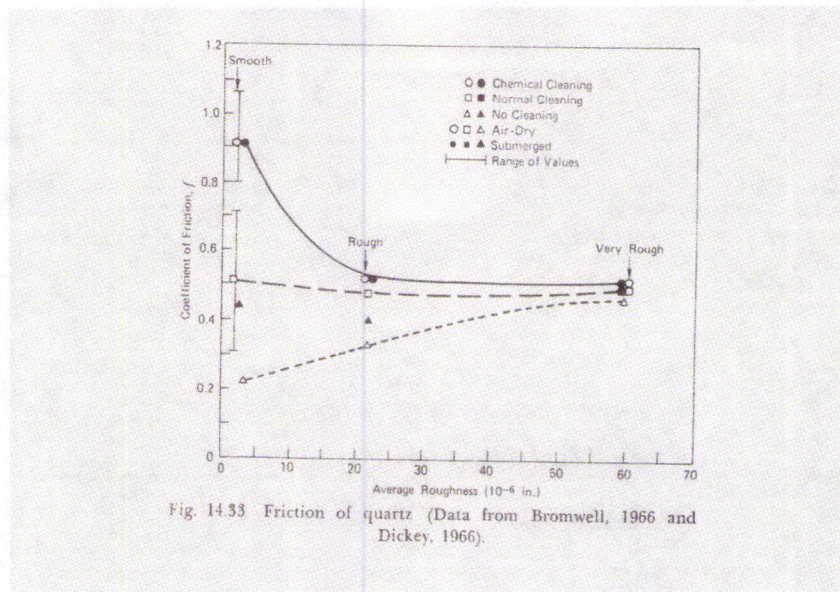Fig. 14.33 Friction of quartz (Data from Bromwell, 1966 and Dickey, 1966).

Figure B-7 - Friction of Quartz on Quartz based on roughness

It is observed that the frictional resistance of quartz contacting quartz is 0.5, which is equivalent to a friction angle of 26.5 degrees. It is also well known that the friction angle of quartz sand is typically much higher than the 26.5 degrees particle friction angle and commonly ranges from about 32 to 38 degrees. The difference is explained by the void ratio of the sand, which either requires that particles seek a denser arrangement (contraction) or expand in volume (dilation) in order for particles to either shear or roll against one another (dilate). Materials that are "contractive" tend to loose strength during shear, whereas materials that are dilative require an increase in volume for shear to occur and thereby possess much higher overall shear strength. At a unique void ratio, the sand particles shear under constant volume. This unique void ratio is often termed the "steady state shear strength and the friction angle at this steady state is termed ϕ_{CV}. This unique "state" is also referred to as the "critical state". The relationship between porosity (inverse of void ratio) and friction angle for a granular material is shown on the following figure (also after Mitchell, 1976). For very dense materials (low porosity), the friction angle may be quite high, up to 46+ degrees, since particles must break in order to slide or roll past one another during shear.
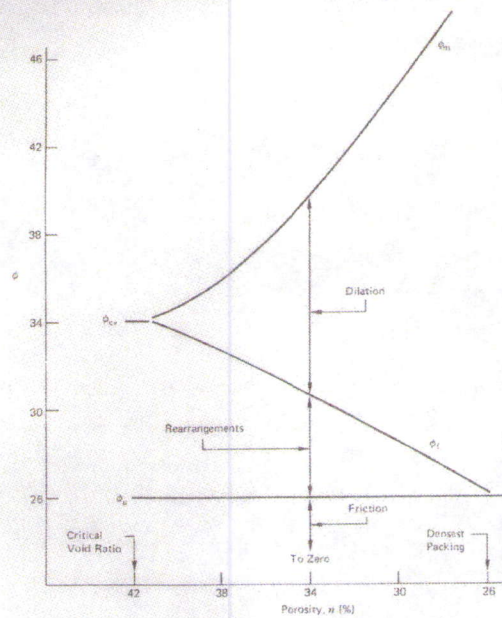
Fig. 14.38 Components of shear strength in granular soils (After Rowe, 1962).

Figure B-8 - Components of Shear Strength: Interlocking, dilation and particle rearrangements

The effect of weathering of particles can be evaluated in terms of fundamental principals of soil / rock fill behavior, even at elevated temperatures. Deep within the dump, it is logical to assume that the waste rock particles have arranged themselves into a dense, dilative state. Observations of previous dump failures indicate that horizontal bedding was present down to depths of 100 to 150-feet in 1000-feet high waste dumps, representing about 10 to 15 percent of the dump height. These horizontal layers were initially placed on the dump surface and are encountered at depth due to settlement and subsequent regrading (short dumping) at the dump surface. Given this degree of settlement, it would be expected that the underlying materials are in a dilative state. Conversely, it is likely that during initial dump placement, the waste rock particles are in a contractive state, hence the high initial settlements. The above principles of particle on particle friction, and contractive / dilatant behavior continue to apply at elevated temperatures.
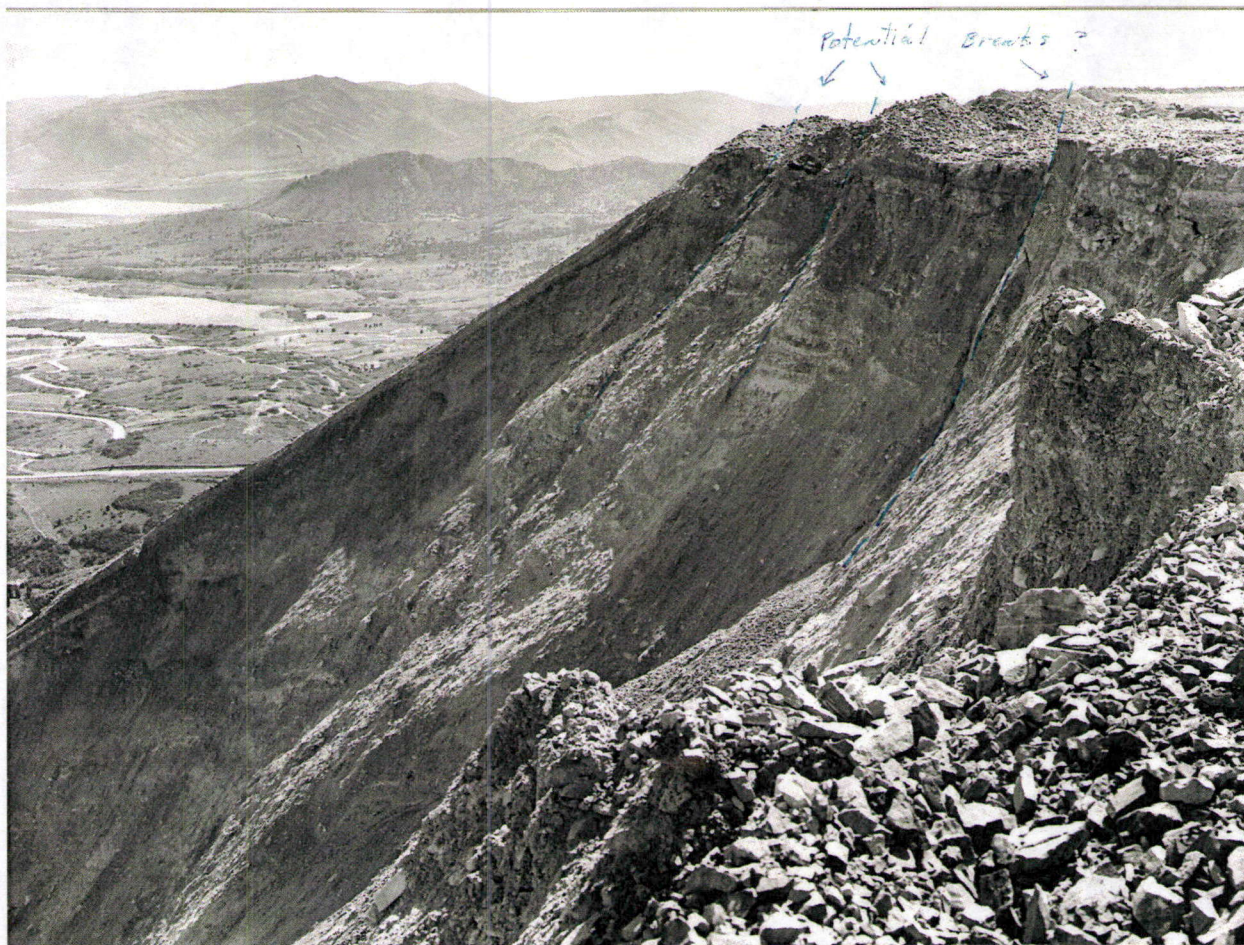

Figure B-9 – Stratification of a dump and horizontally bedded materials observed at depth (1979 photo, J Pilz)

It is also well documented that the Mohr-Coulomb failure surface is non-linear, especially at either very high or low confining stresses. This "curvi-linear" feature of the shear strength envelop is expressed on the "Leps chart" (Leps, 1970), which summarizes the strengths of various rock fills in terms of friction angle versus confining pressure. A plot of the data presented by Leps (1970) is shown on Figure B-10. Based on these data[2], the minimum friction angle for rock fill is on the order of 34 degrees. A decrease in the friction angle with confining stress is one factor that could cause a reduction in stability. However, the existing high truck waste dumps have been stable since the early 1980's with high confining stresses at the base of the dumps. A reduction in shear strength due solely to confining stress is therefore not an explanation for a future reduction in shear strength.

---

[2]   It should be noted that review of the data by Leps indicates that the available testing is only representative of the Santa Rita mine waste materials). The majority of the data represents either tailings sands, slates, sandstone and similar friable materials, along with more durable materials such as granite and basalt.
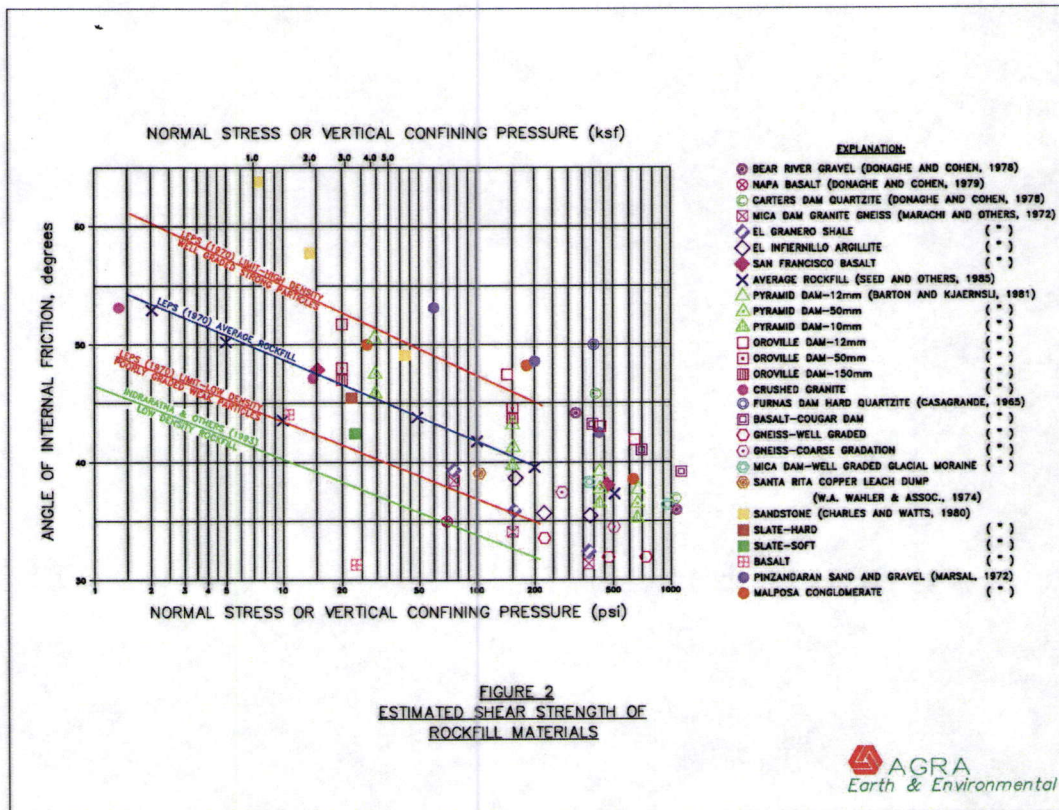
Figure B-10 - Leps chart correlating rock fill shear strength to confining stress

During end dump placement, it is commonly observed that the larger rock particles bounce and break apart as they roll down the end dump slope. This process tends to break the rocks apart along natural planes of weakness into their stronger constituents. Secondly, waste rock materials are generated by mine blasting, which also breaks the rock apart along any in-situ bedding, joint or fractures. These observations indicate that the rock materials that end up along the base of the dump are the most competent materials from the mine. Such materials would fall within the upper range of frictional properties in the Leps chart, Figure B-10.

Cohesive Shear Strength

According to Mitchell (1976), true cohesive shear strength is a function of electrochemical bonding and/or cementation. The definition of cohesion has also been modified by Fredlund et al (1978), who define an apparent cohesion component in terms of matric suction. The form of Fredlund's equation is as follows:

$$T = C' + (\sigma' - u_w) \tan \phi' + (u_a - u_w) \tan \phi^b$$

Where:

C' = true cohesion

σ' = Vertical effective stress

u_a = Pore air pressure

u_w = Pore water pressure

φ' = Friction angle with respect to applied stress

$φ^b$ = Friction angle with respect to matric suction in terms of σ' – u_a.

The last term of the above equation estimates the value of the "apparent cohesion" due to matric suction and essentially turns the 2-dimensional Mohr-Coulomb linear envelop into a 3-dimensional failure surface.

The available gradation data suggest that the percentage of fine grain materials within the dumps is insufficient to provide a significant apparent cohesion component (ie. due to development of negative pore water pressures in the capillary zone).

Cohesion due to cementation by ferric and ferrous iron components may be significant. Observations of the Cottonwood Waste dumps indicate a high degree of cementation is present due to ferric iron precipitates. This form of cohesion is discussed more fully in regards to geochemistry (Appendix C). Since the cementation component has not be quantified by testing, it has been conservatively omitted from the shear strength envelop.

Back Analysis of Minimum Dump Strengths

In general, for cohesionless materials, the critical slip surface in limit equilibrium analysis will converge toward the infinite slope failure condition. For this condition, the factor of safety of the slope is defined as the ratio of the angle of internal friction, φ, divided by the slope angle, i. The infinite slope condition is commonly used to estimate the minimum friction angle of the slope materials, since at a factor of safety of unity (1.0) the friction angle is equal to the slope angle. Since the KUCC waste dumps are observed to "stand" at slope angles of 37 to 41 degrees (where there are more fines), the commonly accepted friction angle at low confining stress is assumed to be within the same range. It is also observed that the WR particles are at their loosest condition at the dump surface.

As described above, the dump materials increase in density due to settlement and the friction angle most likely increases as the materials assume a more dilatant condition. Under very high confining stresses, particle breakage is possible and the interlocking component of friction decreases. Therefore at depth within the dumps, the friction angle may have decreased due to confining stress. It is noted that the parent rock that comprises the waste dump has been subject to significantly higher confining stresses than found in the waste dumps and that blasting and the end dump placement tend to break the rocks apart along pre-existing fractures.

Back analysis can be used to estimate (or bound) the shear strength properties required to maintain stability for observed conditions. Slope stability analysis can be used to provide a lower bound estimate of the minimum shear strength that must be present within the dumps. For existing, stable dumps, the actual factor of safety is not known. However, it is generally accepted that slope deformations are evident at factors of safety between about 1.0 and 1.2. Since there are no present day observations indicating slope deformations within the dumps, it can safely be assumed that the dump factor of safety must be at least 1.2. Secondly, the Bingham pit dumps are subjected to daily blasting. Therefore, it is reasonable to include a seismic coefficient in the back calculations of minimum shear strength. Lastly, if it assumed that the failure surface does not pass through the foundation soil or bedrock materials, the minimum available shear strength of the waste materials can be determined. Based on these considerations, back analysis can also be used to estimate cohesion at various ranges of friction angle.

Back analysis of the minimum shear strengths were completed for a representative cross sections of the Cottonwood dumps on the northwest side of the pit and the higher truck waste dumps on the east side of the mine. The back analysis of the Cottonwood dumps can be utilized to estimate the cohesion that must be present in these well-cemented and stable dumps. The back calculations used the following geometry and assumptions:

Table B-4 – Dump Characteristics

Location	Dump Height, ft	Overall angle of the dump, degrees	Phreatic Surface	Foundation Conditions
Cottonwood Dump	900	48	Several feet above soil/ foundation contact	Gravelly soils and (ortho-quartzite / dacite) bedrock that exceed shear strength of waste materials
Code 30 Dumps (Keystone truck dumps)	1000	37	As above	As above
	1000	Varies with stress	As above	As above, but foundation slopes varies from 0 to 30 degrees
	1000	Varies with Stress	As Above	Weak foundation and slope varies from 0 to 30 degrees

The assumption that the shear strength of the foundation soils exceeds the dump strength is probably reasonable for the Cottonwood dumps, as it would be unlikely that low strength materials comprise the foundation and the dumps are stable. However, the assumption that the foundation soil materials exceed the waste dump strengths on the east side dumps is only a simplifying assumption so that the minimum shear strength of the waste dump can be back calculated. The assumption may be unrealistic. Secondly, the resulting calculations appear to indicate that failure along deep slip surfaces can only occur if a portion of the slip surface passes through weak foundation materials.

For the Cottonwood Dump geometry, a plot of the factor of safety versus minimum cohesion that must be present was prepared. A friction angle of 37 and 40 degrees was selected and the effect of a seismic coefficient to simulate the effect of pit production blasting was also included. The following graph shows the results:

Cottonwood dump Geometry
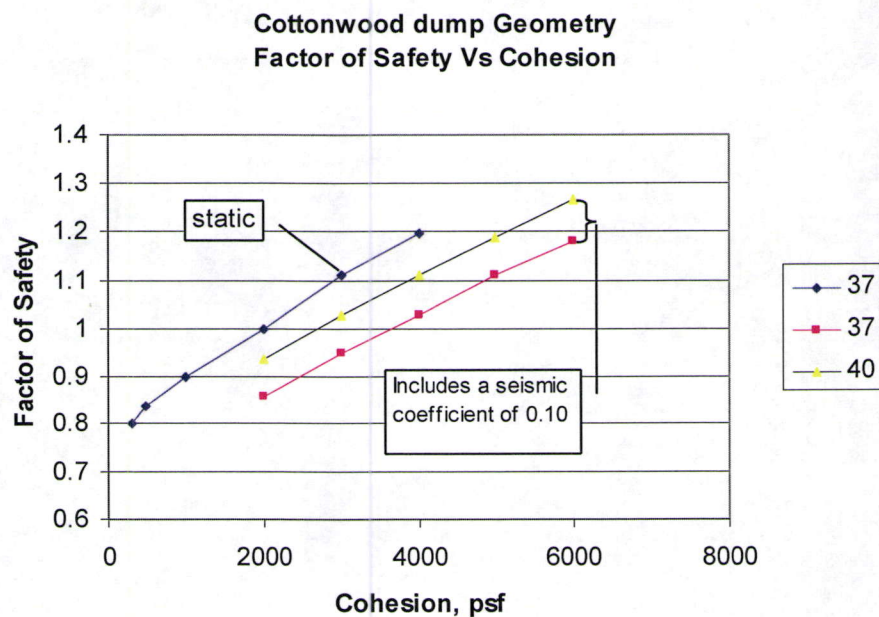**Factor of Safety Vs Cohesion**

Figure B-11 - Factor of safety versus cohesion for a well cemented dump

It is observed that the minimum cohesion required for the cemented dumps to remain stable (which they are) ranges from a low value of 2000 up to 6000 psf. The higher values of cohesion assume both a minimum factor of safety of 1.2 and that the dump has been subjected to a seismic coefficient of 0.1. These back calculations reflect the minimum values of cohesion that are present for cemented dumps and higher values are likely under field conditions.

B.6 EFFECT OF HEAT AND WEATHERING

Hypotheses have been proposed that chemical reactions, elevated temperatures and accelerated weathering of the WR materials could degrade the dump strength over time, thereby reducing stability (Robertson, 2005). As indicated in Appendix C, the majority of the waste dumps are geochemically active and exhibit elevated temperatures. The actual measured range of dump temperatures ranges from 70 to 170 degrees Fahrenheit, as presented in Figure B-12.
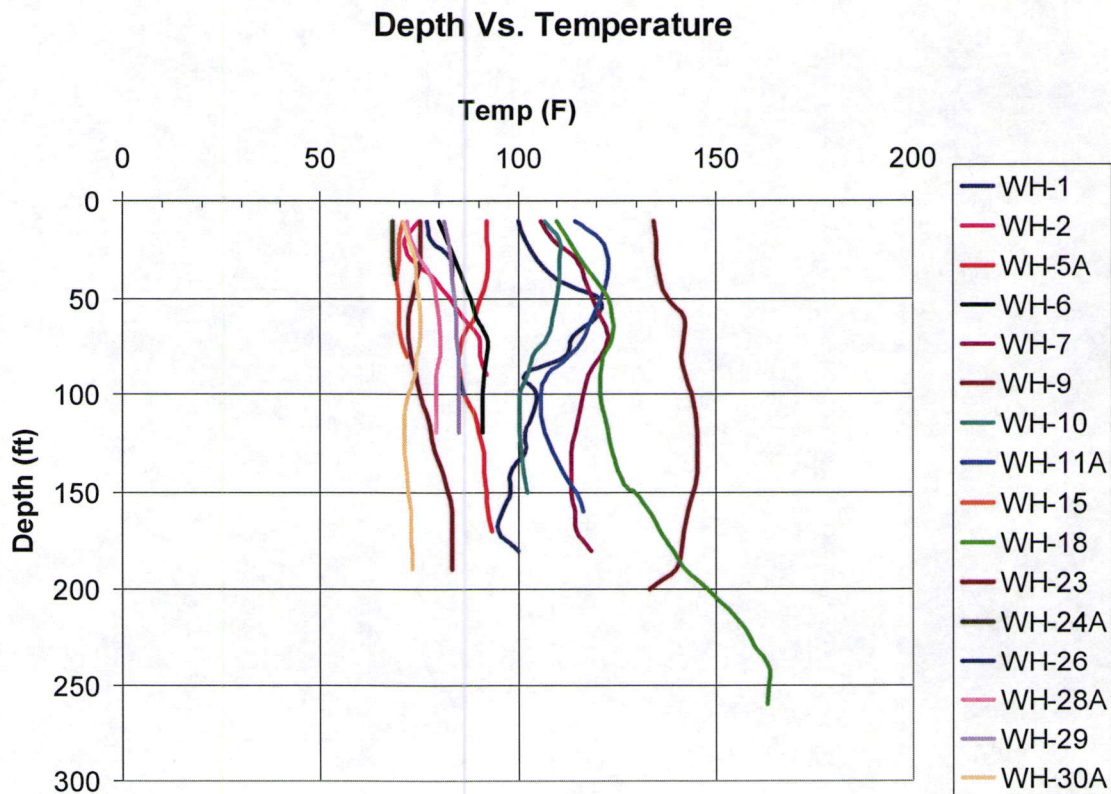
Depth Vs. Temperature

Figure B-12 – Available Temperature Data (Wyoming Mineral drill hole data)

There are few published correlations between the effect of temperature and shear strength at these temperatures. Data are available for more elevated temperature regimes (200 – 300° F). The temperatures measured within the dumps are not sufficient to cause mineralogical changes in the waste rock materials. Since there is no mineralogical change due to the elevated temperatures, it is unlikely that temperature by itself would cause a change in shear strength. Further discussion of the effects of temperature are presented in Appendix C.

Studies Indicating Degradation in Strength

There are a few studies indicating that the shear strength of weathered rock fill is lower than its un-weathered counter-part. One such study was published (Sayao, et al 2005) showing

an approximate 15 percent reduction (depending on confining stress) for unweathered and weathered basalt bedrock. However, it can be argued that the mine waste is already in a weathered state and would have exhibited such weathering effects at the initial placement.

It has been hypothesized that accelerated weathering within dumps of feldspars to clay materials may precipitate waste dump failures (Robertson, 2005). Based on this study, there is an absence of data suggesting that this is occurring within the KUCC waste dumps. This is partly attributed to the fact that many of the dumps are quartzite or quartz monzonite. Conversely, available gradation and mineralogical data suggest that the clay content of the dumps is quite low, due to the low fines contents (% < #200 screen) of the dumps (less than about 20 percent).

Appendix C indicates that the rate of weathering is also quite slow. In the event that weathering does occur, weathering of the waste dump particles other than along the very thin "rind of the waste rock particles" would require time periods on the order of decades. This weathering could affect the "particle to particle" component of frictional strength, but is unlikely to affect the interlocking component of frictional strength.

From a geomechanical perspective, the effect of accelerated weathering would affect the particle interlocking component of friction of materials that break down due to weathering. The primarily quartzite materials do not exhibit such weathering. If weathering of the dump particles to clay mineral would occur, then the particle on particle friction angle is reduced, thereby reducing the available shear strength. However, provided that the particles remain intact, the degree of interlocking is unlikely to change due to the development of a surficial weathering rind.

Secondly, the potential breakdown of the particles and reduction in friction angle appears to be offset by cementation that occurs within the dump, which increases the cohesion and overall shear strength. Cementation appears to be the more pronounced phenomenon observed at KUCC. Given the observations at the Cottonwood dumps, it is more likely that the dumps increase in shear strength over time due to cementation rather than decrease in shear strength due to weathering of the particle on particle friction (it is observed that the particles cement or bond together).

B.7 SUMMARY

The WR dump materials are best characterized using a best estimate relationship and considering:

- o The Leps data on rock fill strength as a starting point
- o Previous estimates from consultant reports (SHB, CNI)
- o Back calculated estimates of the lower bound of shear strength
- o A non-linear shear strength envelope and
- o considering the range in rock types incorporated into the dumps and theoretical "non-linear" shear strength envelop of a fractured rock mass.

Based on the conditions described herein, the best estimate of this range of the waste rock shear strength is presented on Figure B-13. Cementation would increase the available shear strength, particularly at low stresses.
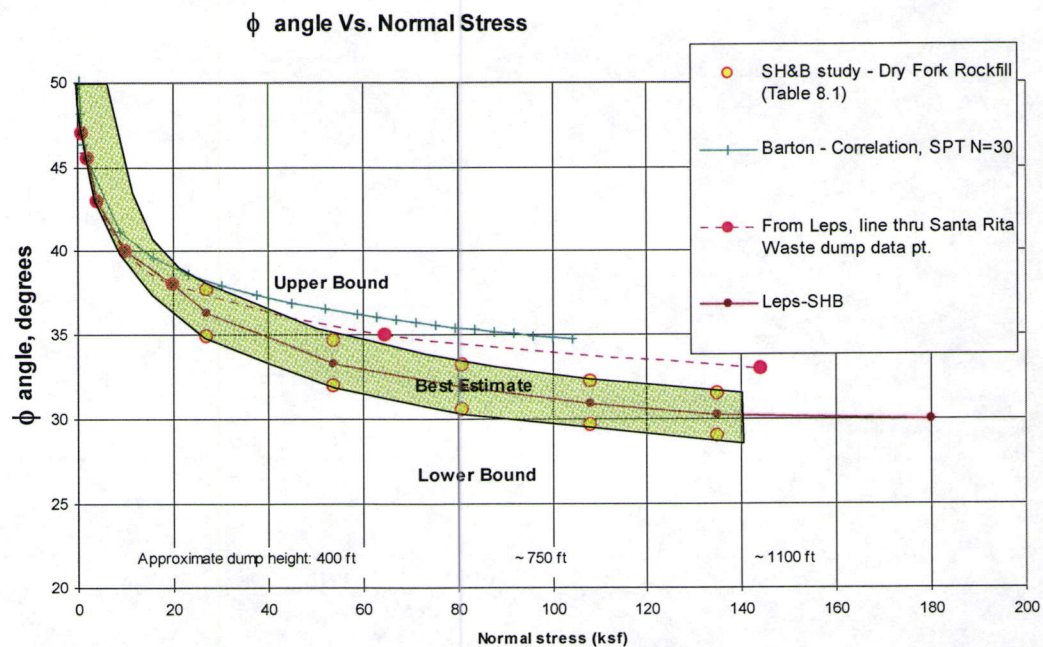

φ angle Vs. Normal Stress

Legend:
- SH&B study - Dry Fork Rockfill (Table 8.1)
- Barton - Correlation, SPT N=30
- From Leps, line thru Santa Rita Waste dump data pt.
- Leps-SHB

Upper Bound
Best Estimate
Lower Bound

Approximate dump height: 400 ft   ~750 ft   ~1100 ft

Y-axis: φ angle, degrees
X-axis: Normal stress (ksf)

Figure B-13 - Best Estimate of Waste Rock Shear Strengths

References:

Abou-zied, S., (1972) "Rock Characteristics and Mineralogy of UCD Midas Dump," Metal Mining Division Kennecott Copper, Salt Lake City, Utah.

Barton, N, (2008) "Shear Strength of Rockfill, Interfaces and Rock Joints and their Points of Contact in Rock Dump Design," in Rock Dumps 2008, Proceedings of the First International Seminar on the Management of Rock Dumps, Stockpiles and Heap Leach Pads, Fourie, A. ed., Perth Australia,

Cathles, L,M., (1973), "An Analysis of the Physics and Chemistry of Waste Dumps," Technical Report, Lexington, Massachusetts.

Gauna, M., (1975), "Permeability Testing Program at the UCD Waste Leach Dumps," Kennecott Interoffice Memorandum, Salt Lake City, Utah.

Grubaugh, P., (1976), "5960 Dye Staining Test," Interoffice Letter, Utah Copper Division, Salt Lake City, Utah.

Gupta, U.K., and Gauna, M., (1976), "UCD Waste Dump in Situ Permeability and Oxygen Temperature Investigation," Metal Mining Division, Salt Lake City, Utah.

Hoek, E., "A brief history of the Hoek-Brown failure criterion," Rocscience, June 2002.

Jueschke, A.A., (1974), "Size Analysis of Waste Rock on Blue Water No. 2 Dump," Kennecott Research Center, Salt Lake City, Utah.

Klinger, P.B. and Schlitt, W.J., (1978), "Mineralogical Study of Samples Recovered" By the Westinghouse Becker Drilling Program on UCD Dumps," Technical Report No. RTR 77-15, Kennecott Metal Mining, Salt Lake City, Utah

Lannacchione, A.T. and Vallejo, L.E., (1995), "Shear Strength Evaluation of Clay-Rock Mixtures," Proceedings of the 35th Symposium on Rock Mechanics," Tahoe.

Leps, T.M., (1970), "Review of Shear Strength of Rockfill," Soil Mechanics and Foundations Division, ASCE, July 1970, pp. 1159-1170.

Logsdon, Mark, J., (2005), "Long term stability of Waste-Rock Stockpiles", draft memorandum, Sept ember 2005.

Malouf, E.E., (1972), "The Plugging of Leaching Columns by Precipitation of Basic Iron Sulfate Salts, Inter-Office Memorandum, Salt Lake City, Utah.

Ream, B.P., (1975), "Freeman Dump Staining Test," Interoffice Letter, Kennecott Mine, Salt Lake City, Utah.

Ream, B.P. to Davey, R.K., May 14, 1982, Internal Confidential memorandum entitled, "Consist Study – UCD Modernization Study.

Robertson, A. "The effects of alteration and weathering of mine slopes and waste rock piles: implications for long-term management," AIME 2005 annual meeting, Salt Lake City.

Stephens, J.D. and Abou-zied, S., (1971), "Rock Characteristics and Mineralogy of UCD Freeman Dump" Technical Report, Salt Lake City, Utah.

Stephens, J.D., (1971), "Study of Copper Mineralization in Eleven Samples of Waste From UCD Keystone Dump", Kennecott Copper Corporation, Salt Lake City, Utah.

TECHNICAL MEMORANDUM

DATE: 10 January 2006 (Updated: 06 August 2009)

TO: **Glenn Eurick (KUC)**

FROM: Mark J. Logsdon (Geochimica)

SUBJECT: **LONG-TERM STABILITY OF SOUTHERN WASTE-ROCK STOCKPILES: PHASE I GEOCHEMISTRY**

cc: **C Kaiser (KUC); Z. Kenyon (KUC); J. Pilz (Rio Tinto T&I); Z. Zavodni (Rio Tinto T&I)**

BACKGROUND

Kennecott Utah Copper Corporation (KUCC) wishes at this time to evaluate the Bingham Canyon waste-rock stockpiles with respect to two major issues:

- What infiltration through the stockpiles to their base is expected?
- What geochemical processes are occurring in the stockpiles that could affect slope stability, and are the rates and extents of these processes sufficient to significantly affect slope stability over reasonably foreseeable periods of time?

In 2001, a geotechnical engineer working on rock-pile issues in New Mexico hypothesized that chemical and physical weathering reactions, particularly accelerated attack by acid-rock drainage (ARD), could adversely affect long-term rock-pile stability. The mechanisms conjectured include:

- Diminution of particle size (by either physical or chemical processes), leading to a loss of internal friction
- Conversion of rock-forming minerals, especially feldspars, to clay minerals, producing zones of low shear strength and potentially high pore-water pressure.

Purpose and Objectives

The purpose of this memorandum is to address the status of the geochemical investigations and evaluations of conditions in the Southern rock piles (focused on detail investigations in the Castro dump) at the level of the Phase I investigations. The hydrogeologic and geotechnical conditions are addressed by others.

Specific objectives of the memorandum include:

- Describing the new geochemical investigations on the Castro stockpiles and their results to date;
- Reviewing the relevant geochemical information from other Kennecott technical studies and other relevant studies of waste-rock stockpiles;
- Synthesizing the historic and recent data to the extent practicable;
- Interpreting the geochemical results in terms of potential impacts to slope stability;
- Recommending further work that may be necessary to reduce uncertainties with respect to the magnitude and timing of geochemical impacts, for both the stockpiles currently studied and for others that have not yet been evaluated.

ISSUES

- What is the nature and extent of geochemical reactivity within the KUCC stockpiles?
- What is the likelihood that geochemical reactions would adversely affect the slope stability of the KUCC stockpiles?
- If adverse outcomes were possible, what are the time frames over which such adverse outcomes might be expressed?
- Are positive outcomes possible due to geochemical reactions, and, if so, over what time frames?
- What geochemical work remains to be done to better define and constrain the risk of adverse impacts on slope stability due to geochemical reactions across the full spatial range of KUCC waste-rock stockpiles?

TECHNICAL APPROACH

Phase I geochemical activities followed three principal tracks:

1. Collection and preliminary geochemical analyses of samples from a suite of test pits.

2. Compilation and critical review of existing Kennecott and contractor studies addressing geochemical and mineralogical aspects of the dumps.

3. Evaluation of the rates of geochemical reactions and their implications for in-situ weathering in the rock piles.

METHODS AND PROCEDURES

Test Pits and Screening-Level Analyses

In early April 2005, KUCC excavated 8 tests pits for the combined infiltration and shallow-geochemical studies. Test Pits 6, 7, and 8 were excavated on the Castro Stockpile, part of the South End Waste Rock Dump complex. The pits were excavated using a KUCC track-

hoe, following standard KUCC construction methods to maintain safety. Vertical faces were limited to 4 feet, separated by benches of 5 feet.

Eight (8) samples for geochemical analysis were taken from the three Castro pits. The samples were collected by a trained professional geologist and logged and photographed in the field. After initial characterization, five of the Castro samples were split into two size fractions (> 6mm and < 6mm) and tested on both a whole-sample and a size-fraction basis, producing a total of 13 Castro samples for geochemical analysis, plus field measurements of paste pH and Conductivity on the eight original Castro samples.

The as-received samples (and also the size splits) were tested for paste-pH and paste-conductivity, modified Sobek acid-base accounting (ABA), and single-addition Net Acid-Generation (NAG) tests. All analytical methods were those standardized by KEL. Three samples were sent to Leslie Research and Consulting (Tsawwassen, BC) for petrographic and mineralogical evaluation. The petrographic evaluations included optical (binocular examination of clasts and transmitted and reflected light microscopy of thin sections), X-ray diffraction (XRD) analysis, and scanning-electron microscopy with energy-dispersion analysis (SEM-EDS) to confirm mineralogical identifications.. The paste measurements assess current acid-base balance within and across pits. The ABA and NAG data address the potential for additional geochemical reactivity within these reaches of the stockpiles. The mineralogical evaluations explain the nature of secondary minerals (e.g., cements) and illuminate the mineralogical basis for the current and future acid-base conditions.

Although the eight test pit samples represent a limited database, the observations and findings are consistent with information and data obtained from previous studies, our understanding of dump leaching operations at Bingham Canyon , and other studies of mined-rock piles.

Document Review

KUCC and contractors on the team identified 19 historical KUCC studies that were relevant to the Phase I activities. Five (5) of these, four dealing with mineralogy (including paste-pH characteristics) and one reviewing the physico-chemical basis for heap leaching, were directly relevant to geochemistry. In addition there was relevant information, for example, on particle-size distributions, permeability measurements, and soils/foundation conditions in other reports, also. The internal reports most important for the geochemical evaluations included

- 1971, Freeman [J.D. Stephens and S. Abou-Zied, Rock Characteristics and Mineralogy of UCD Freeman Dump. MMD-RD TR 71-24]
- 1971, Keystone [S. Abou-Zied, Study of Copper Mineralization in Eleven Samples of Waste from UCD Keystone Dump. MMD-RC Interoffice Memo]
- 1971, Midas [Rock Characteristics and Mineralogy of UCD Midas Dump. MMD-RD TR 72-16]

- 1978, Westinghouse drilling program [P.B. Klinger and W.J. Schlitt, Mineralogical Study of Samples Recovered by the Westinghouse Becker Drilling Program on UCD Dumps. MMD-RC RTR 77-15]
- 1973, Theoretical review [L.M. Cathles, An Analysis of the Physics and Chemistry of Waste Dumps. Ledgemont Laboratory TR C-365 I]
- 1994(?), B.P. Ream and W.J. Schlitt, Kennecott's Bingham Canyon Heap Leach Program. Part I: The Test Heap and SX-EW Pilot Plant. [Undated and unlabelled internal report. There is a 1994 inter-office memorandum from B.P. Ream to R.K. Davey on the SX-EW Pilot study that is the basis for estimating the date of this report.]

A new report on the mineralogy of samples from this investigation has been produced:

- Jambor, J.L., 2005. Mineralogy of Oxidation Products in Bingham Canyon (KUCC) Waste Rocks. Contractor report to Geochimica, Inc. October, 2005. [Electronic copy on file with D. Cline (RT-TS) and Geochimica].

In addition to the KUCC documents, we reviewed other published literature on waste rock geochemistry, particularly that related to (a) porphyry-copper and porphyry-molybdenum systems and (b) experimental and field-scale data on weathering rates. Important work in the published literature included:

- Cathles, L.M., 1994. Attempts to Model Industrial-Scale Leaching of Copper-Bearing Mine Waste, in C.N. Alpers and D.W. Blowes (eds.) Environmental Geochemistry of Sulfide Oxidation, American Chemical Society Symposium Series 550, p. 123-131.
- Ludington, S.D., G.S. Plumlee, J.S. Caine, D. Bove, J.M. Holloway and D.E. Lowe, 2005. Questa baseline and pre-mining ground-water quality investigation. 10. Geologic influences on ground and surface waters in the Red River watershed, New Mexico. U.S. Geological Survey Scientific Investigations Report 04-5245.
- Wels, C, R. Lefebvre and A.M. Robertson, 2003. An Overview of the Prediction and Control of Air Flow in Acid-Generating Waste Rock Dumps, Proceedings, 6th International Conference of Acid Rock Drainage, Cairns (QLD), Australia, p. 630-650.
- White, A.F. and S.L. Brantley, 1995. *Chemical Weathering Rates of Silicate Minerals.* Mineralogical Society of America, Reviews in Mineralogy, vol 31.

We also considered the October 2005 presentations at the Geological Society of America (2005 annual meeting) Theme Session (Number 175, 18 October, 2005) entitled "Mine Rock Piles and Pyritically Altered Areas: Their Slope Stability and Effects on Water Quality" (GSA, 2005). The most relevant geochemical information was presented by Campbell et al (2005), which showed that the jarosite forming in natural weathering of Quartz-Sericite-Pyrite altered volcanic rocks at Questa, NM were 300,000 – 1.8 million years old.

Geochemical Evaluations of Rates and Impacts

Working from literature values, we have made some preliminary calculations of weathering rates (especially rates of generating clay minerals from primary alumino-silicates) and tried to relate them to the observed weathering in KUCC stockpiles. In doing this we follow, in part, screening approaches suggested by Lasaga (1998) and Jambor et al. (2000), and in part a numerical modeling approach suggested by Bethke (1996; 2005) as it might be applied to the KUCC rock piles. The numerical modeling uses both full equilibrium and kinetic models of the geochemical interaction between acidic infiltration and "granitic" rocks.

PHASE I GEOCHEMICAL RESULTS

Field information, acid-base accounting data and mineralogical results are available in the contractor reports (too large to make a credible attachment) on file with Rio Tinto or from Geochimica. The key findings from the geochemical testing for the Castro stockpile to date include:

- In the Castro pile, cap-rock and test pits containing predominantly intrusive rock have low pH and elevated conductivities. However, Test Pit TP06 was excavated into predominantly calc-silicate rock, and below the intrusive cap the pH of this material remains circum-neutral (pH 6.88-7.6), and the conductivity values fall toward the low end (near 2,000 uS/cm) for all samples tested.
- When the samples are split into size fractions, the finer fraction (silt and smaller-size) has lower pH and generally somewhat higher conductivity.
- The bulk-sample paste-pH values measured immediately after excavation tend to be distinctly lower paste-pH and paste-conductivity values than those measured several weeks later. The reasons for these trends are not known at this time. Jambor (2005) reports that no additional minerals precipitate during air drying of samples, so precipitation of soluble salts during evaporation does not seem a likely cause. Perhaps there has been some precipitation of low-solubility phases that incorporate some of the labile acidity, as for instance hydronium (H_3O^+) ion in jarosites that do not re-dissolve in the paste procedure.
- Although moisture contents below the very-near-surface of the pile were low and the system was entirely unsaturated, in the Keystone dump there is moist, warm to hot air venting upward through coarse layers in the waste rocks. Some vents reach the dump surface on Keystone, where they appear as water-vapor "fumaroles" on cool days. Such temperatures or evidence of warm-air movement was not seen in Castro during the 2005 field work.

The mineralogical evaluation (Jambor, 2005) includes the following key results, focusing on the Castro samples:

- The samples from Castro includes not only quartzite and intrusive, but also a significant fraction of carbonate-bearing calc-silicate.

- The only secondary minerals that appear as coatings and cements are jarosite [(K, $H_3O^+)Fe^{III}(SO_4)_2(OH)_6$][1] and gypsum ($CaSO_4 \cdot 2H_2O$). Although very tiny amounts can be identified in SEM-EDS investigations, the effective absence of goethite (FeOOH) or its predecessor, ferrihydrite ($Fe(OH)_3$) is noticeable. There is no significant difference between the jarosites in the leached sample from Code 51 and the jarosite in the unleached samples form Keystone and Castro.

- Limestone remains inside partially skarnified clasts in the Castro sample. This is consistent with the measured Neutralization Potentials. In Castro samples containing the <u>calc-silicate</u> clasts, the paste-pH values are all close to pH 7.

- There are no identifiable examples of either newly-formed clay minerals or secondary, amorphous silica, even in the samples with circum-neutral paste pH and observable limestone in the calc-silicate matrix. There are rare clay minerals in some of the intrusive fragments, but these appear to be hypogene hydrothermal minerals that do not reflect clay generation in the pile after mining. The only silicate mineral that shows alteration is biotite (a hypogene phase), which is transformed to an interlayered mineral, called "hydrobiotite", that has alternating layers of biotite and K-free vermiculite. The incongruent leaching of K form biotite is the source of the K^+ ions that now reside in the jarosite. Where biotite is absent in clasts, the jarosite is either a mixed K^+ - H_3O^+ or a true hydronium jarosite.

The mineralogical results for the 2005 samples are consistent with the observations of jarosite dominance and lack of evidence of newly-formed clays in the 1970's studies by Kennecott.

RESULTS OF THE LITERATURE REVIEW

During the 1970s (particularly), Kennecott staff extensively reviewed the geochemistry and hydrology of the rock piles in order to understand how to optimize leaching. The leaching process was based on reacting strong acids with the rock piles at rates that greatly exceed similar reactions occurring as a result of natural ARD (Acid Rock Drainage). The increased rate of reaction (compared to meteoric conditions) arises from two factors:

- The lower pH and much higher total acidity of the leach solutions compared to meteoric solutions;

- The much higher, and more consistent, application rate of leach solution compared to natural infiltration through the piles.

Key results from geochemical and mineralogical evaluations (especially of the Freeman, Midas and Keystone piles – those investigations did not significantly address the limestone-bearing southern rock piles because they were not suitable for leaching because of their high carbonate content) in the 1970s include:

---

[1] True jarosite contains K; the hydronium-substitution is well known mineralogically, but requires a low-potassium and high acidity system and is rare in most mine-waste systems. The significance of hydronium jarosite is discussed below.

- Paste-pH values ranged from about 2 to about 4, with average values near 3.5, and paste-conductivity values were in the range of several thousand uS/cm. These values are indistinguishable from values obtained in 2005 outside the calc-silicate zone of Castro.
- There were zones within the rock piles with ambient temperatures up to 130 F (50 C), and oxygen contents approached atmospheric levels (15%-20% of total air volume) throughout much of the pile and were detectible (at up to 3%) everywhere tested. These results imply a well-oxygenated pile in which sulfides (especially pyrite) are actively oxidizing to produce the observed heat.
- The principal secondary minerals were jarosite and gypsum, again identical with the 2005 results. [One of the early mineralogical reports discusses clay minerals (especially kaolinite) and amorphous silica in "clay-rich" matrix surrounding some lithic clasts, but the X-ray diffraction, optical, and microbeam reports do not identify these as newly formed, and the text makes a point of stating that the mineralogy of the rocks at the time they were deposited is not known, so the clay minerals cannot be shown to be newly formed.]
- Carbonate minerals were entirely absent from all leached rocks. This also is the observation in the new 2005 work., however limestone was clearly present in some Castro samples in the Southern Rock Pile complex

There are some important results in the older work also in terms of hydrogeology and geotechnical parameters. The significance of these for infiltration will be addressed primarily by others, so this discussion will focus on results potentially important for geochemistry.

- There is a bimodal distribution of particle sizes in the 1970s studies, with a large portion of the tested samples having lower hydraulic conductivities [$K < 10^{-3}$ cm/s; (k < 1 darcy)], whereas other portions represented gravel or larger-sized coarse zones with very high hydraulic conductivities [$K > 1$ cm/s; (k> 1000 darcy)]. In all three leach dumps, 10% - 20% of the particles pass the 200 mesh (and are called "slimes" in the early reports, based on an operating term appropriate to tailing). Hydraulic conductivities in these materials probably would be about 10^{-5} cm/s to 10^{-6} cm/s (k = 1 millidarcy) or less. It seems likely, based on both the site-specific mineralogical analyses and observations in other mine sites, that the fines represent hypogene mineral phases, which may have, in part, migrated through the coarser layers to accumulate with other, finer material (silty-sand sized layers) during settling and infiltration.
- In 1982, KUCC conducted a particle-size distribution study for run-of-mine rock. This study found that only a few percent (certainly < 5%) of the tested samples passed the 200 mesh. Although it is not entirely clear that the run-of-mine rock that reported to the Southern dumps prior had the same particle-size distribution as the samples tested in 1982, there is no reason based on the lithologies to expect much higher fines content, and the available data indicates that the clay-sized fraction is sufficiently small that it would be unlikely to influence the bulk mechanical behavior of the rock pile..

The bimodal permeability structure is the macroscopic fluid-phase expression of the alternating coarse- and fine-layering seen in the piles when they are excavated. This permeability contrast controls the flow of air and heat primarily through coarse layers and fluids migration predominantly in the fine layers as a consequence of the basic physics of fluid flow in porous media under unsaturated conditions.

DISCUSSION

Geochemical Reactivity

There is a body of geochemical data, especially in seepage water-quality, that shows that the rock piles, both those that have been leached and those that have not, are geochemically active. The 2005 observation of residual pyrite in waste-rock samples that have no residual neutralization potential (outside the Southern rock piles) implies that the observed pyrite oxidation that leads to the low-pH conditions will persist well into the future.
The observation, consistent from 1971 to present, that the majority of the secondary minerals produced by reactions in the Kennecott rock piles is jarosite and gypsum, and the absence of carbonates in non-calc-silicate rocks, implies that the principal reactions are:

- Oxidation of pyrite (FeS_2) to release Fe and S that oxidize to Fe^{3+} and SO_4^{2-}. Pyrite oxidation is acid-generating. In addition, the recycled leach solutions contained abundant additional Fe^{3+}, added to the solutions in the Precipitation-Plant reactions. An important matter is understanding the point made by Cathles (1973) that the principal oxidant of sulfides in the piles is Fe^{3+} ion, and that the principal role of the high oxygen levels within the pile is to ensure that the dissolved iron will be maintained overwhelmingly in the Fe^{3+} (ferric) state.

- Incongruent dissolution of biotite to hydrobiotite releases K^+ to pore waters. The oxidation reactions are sufficient to form pH conditions low enough to stabilize jarosite [$(K, H_3O)Fe(SO_4)_2(OH)_6$] instead of ferrihydrite [$Fe(OH)_3$] (see Figure 2). Where there is sufficient K^+ locally available, the jarosite is a classical K-jarosite. Where K is deficient, the pH is sufficiently low to allow abundant H^+ ions to react with water to produce the hydronium (H_3O^+) seen in the hydronium jarosites documented in Jambor (2005). A significant feature of the geochemistry of all Kennecott dumps examined to date is that jarosite, not ferrihydrite, dominates the iron precipitates that form cements and coat clasts.

- Dissolution of calcite ($CaCO_3$) by the acidity generated form sulfide oxidation to eliminate the original carbonate minerals and provide the Ca^{2+} that is now present in newly formed gypsum ($CaSO_4 \cdot 2H_2O$).

- Although one early report (the 1971 Freeman report) qualitatively described kaolinite and amorphous silica in the leach dumps, this was not confirmed in the mineralogical reports, and the 2005 sampling did not identify any clay minerals that were formed in place. The 1971 report concluded that the kaolinite and other clay

minerals in the pile probably were largely if not entirely hypogene and unrelated to any geochemical reactions within the pile after mining.

Figure 1 outlines the major stability fields of secondary minerals and fluid compositions in terms of pH and oxidation state, in the familiar Eh-pH diagram (e.g., Bethke, 1996).

Figure 1 Eh-pH Diagram for Relative Stability Fields of Jarosite, Ferrihydrite, and Pyrite
(Figure calculated in Geochemist's Workbench, Rel 6.0, Bethke, 2005)
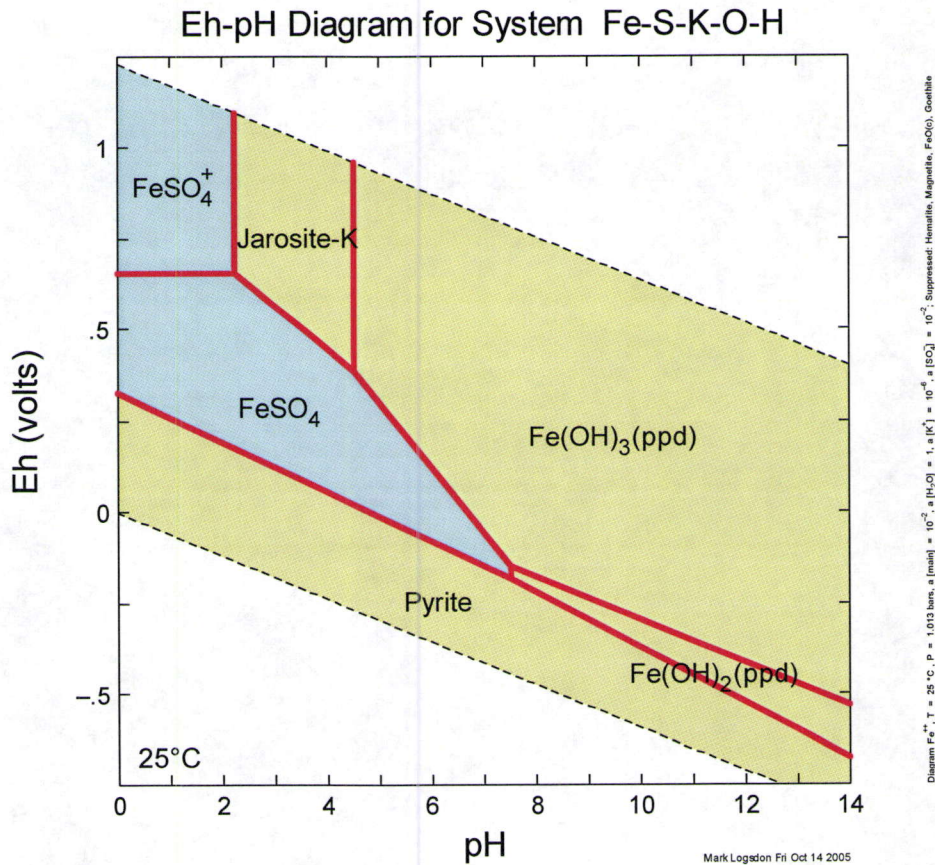
Jarosite is stable under highly oxidizing conditions and pH values between about 2 and 4.5.
Ferrihydrite ($Fe(OH)_3$ is stable at higher pH. Goethite (FeOOH), is an aged, dehydrated
iron hydroxide phase that would form over long time periods, ultimately encompassing the
field of both ferrihydrite and jarosite (Jambor et al., 2000). Calcite, the major mineral in
limestone, is unstable at pH below 6, so a system precipitating jarosite must be dissolving
calcite. The iron disulfide, pyrite, is stable only under reduced conditions. In the waste-rock
pile, which is well oxygenated, pyrite oxidizes, with the iron ultimately reporting to a
secondary hydroxysulfate (jarosite) or hydroxide (initially ferrihydrite).

Reaction Rates and Implications for Dump Stability

Excluding small-scale unraveling and shallow slips near dump toes, dump-stability issues at
Bingham Canyon have been associated with fluid management in the leach systems
(Pennichele, A.D. and M.B. Kahle, 1971. Stability of Waste Dumps at Kennecott's Bingham
Canyon Mine. Transactions of AIME, vol. 250, p. 363-367). The dumps have histories
extending back prior to 1930, so there is at least a 75-year history that shows that the
conjecture of geochemical instability is not significant to time periods on the order of 100

years, so long as fluids are well managed (or the piles are not leached, for example the Castro rock pile). It is worth looking into the fundamental controls that may explain this and trying to estimate some rates for important reactions that may help estimate the long-term stabilities.

One may analyze the basic conditions for slope stability in terms of shear strength:

$$\tau = c + (\sigma_n - p_u)\tan\phi$$

where τ = shear strength
c = total cohesion,
σ_n = normal stress
p_u = water pressure
ϕ = friction angle

[W. Wilson, personal communication, 2005]. The cohesion term (which could, in principle, be measured in intact samples at ambient moisture content) can be divided into a "true" cohesion term encompassing adhesion, cementation and the effects of stress history, and an "apparent" cohesion due to matric suction in unsaturated materials.] The two critical geomechanical parameters, then, are friction angle and cohesion. It should be noted that conventional slope stability analyses generally ignore cohesion entirely and conservatively assess stability in terms of friction angle alone. However, a notable feature of several of the KUCC leach dump is that they have cemented into ferricretes[2] that are so strong, that, at least in some cases, they must be blasted to move the pile (Pennichele and Kahle, 1971; Z. Zavodni, personal communication, 2005; V. Peacey, personal communication, 2005.). In other dumps, the cements exist only as a thin crust on dump surfaces (J. Pilz, personal communication, September 2005), and some dumps can be excavated without blasting (B. Vinton, personal communication, 2005).

Friction Angle and Geochemistry

Friction angle will be a function of particle size, particle interlocking (density) and shape. Processes that would tend to reduce particle size (e.g., conversion of feldspars to clay minerals) or that would tend to smooth rough surfaces would tend to reduce friction angle, and therefore move a pile that originally was stable due to friction alone toward a state of instability. This is the essence of the geochemical-instability conjecture.

The question then arises: at what rates would one expect rock-forming minerals to dissolve? This has been a very active area of geochemical research in the past 10 – 15 years. A useful summary is presented in Lasaga and Berner (Lasaga, A.C. and R.A. Berner, 1998. Fundmental aspects of quantitative models for geochemical cycles. Chemical Geology, vol. 145, p. 161-175.) and reproduced here as Table 1.

---

[2] "Ferricrete" refers to a material, visually similar to concrete, in which clasts (the "aggregate") is cemented by an iron-rich matrix. In the general case, that matrix can be ferrihydrite ($Fe(OH)_3$, goethite ($FeOOH$),or jarosite ($KFe(SO_4)_2(OH)_6$. In the Bingham Creek piles, the cement is primarily jarosite.

Table 1 Mean lifetime of a 1 mm crystal at 25C and pH 5 (minerals directly relevant to
Bingham waste rock highlighted)

Mineral	Lifetime (year)		Mineral	Lifetime (year)
Calcite	**0.43**		**Albite**	**575,000**
Wollastonite	**79**		**Microcline**	**921,000**
Forsterite	2300		**Epidote**	**923,000**
Diopside	**6800**		**Muscovite**	**2,600,000**
Enstatite	10,100		**Kaolinite**	**6,000,000**
Sanidine	291,000		**Quartz**	**34,000,000**

The minerals considered by Lasaga and Berner were pure minerals. If, in a mineral deposit
such as Bingham Canyon, some of the minerals had been affected by hydrothermal
conditions prior to mining, it could be that their dissolution behavior would be different
from that considered by Lasaga and Berner. Additionally, reaction rates would be slightly
higher at 50 C and at pH 3.5 than those considered in the original study.   It should be
noted, however, that in Jambor's detailed evaluation of current samples (Jambor 2005), he
found no evidence for alteration of any hypogene phase except biotite. In any event, the
relative rates would remain the same, and even if the rates were 10 times higher, the basic
information remains the same. The most important features of this table are:

- The only fast-reacting (less then several decades), rock-forming mineral is calcite.
  This is expected to be the case also at Bingham, based on the mineralogy of country
  rocks and intrusives.
- Skarn minerals known at Bingham include wollastonite and diopside, and the
  reaction rates for these are long compared to calcite. Therefore clasts of calc-silicate
  rock may contain residual limestone that is protected against acid attack by the rind
  of skarn minerals (see Jambor 2005 for an example from Castro dump).
- The principal rock-forming minerals of the intrusive rocks and quartzite would not
  be expected to dissolve in any time period of interest to this evaluation.

In summary, except in limestone-rich rocks that may come in contact with ARD, large-scale
dissolution, sufficient to reduce friction angles significantly in the rock-forming minerals at
Bingham would require tens to hundreds of thousands of years. Where carbonates are
present, as in the calc-silicate rocks at Castro in the Southern complex, the natural acidity
(these were not leached) would be neutralized and all reactions would be very slow.
Certainly, coarse-rock zones in the piles would be almost entirely unaffected, unless the
clasts were limestone that is not rimmed with skarn. Supporting this long time frame,
radiometric dating of weathering minerals (jarosites) in naturally weathered Quartz-Sericite-
Pyrite altered igneous rocks at Questa, NM show that the alteration process there has taken
300,000 to 1,8 million years to produce the natural "scars" seen on the sides of the valley
there (Campbell et al., 2005).

Cohesion and Geochemistry

The most extreme cohesion seen in rockpiles arises from the precipitation of secondary cements in open pore space. This is very evident in the calc-silicate zones of the Castro rock pile, where jarosite has completely filled the open pore space, producing a "ferricrete": a ferric-iron cemented material that resemble concrete, in which the "aggregate" is the pre-existing rock fragments of what was a porous medium. The effect is striking in Figure 2 (from Jambor, 2005).

Figure 2 Cementation (as ferricrete) of limestone clasts by jarosite (reddish-brown) in Castro Dump ['puck' diameter ~32 mm]

 A ferricrete such as illustrated in the two clasts on the left side of Figure 2, must be sawed with a diamond blade or broken by percussion with a heavy hammer

The sort of cementation seen in Figure 2 is not limited to Castro. Other parts of the leach dumps, which were under leach for decades, have yet more extensive cementation, as shown in Figure 3. As discussed above, in some places in the leach dumps, the cementation is sufficiently robust that, if the dumps need to be deconstructed, drilling-and-blasting is required, as has been observed recently on historic dumps rimming the east, west and northwest walls of the Bingham pit, and some faces of up to 50 feet remain vertical after excavation (V. Peacey, personal communication, 2005).

Figure 3 Major zone of ferricrete cementation in West-Side leach dump (Photo is courtesy of Z. Zavodni, RT-T&I, 2005)

The leach solutions used by KUCC were a very advanced form of "acid-rock drainage": low-pH, high-iron; high sulfate solutions derived, ultimately form pyrite oxidation in the rock piles themselves. The mineralogy, based on X-ray diffraction and scanning electron microscopy as well as by standard methods of optical petrography, of the cements examined in 2005 (and as described in the 1970s) is essentially identical whether the rocks have or have not been leached. Therefore, it is geochemically reasonable to infer that the process of cementation seen in the leach dumps also would occur in the non-leached dumps, although the extent of iron precipitation in the leach dumps is related to the very high concentrations and large total mass fluxes of iron in those systems during the leaching history. There are some bounding calculations that one can use to assess the differences between the leached and unleached dumps and to assess whether, and when, an unleached dump can achieve the degree of cementation seen in the leach dumps.

The amount of jarosite present as a cement in a dump is a function of the amount of iron and sulfate that has flowed through that pore space, because there is 1 mole of Fe and 2 moles of SO_4 for every mole of jarosite [$KFe(SO_4)_2(OH)_6$] present. Now, the flux of Fe^{3+} and SO_4^{2-} through the forced-leach dumps is several orders of magnitude (probably >3 orders of magnitude) greater than in non-leached dumps. This arises from the high water application rates and the high concentrations typical of the recycled leach solutions. Cathles (1973) states that the application rate of leach solution on the full-scale Midas dump was about 0.25 gal/ft^2/hr[3], or 8.92E+1 m/yr (per m^2), which is about 2 orders of magnitude higher than the average annual precipitation (estimated at 700 mm). In fact, because the dump application was maintained as ponded water for long periods, the infiltration was probably another order of magnitude higher than that under natural conditions (estimated at about15% and certainly less than 30% of annual precipitation by M. O'Kane, personal communication, 2005). In addition, total iron concentrations in acidic drainage from porphyry-style rocks is usually around 100 mg/L (e.g., Plumlee, 1999), whereas the recycled leach solution would have been close to 10 g/L, and certainly above 1 g/L, so there would be another 1-2 orders of magnitude increase in flux associated with concentration alone. Thus, the flux of Fe^{3+} in the system while the rocks were under leach was probably 3 to 7 orders of magnitude higher than would be expected in the unleached rock piles, and this is the principal reason why there are extensive zones of dense, jarosite-rich ferricrete in the leach dumps, whereas cementation in the unleached zones that we observed in 2005 in Keystone and Castro were limited and somewhat ephemeral (except in the calc-silicate zones as shown in Figure 2).

In his 1973 paper, Cathles calculates a "characteristic time" for complete leaching of the Bingham dumps. The "characteristic time" is a concept derived from chemical engineering, where it represents the period required for full reaction in a given volume undergoing flow at a given average rate. Cathles' calculations, supported by laboratory and field-scale data,

---

[3] Cathles (1973) states that the application on the Midas test Pad was 0.26 gal/ft2/hr and that the application rate to the full-scale pile was 10 times higher.

showed that the characteristic time for UCD dumps under leach was about 380 months, or 30 years. Given that the flux rate of Fe^{3+} was very much greater than that expected for the non-leach dumps operating under meteoric flow, suggests that for natural meteoric conditions to approach those seen in a fully-leached dump (e.g., Figure 3) would require very long times.

Despite the likelihood that meteoric dumps would not achieve the degree of cementation seen in the leach dumps for very long times, the basic geochemical behavior is such that the dominant outcome is clearly a trend toward increased cohesion. The geochemical reactions that tend to increase cohesion by producing cements occur very much faster (weeks to months, as seen in the leach dumps during operations), compared to thousands or tens of thousands of years needed for dissolution to adversely affect internal friction characteristics of even fine-grained portions of the system.

CONCLUSIONS AND RECOMMENDATIONS

The principal conclusions of the Phase I study with respect to the Southern Rock Piles include:

- Rock piles are geochemically active and producing acidic drainage or locally (where limestone is present) neutralized but high TDS seepage that precipitates gypsum.
- Pyrite oxidation reactions will persist far into the future, probably hundreds of years or more, based on the amount of pyrite remaining and the oxidation rate of pyrite in air.
- There is no evidence from the new or old mineralogy reports that feldspars and other alumino-silicates are being converted to clay minerals at rates that lead to observable amounts of clay minerals in periods of several decades.
- There is active precipitation of secondary, cementing minerals, largely jarosite $[KFe(SO_4)_2(OH)_6]$ and lesser amounts of gypsum $(CaSO_4.2H_2O)$, in both leached (Code 51) and non-leached (Keystone and Castro) dumps.
- The mineralogy of the cements does not depend on the lithologies of the local clasts.
- The amount of cementation is greater in the leach dumps than in the non-leach dumps, because a very much greater flux of Fe^{3+} and SO_4^{2-} have passed through the leached dumps.
- There is no reason to expect that the ferric minerals precipitated in the waste-rock dumps would become chemically unstable and dissolve. They may convert over time to a more goethite-like ferric hydroxide $(FeOOH)$, but this is expected to occur over centuries or even longer and would leave the dumps still iron-cemented. Gypsum in very shallow zones may be subject to dissolution and re-precipitation cycles, during shallow infiltration events, but this is unlikely to be important more than a very few meters below ground surface.
- Because the geochemical processes and the initial rocks are identical mineralogically, the non-leach dumps will evolve toward conditions such as those seen in the leach dumps, i.e., increasing cementation (cohesion) over time.

- Dissolution of particles as a mechanism for grain-size reduction cannot occur at a rate sufficient to significantly reduce internal friction in the dumps over time periods on the order of hundreds to a few thousands of years, and probably would require tens to hundreds of thousands, or even millions of years.
- Therefore, we conclude that the geochemical trends in waste rock dumps, specifically including Castro and the other Southern Rock Piles, are toward greater stability, through addition of true cohesion, rather than toward instability due to particle-size reduction and loss of internal friction.

We recommend that the Phase I team and KUCC personnel meet to discuss the outcomes, conclusions, and limitations of the interim study and determine whether additional studies are warranted at this time. A further search for relevant in-house files is justified. Expansion of the program to other dumps on a near-surface basis could be accomplished with a scope very similar to that used in Phase I.

REFERENCES CITED

Bethke, C.M., 1996. *Geochemical Reaction Modeling*. New York: Oxford Press.

Bethke, C.M., 2005. *The Geochemist's Workbench, Release 6.0*. University of Illinois.

Campbell, A.R., Lueth, V.W., and Pandey, Shubha, 2005. Stable Isotope Discrimination of Hypogene and Supergene Sulfate Minerals in Rock Piles at the Questa Molybdenum Mine, New Mexico. GSA Program with Abstracts, 2005 Annual Meeting, 16-19 October, 2005, Salt Lake City, Utah, Abstract No. 175-5.

Cathles, L.M., 1973. An Analysis of the Physics and Chemistry of Waste Dumps. Ledgemont Laboratory TR C-365 I.

Geological Society of America, 2005. Program with Abstracts, 2005 Annual Meeting, 16-19 October, 2005, Salt Lake City, Utah.

Jambor, J.L., D.K. Nordstrom, and C.N. Alpers, 2000. Metal-sulfate Salts from Sulfide Mineral Oxidation, in C.N. Alpers, J.L. Jambor and D.K Nordstrom (eds.), *Sulfate Minerals – Crystallography, Geochemistry, and Environmental Significance*. Reviews in Mineralogy and Geochemistry, Vol. 40, p. 303-350.

Jambor, J.L., 2005. Mineralogy of Oxidation Products in Bingham Canyon (KUCC) Waste Rocks. Contractor report to Geochimica, Inc. October, 2005.

Lasaga, A.C. and R.A. Berner, 1998. Fundamental aspects of quantitative models for geochemical cycles. Chemical Geology, vol. 145, p. 161-175

Plumlee, G.S., 1999, The Environmental Geology of Mineral Deposits, in G.S. Plumlee and
M.J. Logsdon (eds), *The Environmental Geochemistry of Mineral Deposits*. Reviews in
Economic Geology, Vol. 6A, p. 71-116.

Additional citations, especially internal Kennecott documents, that were consulted, are cited
in full in the text.

RioTinto

Project code	12094	**Report number**	12094-02	**Version**	1.0

Technology and Innovation

Appendix D - Construction of the South KUCC Waste Rock Dumps Over Time

20 Oct 2009

Prepared for	C. Kaiser	**Author/s**	J. Pilz
Distribution	C. Kaiser, K. Payne, Z. Kenyon, M. Robothym		
Project manager		**Reviewer**	
	J Pilz		Z.M. Zavodni

Section 1 - Executive summary

This appendix places the construction of the South KUCC Waste Rock Dumps into a historical context by evaluating the progression of the dumps over time. By understanding the dump progression, subjective inference can be made of the materials placed in the dumps based on the geology of origin of those materials in the pit. The progression of the dumps elsewhere around the Bingham Pit also qualitatively attests to the historic stability of the dumps, as some of the dumps are now over 100 years of age and most dumps are older than 25 years before present. In comparison, the South dumps were placed beginning in about 1970's and have been incrementally added to since that time.

Contents page

List of figures

List of tables

Appendix D – Development of the KUCC Waste Rock dumps over time

D.1 Overview

This appendix summarizes a review of historic aerial photographs to trace the construction history of the KUCC waste rock dumps over time. The purpose of this work is to review the construction history of the dumps, understand the historic stability of the dumps and gain a perspective of the materials placed into the dumps.

As indicated in Appendix B, from the beginning of mining at the turn of the century to the late 1990's approximately 140 Billion tons of waste was moved and placed into dumps surrounding the pit. Large quantities of waste production began in the late 1940's and from the 1970's to 1980, waste production (stripping) was generating approximately 3 to 6 Million tons per year of overburden material.

Total overburden production estimated from ore produced and the stripping ratio is depicted on Figure D-1.
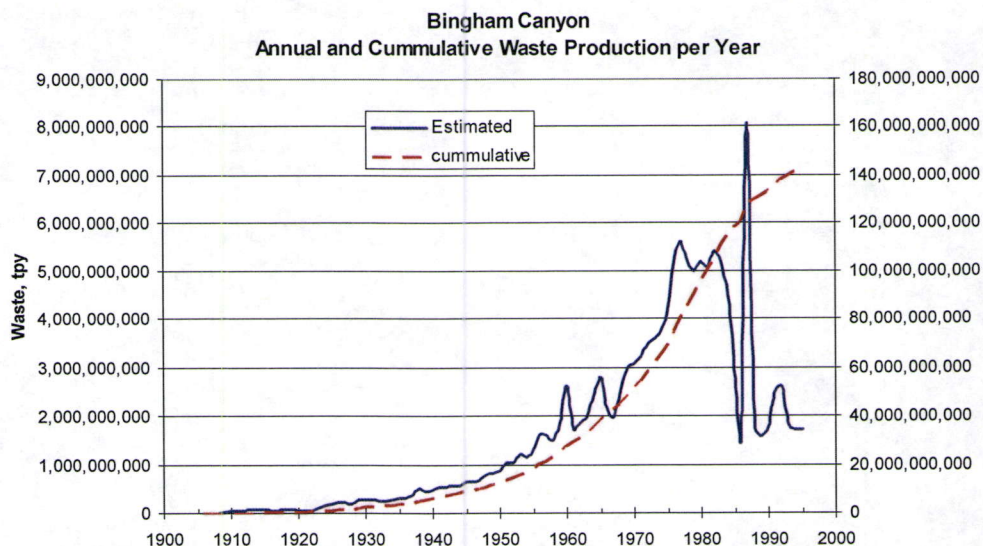
Figure D-1- Estimated Bingham Canyon waste production estimated from ore production and strip ratio (after Krahulec, 1997)

Information that may be obtained from the aerial photograph review includes the following:

- Dump progression (i.e. foot print crest / toe at various points in time). The advance of the dumps was mapped by identifying the toe of the dumps at approximately 10 year intervals in time.

- Approximate <u>material composition</u> can be estimated by reviewing the open pit foot print and making inferences about the general types of materials that were being mined and placed in the dumps. The dump composition information is supported by anecdotal information regarding the dump construction.

- <u>Leached areas</u>. The leached areas of the dumps (either by flooding or trickle irrigation) are quite apparent on aerial photography. These areas could be digitized and the dump areas that have been subject to leaching be determined.

D.2   Dump Progression

The principal drainages surrounding the Bingham Pit and dumps are as follows:

Table D.1– Summary of Dumps and Materials placed into them

Dump Group	Drainages Filled	Waste Materials Placed
North and West Pit Dumps	Markham Gulch	Primarily Quartzite with intrusives
	Cottonwood Gulch	
	Dry Fork	
	Freeman Gulch	
Bingham Canyon Dumps	Bingham Canyon	
Eastside Rail Dumps	Bluewater 1, 2 and 3	About 32 percent intrusives and 60+ percent quartzites, other minor constituents.
	Midas 1 and 2`	
	Congor 1, 2 and South Congor	
	Crapo	
Eastside Truck Waste Dumps	North Keystone and Keystone	Quartzites and intrusives
	Lost	
	North Copper and Copper	
South Dumps	Yosemite	Intrusives, quartzites and calc-silicates / limestones (these are

Dump Group	Drainages Filled	Waste Materials Placed
		primarily limestone dumps)

Historic aerial photographs were reviewed to determine the location of the dumps at approximate 10 year intervals. The approximate progress of the extent of the dumps in 10 year time increments was developed. The following figures show the dump progression overlying various base maps:

- Figure D-2 – Extent of dumps overlying USGS topographic maps.

- Figure D-3 - Extent of dumps overlying Bingham Mine generalized geology.

- Figure D-4 – Extent of dumps overlying a 1977 aerial photograph of the mine area.

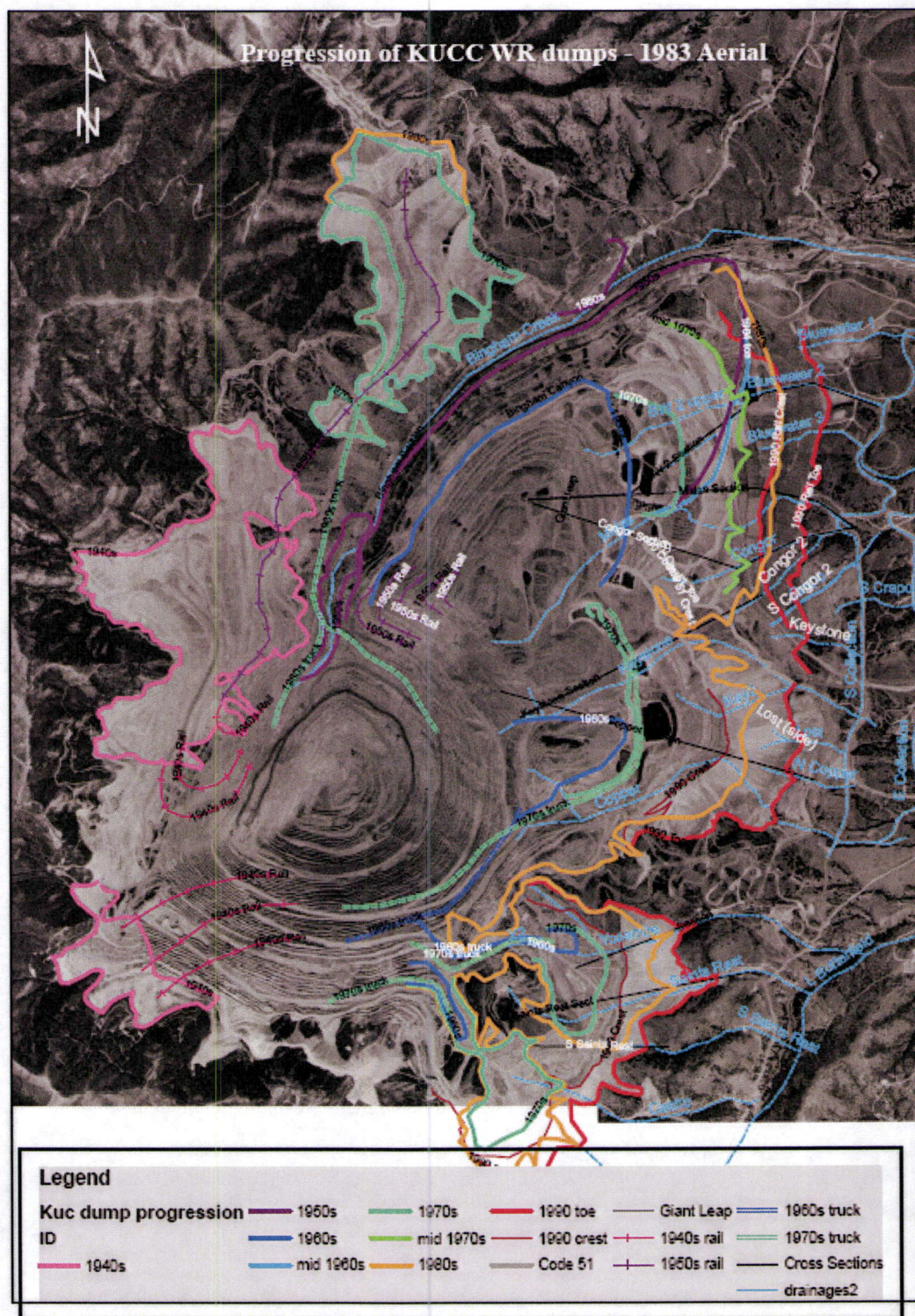- Figure D-5 - Extent of dumps overlying a 1983 aerial photograph of the mine area.

- Figure D-6 – Extent of dumps overlying underground mine workings.

Other combinations and permutations of the dump footprint overlying the original topographic maps, historic mapping by others and the other base maps can be generated within the GIS database used to develop these maps.

Table D.2- Summaries of the areas were materials were placed over time

Date Range	Location of Primary Waste Dumps	Color on Figures D-1 through D-5
Prior to 1940's (>70 yr old)	Markham (north) and west wall of pit [Note some of these materials were subsequently remined.]	violet
1940 to 1950 (60-70 yr old)	Along south slope of Bingham Canyon via rail	Purple
1950 to 1960's (50 – 60 yr old)	Extending outward from Bingham Canyon and around the East side via rail	Blue
1960's to 1970's (40 – 50 yr old)	Extending out from Yosemite notch and extending further south along the East side (rail and truck). Some waste being placed in Dry Fork	Green
Mid 1970's (~45 yr old)	Extending further out along North half of East Side	Light green`

1980's	High truck waste dumps established late in the 1970's	Yellow
(20 - 30 yr old)	immediately north of Yosemite Notch. Toe of East side rail	
	dumps was extended. South dumps were established.	
1990's	Material placed in Dry Fork Canyon and in South dumps	Orange
(10-20 yr old)		
2000	Bingham Canyon dumps developed	Not shown in color

In the 1940's, waste was hauled by rail to the west dumps and to the north (Markham Gulch) dumps. Old photos show railroad trestles, which were required to cross the former Bingham Canyon. The rail dumps were generally constructed from the bottom upwards using side dump rail cars. The dumps were essentially constructed in approximate 50 feet high lifts. Some of the waste was also hauled out the lower portion of Bingham Canyon and dumped along the side of the canyon.

Beginning in the 1950's, most of the waste was hauled down Bingham Canyon. The dumps were progressively advanced to the northeast until the mouth of the canyon was reached. Dumping subsequently "wrapped around" southward along the East side. Waste was placed in lifts and grade changes between loading and dumping were minimized. Dumps were terminated against major drainages. Acid leaching was initiated in 1965.

D.3 Progression of Dumps Over Time

The following figures show the approximate advancement of the dumps over time by depicting the approximate toe of the dumps in 10 year time increments.
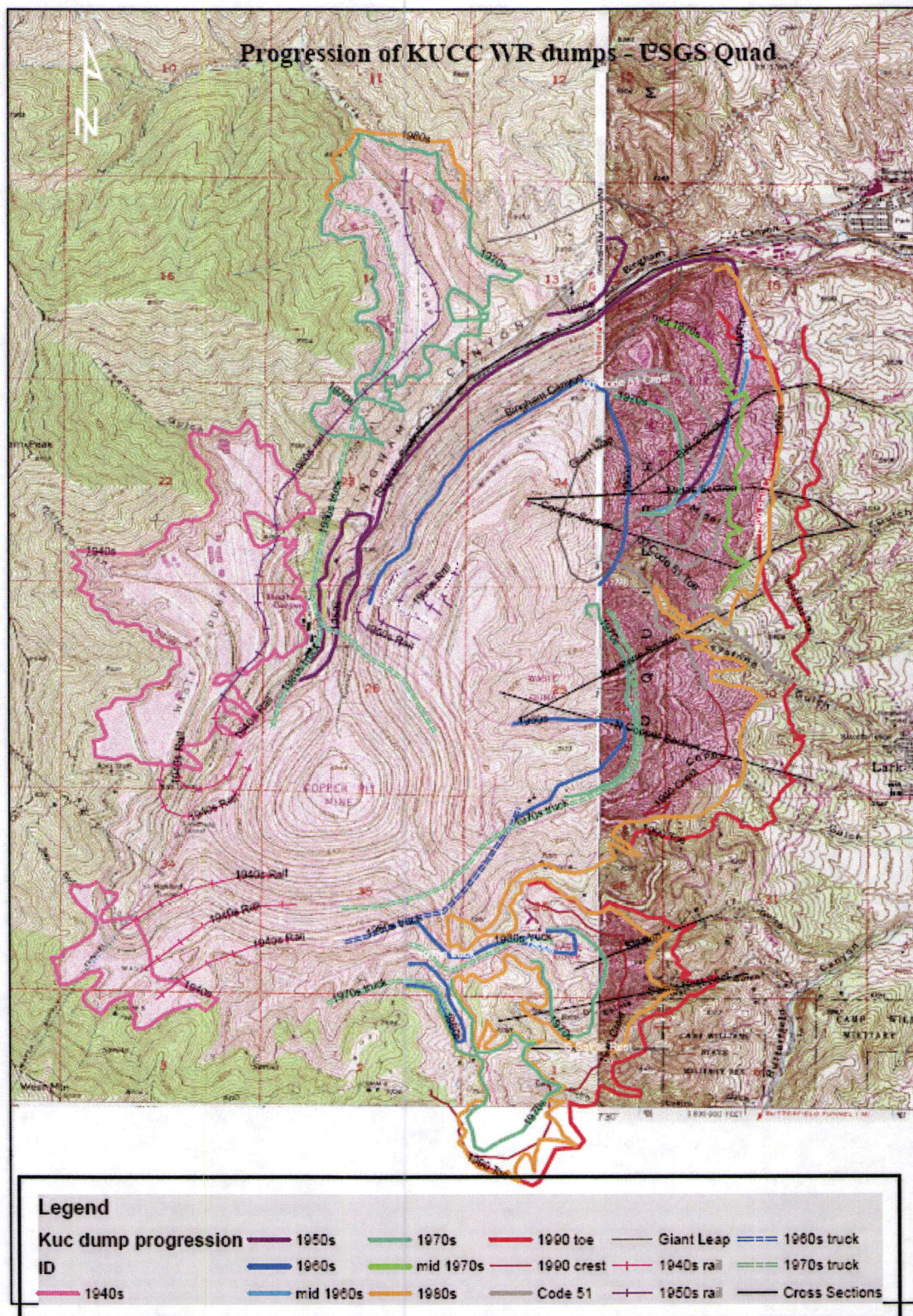
Figure D-2 - Extent of dumps overlying USGS 1980's topographic maps
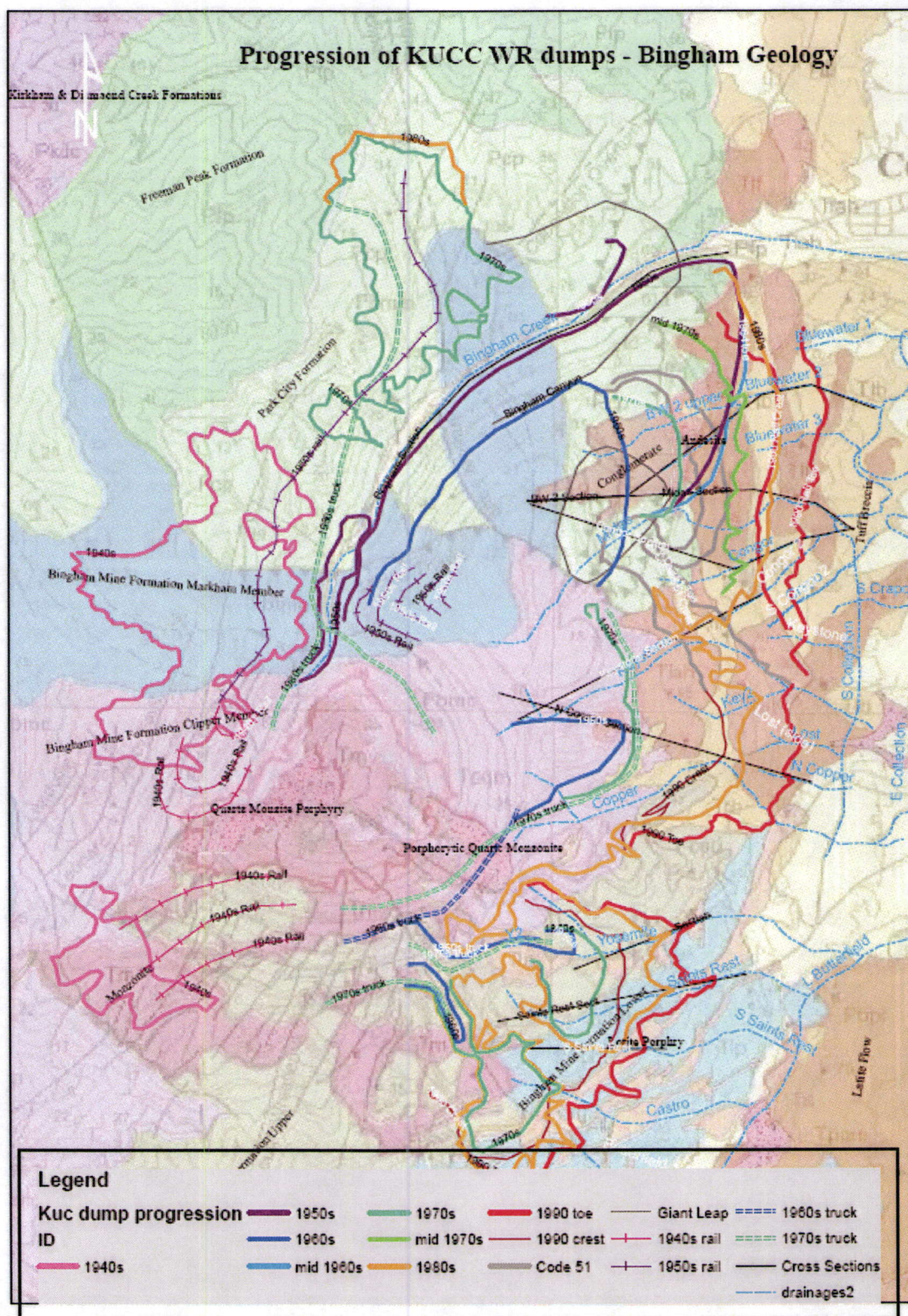
Figure D-3 - Extent of dumps overlying Bingham Geology dumps

Figure D-4 Extent of dumps overlying a 1977 aerial photograph of the mine area.

Figure D-5 - Extent of dumps overlying a 1983 aerial photograph of the mine area.
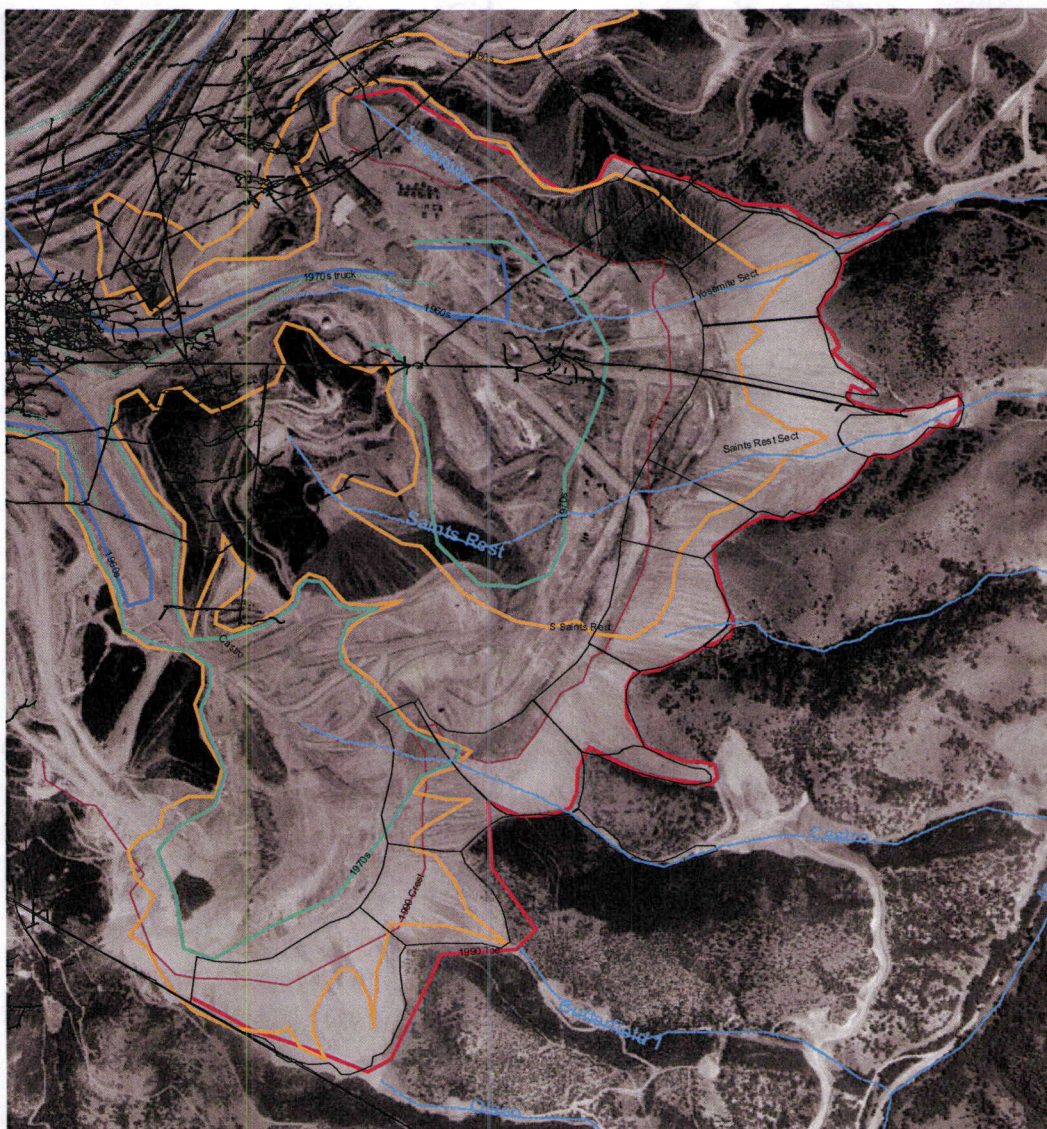
Figure D- 6 - Detail of progression of the South End dumps overlying historic underground workings

RioTinto

Project Code	12094	**Report Number**	12094-2	**Version**	1.0c

Technology and Innovation

Appendix F –

South End Dump Debris Flow Analysis

21 October 2009

Prepared for	Kelly Payne, KUCC	**Author/s**	J. Pilz
Distribution	C. Kaiser, Z. Kenyon, Z.M. Zavodni		
Project Manager		**Reviewer**	

_____   _____
J Pilz, PE, PG   Z.M.Zavodni, PE

Section 1 - Executive Summary

Project Purpose and Scope

Rio Tinto Technology and Innovation (T&I) was requested by KUCC to address the potential for debris flows to overtop the detention basins situated at the base of the South End drainages. This work involved a review of aerial photography, development of input parameters for utilizing Dan-W (a debris flow run out distance software package), completion of Dan-W analyses, development of alternative mitigation schemes and preparation of this summary report. This work was a follow up on effort to evaluate a debris flow that occurred on July 27th 2007 and is in response to a Notice of Violation (NOV) by the Utah Division of Oil, Gas and Mining (DOGM).

Findings

Dan-W analyses indicate that it is highly unlikely that debris flow events travelling down the dump face have or will overflow the catch basins as an intact debris flow. Parametric Dan-W analyses[1] indicate that there are few combinations of reasonable input parameters that would have caused the travel distance to exceed the basin location. In the case of the July 27, 2007 event, the most likely scenario is that the debris flow clogged the basin outlet, which subsequently caused silt laden water to overflow the basin. The parametric analyses found that for sediment to travel the distances observed the debris flow characteristics would need to change or the material must become highly fluid during its travel path. Since fine grain material has migrated off site on several occasions, the possibilities to explain this observation include:

- The debris flow filled the basin in the early part of a storm, either plugging the basin outlet or reducing the available storage for the storm event that subsequently occurred. Sediment-laden water then overtopped the basins.

- The debris basin was already full of water at the time that the debris flow occurred and the debris flow displaced the water causing the finer sediment to overtop.

The observation that most of the off site incursions involved fine sand and silt sediment while granular materials were observed in the basins corroborates these findings. There is little evidence that debris flows containing the large gravel and cobble size constituents extended beyond the debris flow basins.

Recommendations

Historic review of previous debris flow events indicates that a typical debris flow is on the order of 750 to 1200 cubic yards of material. It is recommended that the catch basins at the

---

[1] Parametric analyses were performed by varying R_u within the geometrical, material property and geometry constraints described in Table 3.

toe of the dumps be provided with the supplemental storage capacity to contain such a debris flow event and the 10 year 24 hour storm described in a companion report by URS Corporation.

An alternative method to containing the debris flow within a basin is to reduce the debris flow velocity such that the debris is unlikely to enter the basin itself. Dan-W modelling found that there may be several means to reduce debris flow velocity and reduce run out distance. One of the more promising approaches was to terrace the toe of the dumps, by shaping the apron of debris at the toe of the dumps into a "stair step" pattern. The concept is to use these stair steps to dissipate the energy of the debris flow and thereby reduce the travel distance. There are limitations to the stair-step geometry and Section 5 of this report should be consulted for specifics.

Contents page

List of figures

List of tables

Section 2 – Dan-W Modelling and Findings

1. Introduction - Waste Rock Dump Construction and Erosion Processes

During waste dump operations, particle segregation occurs down the dump face. In general, the finer grains size silt and silty sand particles deposit near the crest of the dumps, while the large cobble to boulder size particles roll or *saltate* down the dump face. Very large boulders often break up as they bounce down the dump face. In general, this particle segregation causes a slight over-steepening of the dump face with slope angles in the upper portion of the dumps extending at over 40 degrees. The over-steepening is attributed to "apparent cohesion" within the fine grain particles (a function of partial saturation of these materials). The angle of repose of the coarser particles is generally between 35 to 38 degrees, which is also considered to be close to the angle of internal friction (or ϕ angle) of the dump materials under low stresses. Over time, there is a tendency for the dumps to flatten slightly from their initial angle of repose of 37 to 38 degrees to the presently observed 35 degree slope angle. The flattening may be attributed to settlement and erosion processes.

The more erodible sand, silty sand and silt (with trace clay) particles are situated at the crest of the dump as described above. The less erodible gravel to boulder size particles congregate at the dump toe. The overall dump composition therefore varies from fine particles at the crest to coarser particles at the toe. However, trenching through dumps at the Questa Mine (Gutierrez, 2008) in New Mexico indicates that this general process is quite complex in the field. This is due to the fact that different sizes of waste materials are placed onto the dump with each truckload. The differences are due to varying composition of the overburden waste rock, varying energy levels during the actual dumping and variations in blasting (which influences particle size). It is not unusual that waste rock was hauled from several locations or shovels at one point in time, therefore the dump composition can be quite heterogenous at any given point. Weather and moisture conditions at the time of dumping can also influence the energy levels for the dumps.

A good description of dump stratification at the Questa Mine is provided by (Gutierrez, 2008). Excavations within the Bingham Pit through the Markham dumps reveal that similar processes are observed at KUCC. A sketch of typical waste rock dump deposition is shown on Figure 1.
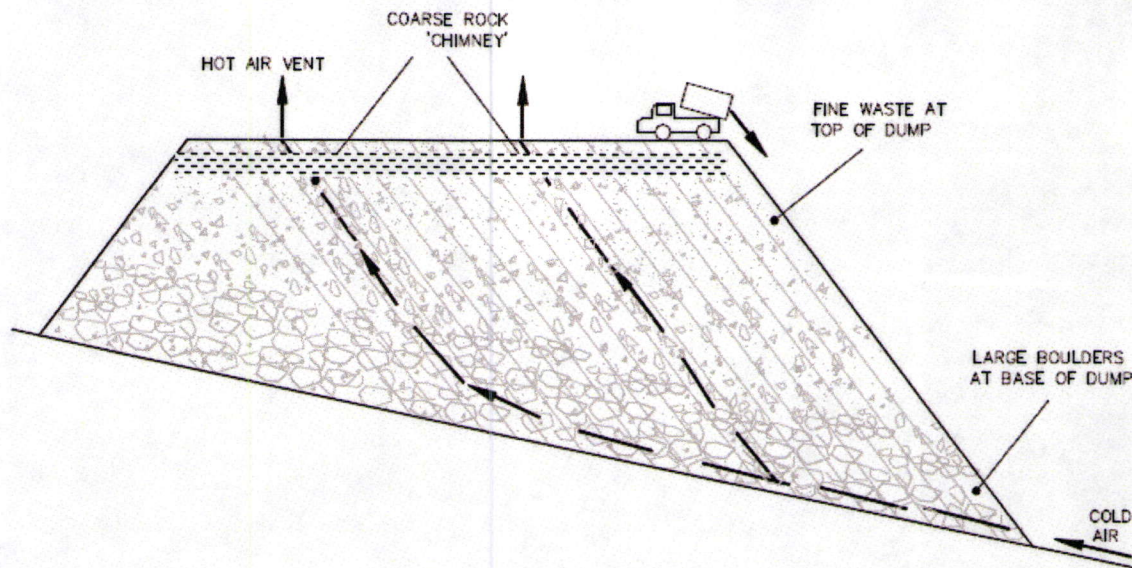
Figure 1 -   *Typical dump deposition (modified after www.infomine.com). A zone of horizontal stratification has been added at the dump crest to simulate short dumping to maintain dump elevation due to dump settlement. Coarse rock chimneys are zones where heat released during acid generation is released.*

As more materials are placed on the dump face, settlement occurs. Settlement is caused by the particles rearranging from a loose state (dumping) to a denser state. This particle rearrangement changes the internal shear strength of the dump materials as particle interlocking increases. However, at very high stresses near the base of the dump, shearing of some asperities occurs, causing a slight reduction in shear strength. Shear strength is often plotted in terms of the Mohr-Coulomb shear strength envelope. Under low stresses, the Mohr-Coulomb envelope is generally considered to be linear. However, due to the high stresses at depth, the Mohr-Coulomb envelope for the dump materials is considered to be non-linear.

To maintain a level dump surface at a given elevation, mine operations typically *short* or *plug dumps* by placing piles of loads on the dump surface. A dozer is then used to level out the dump surface, causing pseudo-horizontal stratification. As settlement occurs and the process is repeated over time, the crest of the dump often results in a series of near horizontal layers that mimic the original complete gradation of the material hauled to the dump. Since dump settlement can constitute 10 to 15%[2] of the dump height, the zone of horizontal layering can extend 70 to over 100 feet thick in a 700 feet thick dump[3].

Settlement near the dump crest also occurs in the form of *infinite slope* type displacements, where slippage of the outermost over-steepened materials occurs. The infinite slope displacements are evidenced by a series of steps at the Yosemite dump crest and elsewhere on the dumps (see Figure 2).

---

[2] Representative void ratios for loose to dense materials can be used to perform void ratio calculations that indicate the 10 to 15% settlement number is a reasonable range.

[3] The actual dump thickness is not the toe to crest height at KUCC because the dumps were placed on sloping topography, therefore the dump thickness is less than the height from crest to toe.

Figure 2 – View of settlement cracks and surficial movement at crest of Yosemite dump. There is abundant evidence that shallow slips of the surface continue to occur. Tension cracks are sometimes observed as far back as 500 feet from crest. Cracks tend to "heal" themselves over time. Survey monuments situated up slope of these cracks settled 3 ½ to 4 ½ inches from Oct 2005 to April 2007. Displacement along these scarps is much greater and on the order of tens of feet.

Observation of aerial photographs during the period 1977 through 2006 indicates there are several surface erosion processes occurring (see Attachment A for detail). Factors that influence the erosion processes include:

- The grain size of the dump materials: fine silts and sands are more highly prone to erosion than coarse particles.

- The fine grain size materials also have a high moisture retention value and tend to maintain higher moisture contents.

- There are generally few clay particles present in the dump that provide cohesion.

- Concentration of surface water flow along the dump crest leads to erosion gullies.

- Some berms at the dump crest tend to impound water, which ultimately impacts infiltration on the dump surface and contributes to the high antecedent moisture conditions.

- If water overflows the berms at the dump crest or there is a breach, then a debris flow may occur.

- There are *scars* present on the dump slope, indicating that some of the infinite slope movements may have become saturated and caused debris flow events.

In addition to surface erosion by overland water transport, a number of earth movement processes may influence dump erosion. These processes are defined in Table 1.

Table 1 – Earth Movement Processes

—

Sediment Flows (reference: http://www.tulane.edu/~sanelson/geol204/masswastproc.htm)

Sediment flows occur when sufficient force is applied to rocks and regolith that they begin to flow down slope. A sediment flow is a mixture of rock, and/or regolith with some water or air. They can be broken into two types depending on the amount of water present.

Slurry Flows- are sediment flows that contain between about 20 and 40% water. As the water content increases above about 40% slurry flows grade into streams. Slurry flows are considered water-saturated flows.

Granular Flows - are sediment flows that contain between 0 and 20% water. Note that granular flows are possible with little or no water. Fluid-like behavior is given these flows by mixing with air. Granular flows are not saturated with water.

Slurry Flows   **Granular Flows**

Velocity	
400 km/hr	
100 km/hr	Debris Avalanche
	Mud Flow — Grain Flow
1 km/hr	
100 m/hr	
1 m/hr	Debris Flow — Earth Flow
1 m/day	
1 m/yr	
1 cm/yr	Solifluction — Creep

~40%   ~20%   0%

← Stream Flow
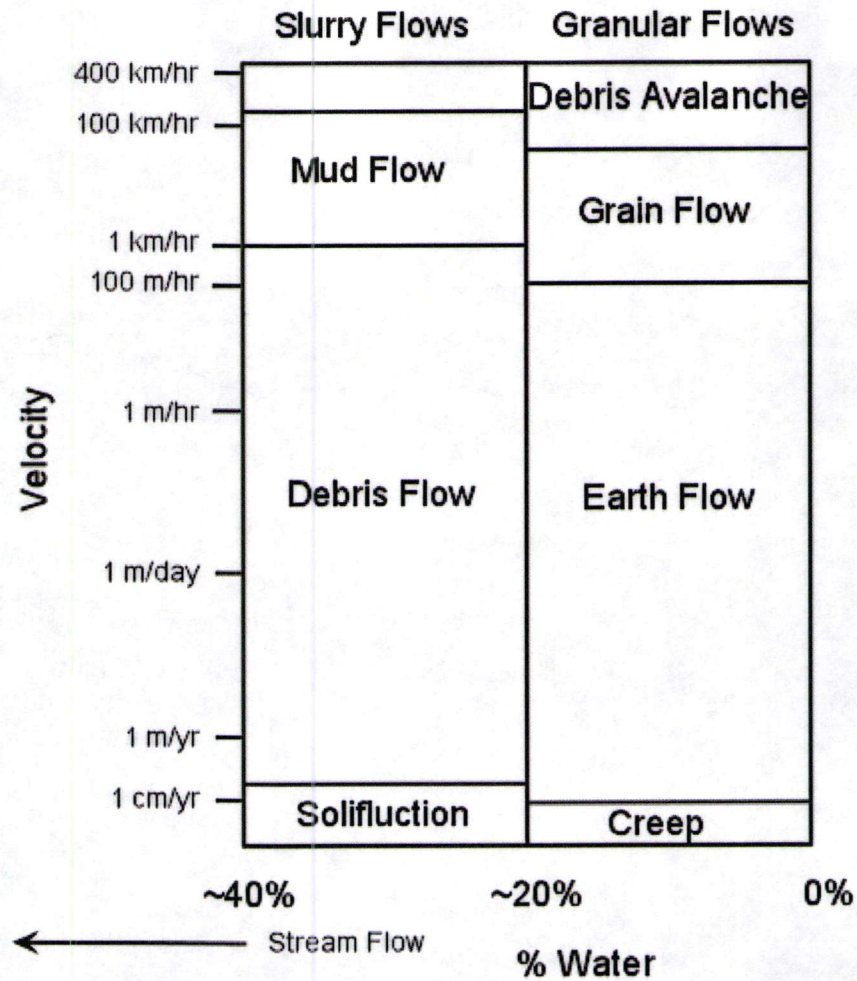
% Water

Each of these classes of sediment flows can be further subdivided on the basis of the velocity at which flowage occurs.

Slurry Flows

- **Solifluction** -flowage at rates measured on the order of centimeters per year of regolith containing water. Solifluction produces distinctive lobes on hill slopes. These occur in areas where the soil remains saturated with water for long periods of time.

- **Debris Flows** - these occur at higher velocities than solifluction, with velocities between 1 meter/yr and 100 meters/hr and often result from heavy rains causing saturation of the soil and regolith with water. They sometimes start with slumps and then flow downhill forming lobes with an irregular surface consisting of ridges and furrows.

- **Mudflows** - these are a highly fluid, high velocity mixture of sediment and water that has a consistency ranging between soup-like and wet concrete. They move at velocities greater than 1 km/hr and tend to travel along valley floors. These usually result from heavy rains in areas where there is an abundance of unconsolidated sediment that can be picked up by streams. Thus, after a heavy rain, streams can turn into mudflows as they pick up more and more loose sediment. Mudflows can travel for long distances over gently sloping stream beds. Because of their high velocity and long distance of travel, they are potentially very dangerous.

Granular Flows

- **Creep** - the very slow, usually continuous movement of regolith down slope. Creep occurs on almost all slopes, but the rates vary. Evidence for creep is often seen in bent trees, offsets in roads and fences, and

inclined utility poles.

- **Earthflows** - are usually associated with heavy rains and move at velocities between several cm/yr and 100s of m/day. They usually remain active for long periods of time. They generally tend to be narrow tongue-like features that begin at a scarp or small cliff.
- **Grain Flows** - usually form in relatively dry material, such as a sand dune, on a steep slope. A small disturbance sends the dry, unconsolidated grains moving rapidly down slope.
- **Debris Avalanches** - These are very high velocity flows of large volume mixtures of rock and regolith that result from complete collapse of a mountainous slope. They move down slope and then can travel for considerable distances along relatively gentle slopes. They are often triggered by earthquakes and volcanic eruptions.

The processes that have been observed on the surface of the KUCC dumps include primarily particle erosion due to water transport resulting in gullying, and debris flows / mudflows. These are described as follows:

- Particle erosion includes the continuous movement of individual particles due to wind and water. Particle erosion is largely attributed to the fact that there is no vegetation cover or other stabilizing agent present on the dumps.

- Gullying and rilling occurs due to water transport. At slope distances greater than approximately 50 to 100 feet from the dump crest, erosion gullies are observed. These gullies form as overland transport coalesces into small "streamlets" and these "streamlets" continue to coalesce into more pronounced flow paths. Gullying of this type is attributed to precipitation and snowmelt.

- Debris or mudflows occur when the uppermost fine grain size materials become saturated and flows as *lobes* down the slope. Such *lobes* of material are evident along the surface in aerial photographs and can be observed extending from near the dump crest all or part way down the slope. Moisture conditions at the surface of the KUCC dumps are quite close to 20 percent moisture, indicating that the materials are at the boundary between slurry and granular flows.

- At the toe of the dump an apron of material forms from these erosion processes. The distribution of slope angles of these apron materials is bimodal, as follows:

  - The steeper apron materials average 20 +/- 5 degrees (mean +/- standard deviation)
  - The flatter apron materials average 6.5 +/- 1.5 degrees.
  - The overall average is 13.5 +/- 6 degrees.

Out of the above processes, debris flows are most problematic because they are episodic in nature and associated with meteoric events. When such debris flows occur, sufficient containment must be present along the toe of the dumps to contain the material. Otherwise, overtopping of the containment structures occurs and the fluid flows can migrate off property.

2. Information that Dan-W can provide

The Dan-W software program provides the following useful output:

- Dan-W can predict the distance that a debris flow will travel. This prediction is based on developing realistic input assumptions, calibrating to some known events and assessing a range of those conditions in the profile of interest.

- Likewise, Dan-W can predict the velocity that a debris flow will travel at various locations along the debris flow path. At KUCC, this is not considered a major concern because historic evidence suggests that the debris flows are relatively slow traveling (1 to 100 m/hr, see Table 1). Velocity was a major issue in the development of Dan-W because the model was developed to predict run out distance and velocity in terrain where failures achieved very high velocities.

- For the KUCC analyses, one of the more useful features during Dan-W execution was the velocity at the front and tail of the debris flow. It was observed that any means to reduce the velocity at the front of the debris flow was very effective at causing deposition to occur and ultimately reducing the travel distance. By reducing velocity at the front of the debris flow, material would accumulate, essentially causing the remaining material to begin to "pile up", which then reduced the velocity along the remainder of the travel path.

- The geometry along the path of the debris flow can be varied to assess the impacts to velocity, distance and depth of deposition. Impacts from geometry changes include changes to velocity (either accelerating or decelerating), the initiation of deposition and changing the depth of deposition. It is noted that increasing steepness in the run out zone can also increase velocity and travel distance. For example, a debris basin located too close to the toe of the dump may be overtopped, and the steep downstream slopes of the debris basin could extend the travel distance. In this manner, Dan-W can assess whether debris basins are located appropriately at the toe of the dump.

- Geometry changes also impact the continuity of the debris flow. Dan-W can model the debris flow splitting into one or more separate flows. Additionally, if a known geometry causes the debris flow to become "airborne" (which is considered to be unrealistic), then such a known geometry inflection point can be used during calibration to rule out unrealistic input parameters.

3. Information that Dan-W can not provide

- The program requires input of the material parameters, which are related to precipitation data and the material properties in the debris flow. Dan-W can not predict the amount of precipitation required to cause the debris flow. This is an input assumption, which in the cases evaluated for the KUCC waste dumps, requires an assumption for either the pore pressure parameter, R_u, (for the Mohr-Coulomb input assumption) or a definition of the rheology of the debris flow (Voellmy input assumption).

- Dan-W does not provide any information in regards to the return period of the debris flow event. The return period is ultimately related to the precipitation required to cause sufficient saturation for the debris flow to occur.

- Dan-W also requires an assumption of the volume of material involved in the debris flow. Volumes can be assessed parametrically by calibrating to the material deposited, but ultimately the size of the debris flow must be input at the initiation of the analysis. Debris flow volume is critical to sizing a catch basin and must be established by other means. Several sources of information were available to estimate the "typical" debris flow volume. The primary sources of the input information include the historic database and review of aerial photography. Aerial topography combined with accurate topographic contours can provide an estimate of the size of gullies and also size of semi-circular 'scars" observed on the dumps. Since aerial photography and topographic data are two-dimensional, the depth of the debris flow at initiation must be estimated from the inflection of the contours.

- The maximum depth of erosion along the travel path is another input parameter. This depth must be assessed based on field observations. Dan-W <u>does</u> make an assessment of whether material is eroded or deposited along the debris flow path and uses the velocity, shear strength and depth of erosion input parameters in this calculation.

4. Dan – W Analysis Methodology

The software program, Dan-W (Hungr, 2006) was used to assess debris flow run out distance and velocity. However, before such analyses could be conducted, there was a significant data gathering component, which is summarized in Attachment 1. The Dan-W analysis consisted of gathering the required input information and completion of parametric analyses where one of the unknown input parameters was varied to calibrate to known conditions. The parameter that was varied was the pore pressure parameter, R_u, which is a measure of pore pressure and the water entrained in the debris flow. The following sections summarize:

- Dan-W software
- Historic debris flow events
- Development of input parameters
- Summary of Dan-W findings

In general, it was found that some of the most useful information obtained was development of the input parameters for the Dan-W analysis itself. This observation is discussed in further detail in the following sections.

4.1 Dan-W Software:

Dan-W was developed primarily to assess hazards from high velocity and long distance debris flows generated from coal mine refuse and waste in British Columbia, Canada. The program was developed by Oldrich Hungr whose papers are referenced in Attachment 3 (the Dan-W manual). During development of Dan-W, travel time, distance and depth of deposition were the primary areas of interest. The software program incorporates the complex kinematics of debris flow (viscous fluid) movement and uses a pseudo method-of-slices approach, which is a dynamic form of the ordinary method of slices used in slope stability analysis. The primary output includes the following graphs:

- Velocity versus time graph, which is presented in real time during the analysis execution.

- Travel distance along slope based on the material input parameters.

- Impacts of slope geometry changes along the travel path. These changes include the one-dimensional profile of the travel path and the width of the debris along that travel path (yielding a pseudo two dimensional analysis).

- Depth of debris flow deposition.

- Various analysis statistics, such as maximum velocity and where it occurs, location of the final toe of the debris flow, location of the debris flow heal, etc.

During the program execution, Dan-W simulates the debris *slug* travelling down the dump face / apron and graphically displays the velocity, depth and distance the material has travelled. Figures 3 and 4 show typical output, which consists of an oblique view of the debris flow (Figure 3) and a travel distance and velocity graph (Figure 4).
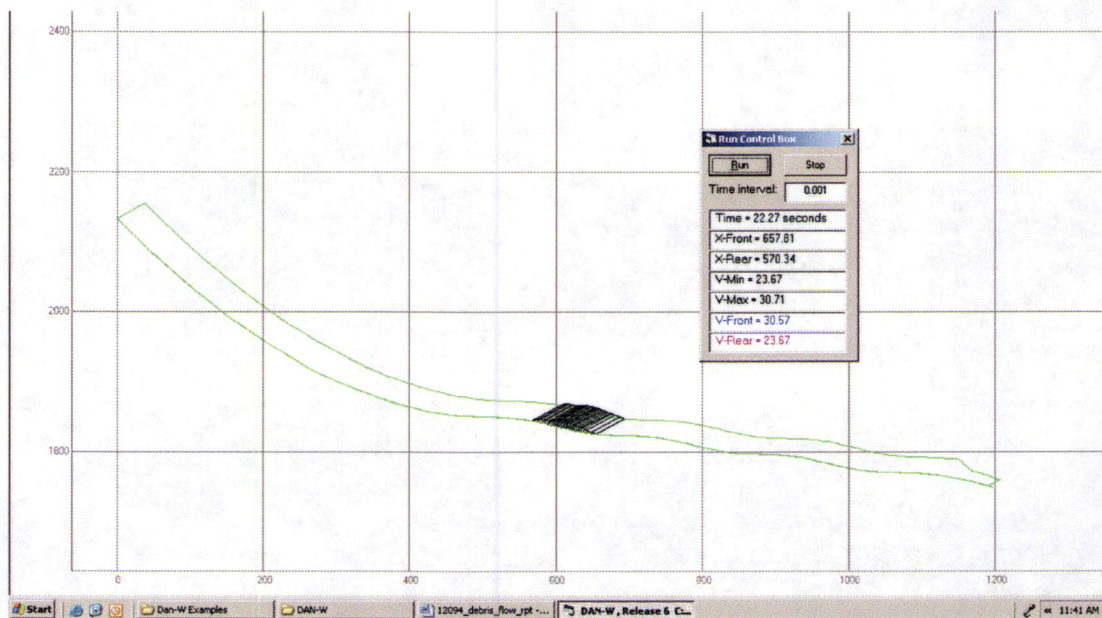

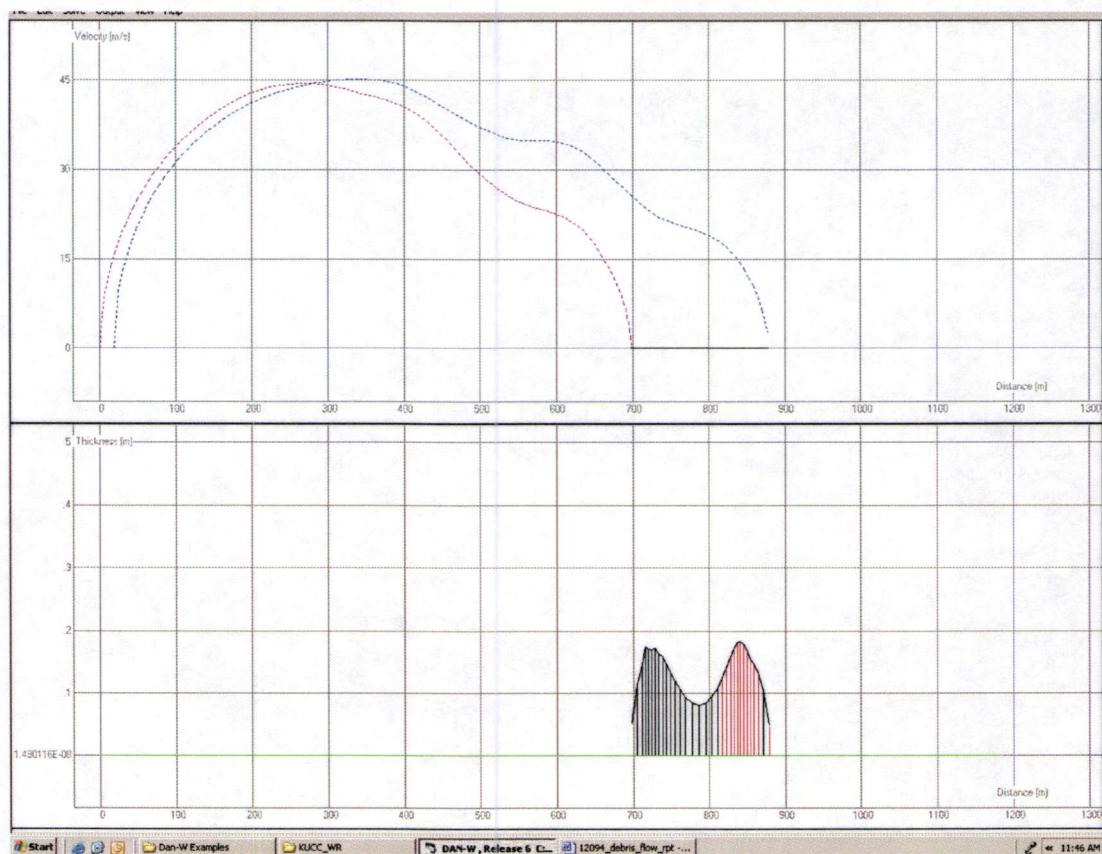Figure 3 - Dan-W output showing debris flow "slug" travelling down terraced apron

Figure 4 - Dan-W velocity, travel distance and depth of deposition graph

4.2   Historic Debris Flow Events

Debris flows often occur in mountainous regions and have been an identified geologic hazard in some communities, such as the east bench areas of Farmington Canyon in Davis County and the Provo bench area in Utah County, Utah (Case, 2000). Debris flows often occur in areas where there is shallow soil cover above fractured bedrock. It is postulated that flow through the fractured bedrock often causes the saturated *debris flow scars* to occur at a particular location. Alternately, surface runoff may concentrate in a particular area, saturating the ground. These *natural* debris flow occurrences are significantly different than the waste rock dumps, where bedrock is situated many hundreds of feet below the outer dump surface. Debris flows in the waste dumps are postulated to occur due to either overtopping of concentrated runoff at the crest of the dumps, or possibly development of perched water tables near the dump crest day-lighting at the surface. Although both sources are possible, concentrated runoff overtopping the dump crest can be prevented by maintaining proper berms and routing runoff away from the dump face. Subsurface perched water tables are more difficult to prevent or address although compacting the dump surface to reduce infiltration is effective.

Historic review of documented KUCC events found that debris flows are usually characterized by the following:

- A period of high, concentrated or above normal antecedent precipitation saturating the surface.

- A period of highly concentrated precipitation in excess of 1 inch per hour.

- Generally occur in the summer months and are associated with thunderstorms.

- Conversely, debris flows associated with spring snow melt appear to be less prevalent.

Table 2 summarizes the documented debris flows at KUCC which migrated off property plus two cases where the material remained on property. A number of other debris flow events have occurred. Because these events were captured within the debris flow basins, they are not documented.

Table 2 – Summary of Historic Debris Flows Documented at KUC

Date	Location	Rainfall, in/hr & duration	Ultimate deposition	Quantity / Comment
1967	Castro		Butterfield Creek	Reportedly dammed up portion of creek
1979	Saint's Rest (south of Yosemite)	Not applicable; debris flow caused by excessive dump leaching	Contained in drainage	Large failure due to excessive leaching for 30 days.

Date	Location	Rainfall, in/hr & duration	Ultimate deposition	Quantity / Comment
1983 – 84	Various	High spring runoff	Some deposition in Butterfield	Yellow-brown layer encountered downstream of the Canyon mouth
June 9, 1997	Olsen drainage[A]	1.32 inches in 1 hour; 1.27 in 30 minutes	Butterfield Creek	750 yd^3 or about 1100 tons; 50% had been contained in Olsen structures
August 4, 1997	Castro Basin overtopped	Antecedent Precip: 1 inch; prior to event: 0.58 inches	Traveled along access road to Butterfield Creek & then to irrigation system	
1998	Olsen		Butterfield Creek	Plugging of pipe
Sept 3, 2005	Castro Gulch	Unknown	Butterfield	Overflow from collection pipe into Eastside Collection System
2006	Castro	Unknown	Contained on property	
July 27, 2007	Yosemite	URS 2009 report	Butterfield Creek	Filled Yosemite basin

Notes:

A – A 4 feet deep gully extending to the crest of the Olsen dumps was observed corresponding to an approximate volume equal to the reported release.

4.3   Development of Dan-W Input Parameters

Based on the above discussion, the required input for the Dan-W analyses was developed using the following approach:

- Geometry: The program requires input of the one-dimensional travel path (cross section) and the width along the travel path. The program can model constrictions, such as in the case of the debris flow entering a narrow stream channel. Conversely, the program can model the impact of widening the travel path, as a debris flow enters the *apron* at the toe of the dumps. The geometry is based on profiles taken along the

main drainages. It is observed that for most of the dumps, the profiles are quite similar allowing one analysis to model the general debris flow characteristics along all basins. The cross-section geometry was based on 2 foot contour intervals along the dump and toe of dumps using the 2008 aerial photography provided by KUCC. USGS topographic maps were used to extend the topography beyond the most recent maps, as necessary. Figure A-14 shows the cross-section geometries that were developed.

- Material types: The material types along the potential flow paths were assumed to be uniform, granular materials. Based on surface inspection this is reasonable. Likewise, inspection of the drainages reveals that most of the drainages comprise granular materials. Where vegetation or other materials are present within the drainages, this assumption is conservative, because such materials would tend to slow the debris flow velocity (and this would not be accounted for in the analysis).

- Strength Parameters: The Mohr-Coulomb (M-C) criteria were used to assess the material type and behavior (shear strength). The M-C criteria are the best known and understood material property type because the dump surface is at the angle of repose, essentially exhibiting a 35 degree friction (ϕ) angle. Secondly, the materials consist of silt to gravel (and larger) size particles so that no cohesion can be assumed. The only assumption required when using the M-C parameters is the pore pressure parameter, R_u. R_u was bounded by varying this parameter between a low value (where no movement occurred) and an upper bound value where the debris flow was observed to "go airborne" during the analysis (essentially giving the analysis unrealistic results). [This usually occurred as a fluid debris flow overtopped the debris flow basin.] This sensitivity analysis yielded a range in R_u from 0.2 to 0.6 (no movement to excessive velocity) with a best fit parameter of approximately 0.4.

- Unit Weight: The unit weight of the debris flow was based on characterization of the surface of the dump by AMEC, who had completed a variety of density tests on the top surface of the dump. The input parameters were corrected for saturated conditions (versus total unit weight).

- Debris flow volume at initiation: The size of scar or volume of debris at the start of the analysis was based on the following:

  - Historic records of debris contained in the basins were checked. This data source revealed an input volume of about 750 to 1200 yd^3 for a typical debris flow.

  - Historic aerial photographs were reviewed to estimate the size of "debris flow scars" (See Attachment 1 Figures A-3 and A-12). The assumption was made that such features generated the larger debris flow events. The area of the scars were measured in ArcGIS and corrected for the 35 degree slope angle. The potential volume was developed by estimation from the inflection of the contour outlining the scar. A maximum depth of 1 meter (3 feet) was used.

  - Estimates of the volume of gullies present on the surface of the dump were also made. Such estimates were made in a similar manner to the debris flow scars, however, there was better depth control due to the incision of the "V" that the gullies exhibit on topographic maps. It is known, however, that individual debris flows did not generate each gully, because the location of the gullies tend to be stable over decades. It was assumed that the gully volumes would generate debris flows no greater than 10 percent of the gully itself, an assumption which is believed to be conservative.

Table 3 summarizes the Dan-W input parameters and the basis for the parameter selection.

Table 3 – Dan W Input Parameter and Basis

Parameter	Value (units)	Basis	Supporting Attachment Figure
Slope Profile	Yosemite drainage and average profile normalized along remaining drainages averages 35.2° Average along "apron" is 12.5° (+/-)	KUC 2 ft topography along main axis of drainage	A-18
Scar Width (profile width in Dan-W)	Average = 30 ft Range: 10 to 55 ft Average acreage: ~ 0.6 acres	As measured from aerials	A-6 to A-17 (Figures developed from ArcGIS)
Shear Strength: Friction Angle (ϕ) Cohesion Intercept	$\phi' = 35°$ Cohesion = 0	Average angle of repose / non cohesive materials	A-18
Pore Water Pressure Parameter, R_u	Varies from 0.2 to 0.6 (Ave = 0.4 to 0.45)	R_u varied to provide a reasonable correlation with observed travel distance. At $R_u < 0.2$, the debris flow does not extend past the toe of the dump. At $R_u > 0.6$, debris flows would become airborne. $R_u = 0.4$ best fit.	A-19
Dynamic Shear Strength	Governed by the equation: $\phi_{bulk} = \tan(\phi'(1 - Ru))$	Reduces the effective friction angle, ϕ', by 0.4 to 0.8 ϕ' with the best fit ϕ_{bulk} angle of 21 degrees (close to the observed 20 degree slope angle of the steeper apron materials.)	n.a.
Unit Weight	19 KN/m^3	AMEC 2006 dump surface test work	n.a.
Erosion Depth, m	3 meters	Estimate	n.a.
Volume of Debris, m^3, as based on: length of scar, width and depth	Depth held constant at 1 meter, width and length varied	As described in text: average value is 750 yd^3 (575 m^3) with range of 750 to 1200 yd^3	A-6 through A-17
Note: Dan-W requires metric input parameters; all English units converted to SI for input.			

5. Summary of Dan-W Findings

The first step in the Dan-W analyses was to gather the relevant input parameters, summarize the basis and complete back analysis of the documented information to develop an

appropriate range of input parameters. This data-gathering exercise is summarized in Attachment 1. The unknowns in the input parameters largely revolved around uncertainty in the pore pressure parameter, R_u, and the volume of the debris flow itself. To address these uncertainties, these parameters were varied so that reasonable output based on the historic data was obtained. It was found that the software was most sensitive to the pore pressure parameter, R_u, in terms of calibrating what was known about prior events.

Additionally, development of the input parameters yielded some of the more useful information. For example, the following information was developed:

- The historical review of scars showed that such features are periodically evident on the dump surface and represent slumps and / or potential sources of the debris flows.

- The size of gullies was estimated, which yielded approximate values for the erosion that may be occurring from the dumps. It was assumed, however, that the maximum individual debris flow event would represent no more than 10 percent of the gully volume, because individual gullies are evident over several decades of aerial photographs.

- Two mechanisms for the occurrence of debris flows were developed:

    o Overtopping of the dump crest by water, which was originally the postulated cause of the debris flows.

    o Day-lighting of a perched water table near the embankment crest.

- The effect of varying the geometry and grade changes was evaluated during back analysis. This constrained the pore pressure parameter, R_u, and also demonstrated that increasing slope steepness in the deposition area would ultimately increase the run out distance.

5.1   Recommended Options to Mitigate Erosion

There are two basic approaches to mitigating the erosion rate and amount of water flowing down the dump face. The most obvious approach involves methods to reduce concentrated water flow down the dump face, which include:

- Maintaining the berms along the dump crest to assure that concentrated flow is not occurring.

- Sloping or regrading the dump crest area inward to promote drainage away from the crest to a point where drainage be routed safely down the down face or groin area, such as using a drainage pipe.

- Avoiding concentrateing areas of surface runoff near the dump crest.

Controlling erosion due to direct surface precipitation onto the dump face is difficult. Therefore, some rilling and erosion must be expected with the current angle of repose dumps. Field observations indicate that dumps must be terraced every 50 to 100 feet to curtain development of large gullies. Assuming that some erosion is inevitable, controlling the sediment at the toe of the dump provides a means of containing the material on KUCC property. The means to collect surface water are discussed in a companion URS report and

has been implemented as of October 2009. The URS report indicates that the second detention basin, situated up slope of the current east side collection system basin will provide supplemental storage for runoff in the Yosemite basin and contain a potential debris flow event.

One of the findings of the parametric Dan-W analyses (analyses where R_u was varied) was that geometry changes could impact the travel distance. Such geometry changes could be used to reduce debris flow velocity and run out distance. Ideally, one would prefer to have a debris flow come to rest before entering the catch basin. In this manner, the full capacity to store a 10 yr 24 hour event would be available. Practical application of reducing the debris flow velocity includes concepts such as:

- Installing constrictions on the alluvial fan or apron at the base of the waste rock dumps.

- Constructing the supplemental debris flow basin upslope of the current basin (as has been completed by KUCC).

- Changing grade to reduce velocity (thereby getting the debris flow to stop before the basin is reached. Recontouring the apron of materials at the toe of the dump has also been accomplished to the maximum extent practical.

Should field evidence indicate the measures implemented need augmentation, creating a constriction would involve placement of physical barriers, such as piles of non-erodible large boulders across the dump toe. Material that is subject to erosion should not be used, as such material could become incorporated into a debris flow. Alternately, steel piling could be driven vertically into the dump apron to provide constructions and reduce debris flow velocity. However, as material collects behind these *vertical barriers* the grade would be changed. Such future increases in the grade could cause additional material to combine into the debris flow, therefore enlarging the amount of debris and increasing the travel distance. Such barriers would require continued maintenance similar to the current debris flow basins.

Dan-W analyses indicate that one of the more effective methods to reduce debris flow velocities is to terrace the toe areas of the dump. There are limitations on the dump terracing since cutting steep terraces into the dump toe creates new sources for erosion. Since the average angle of repose of the saturated materials at the toe of the dump is about 13 +/- 6 degrees, increasing the steepness of areas at the toe of the dump beyond 20 degrees would be likely to cause further erosion. Secondly, any grading performed at the dump toe needs to ultimately match the current dump toe. These two considerations place constraints on practical grading options. Given these considerations, it appears that the best means to terrace include cutting benches between 0 to 2 degrees dip and cutting slopes areas between 10 and 14 degrees dip. For example, at the toe of the Yosemite dump, a terracing pattern of 4 degrees benches and 12 degrees slopes or 2 degree benches and 14 degree slopes would match the current topography. Within practical limits, such terracing has been accomplished in conjunction with construction of the supplemental debris flow basin. Other configurations are viable at locations other than Yosemite and these can readily be evaluated with the current Dan-W model. The minimum bench width should be 200 feet and the number of benches should be dictated by site-specific conditions. Such a terracing scheme is shown on Figure 5.
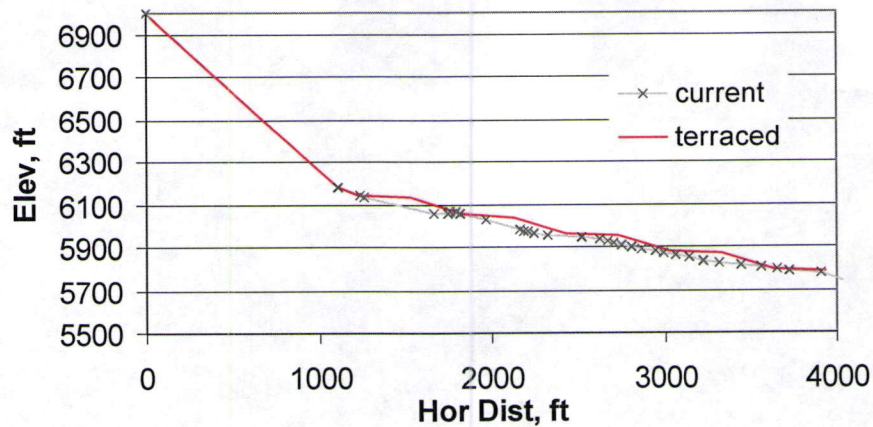
Figure 5 - Possible terracing of dump toe (2 degree benches with 12 degree terrace slopes shown)

5.2 Evaluation of Supplemental Detention Basin Recommended by URS

The calibrated Dan-W model was used to evaluate the impact of the supplemental detention basin situated at a horizontal distance of approximately 1500-1550 feet from the crest of the Yosemite dump. The analysis found that at R_u values less than about 0.3, a 750 yd^3 debris flow would be contained in this basin. At R_u values between 0.3 and 0.4, the debris flow velocity would be appreciably reduced and the debris itself would be deposited immediately down slope of the new basin (and upslope of the current basin). At fluid R_u values greater than 0.4, the basin is situated too close to the dump toe. The debris flows would either become airborne (unlikely) or cause erosion of the upper basin. In either case, containment is provided in the current lower basin. Based on the Dan-W analyses, it appears that the second basin would reduce debris flow velocities in most circumstances. For very fluid debris flows, it is recommended that additional armouring be placed on the debris basin crest (large boulders) to reduce the likelihood of overtopping erosion of the basin embankment.

5.3 References

Case, W.F., 2000, "Debris Flow Hazards," Utah Geologic Survey Public Information Circular Series 70.

Hungr, O, 2004, "Dan-W Release 4, Dynamic Analysis of Landslides" Hungr Geotechnical Research, 4195 Almondel Rd. West Vancouver, B.C. Canada.

Hungr, O. and Evans, S.G.," Rock Avalanche runout prediction using a dynamic model" in Landslides, Senneset (editor), Balkema, 1996.

Guttierrez, et al "Geotechnical and Geomechanical Characterization of the Goathill North Rock Pile at Questa Molybdenum Mine, New Mexico, USA," in Fourie, A. "Rock Dumps 08-Proceeding of the First International Symposium of Rock Dumps, Stockpiles, and Heap Leach Pads," Australian Centre for Geomechanics, CSIRO, Perth, WA.

URS, February 2009, "Hydrologic Assessment of South End Drainages," unpublished report URS Corporation.

Attachment A – Aerial Photo Review

The process of erosion can be observed on the following sequence of aerial photographs. Figures A-6 through A-8 show the erosion sequence for the northern[4], high truck waste dumps (Keystone / Lost Copper); figures A-9 through A-13 show a similar sequence for the Yosemite dump and the Saints Rest dump dump area is shown on Figures A-14 through A-17. The Saints Rest dump was selected because it has exhibited a number of debris flow events over time and contains evidence of 1979 failure debris.

Figure A-6 - Footprint below the Keystone dump in 1977 – debris from previous failure is evident.

---

[4] The Burma road or the road heading up to the former Yosemite truck shop area is the divide between the North and South dumps.
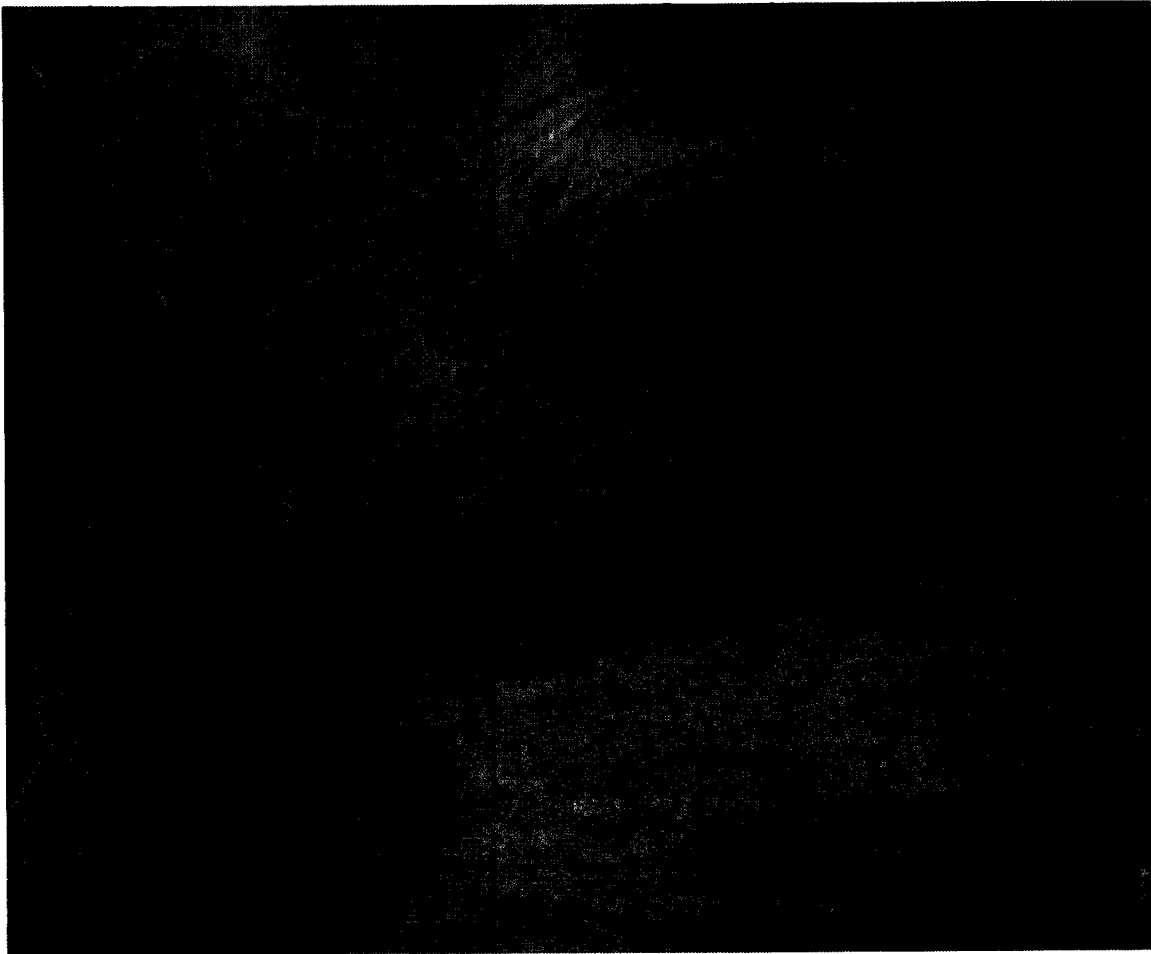
Figure A-7 - The Keystone dump in 1983. Note that minor erosion gullies are already present and previous failure debris has been overtopped.

Figure A-8 - Erosion and gullying in 2003 color aerial photograph of same area. Also note the "scar" formed from a debris flow emanating from near the crest (left of the word keystone). The 2006 aerial is not as good quality and is not shown. However, it shows slight enlargement of scar and apparent deepening of the major gullies shown on this photograph. Piles of "plug dump" waste rock are evident in the lower left corner.

The following photographs show a similar sequence for the Yosemite dump area.
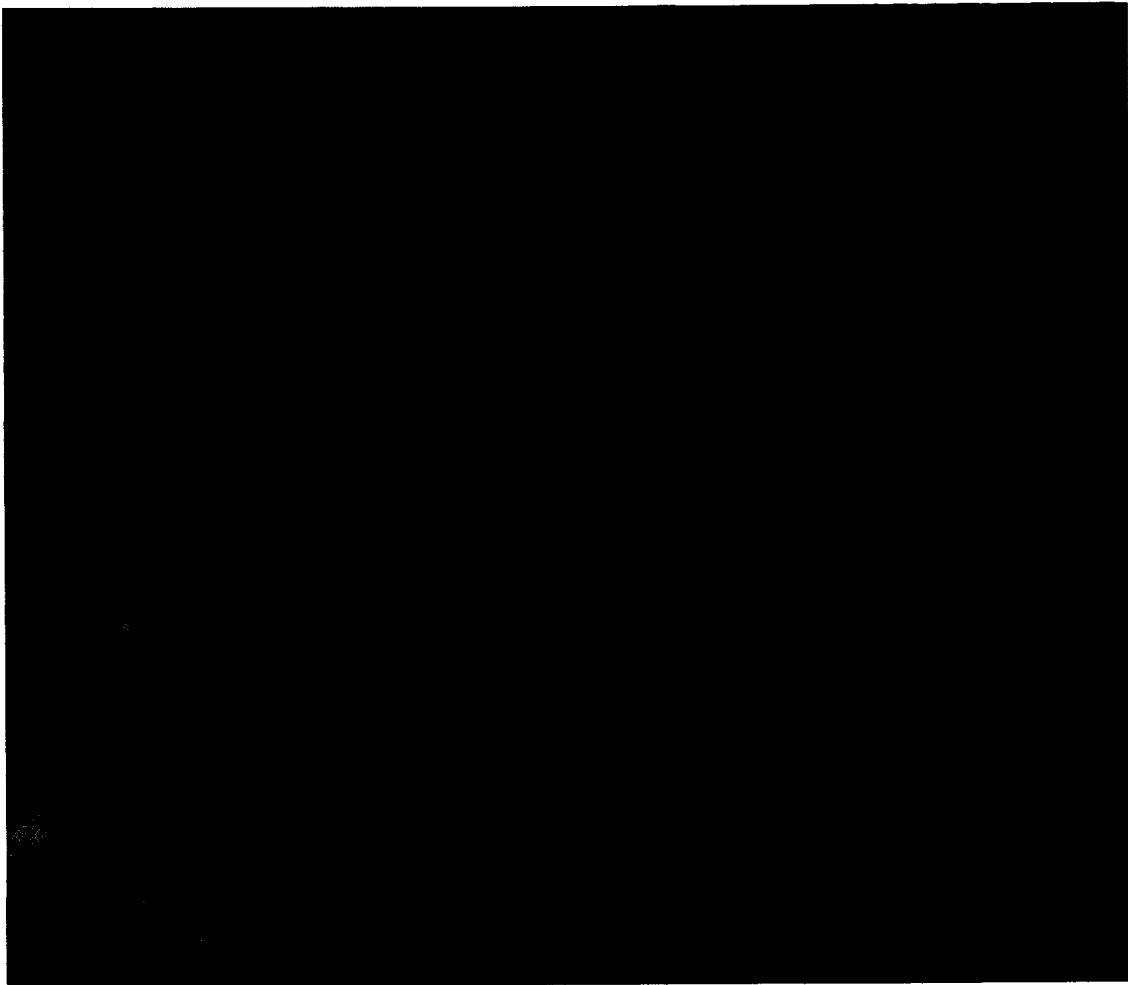
Figure A-9 - 1977 Yosemite aerial photograph. The red circle identifies a major erosion gully.
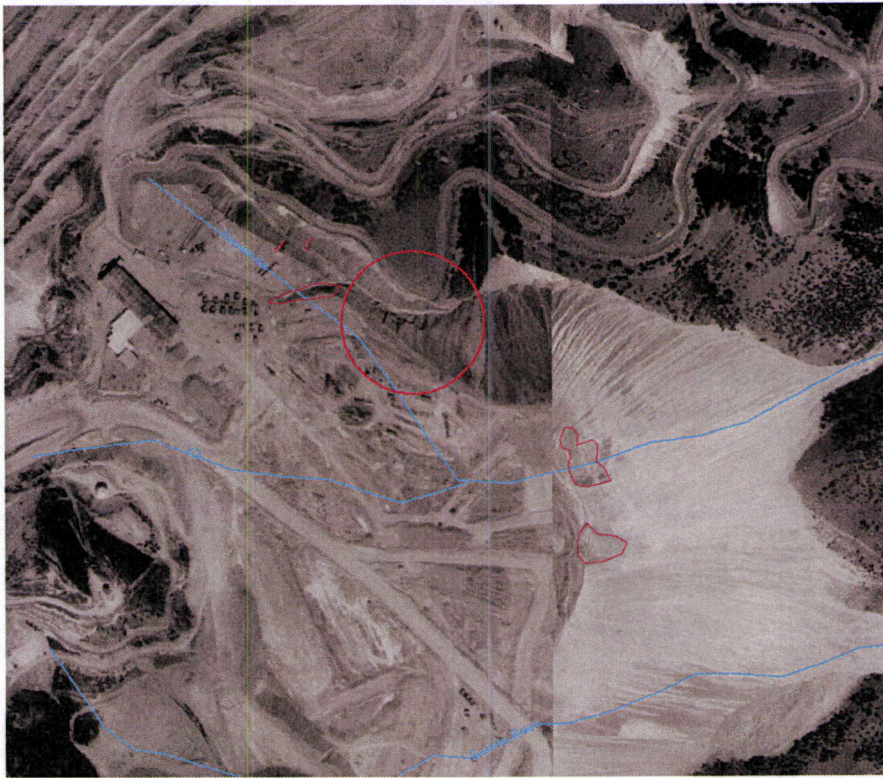
Figure A-10 - 1983 Yosemite Aerial photograph
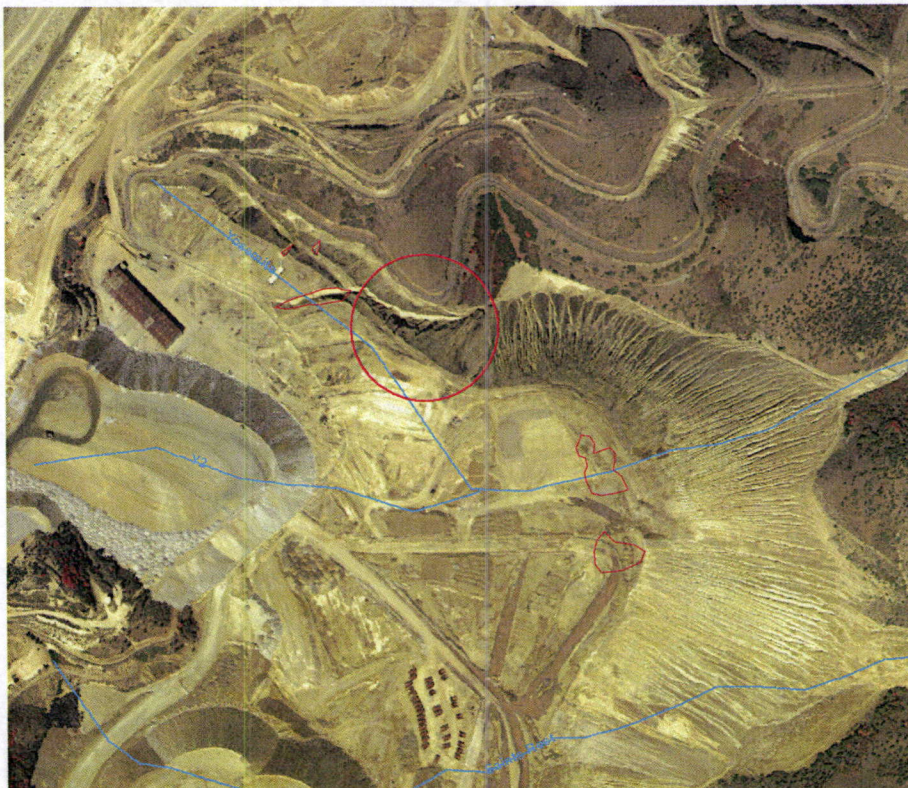
Figure A-11 - 2003 Yosemite Aerial Photograph
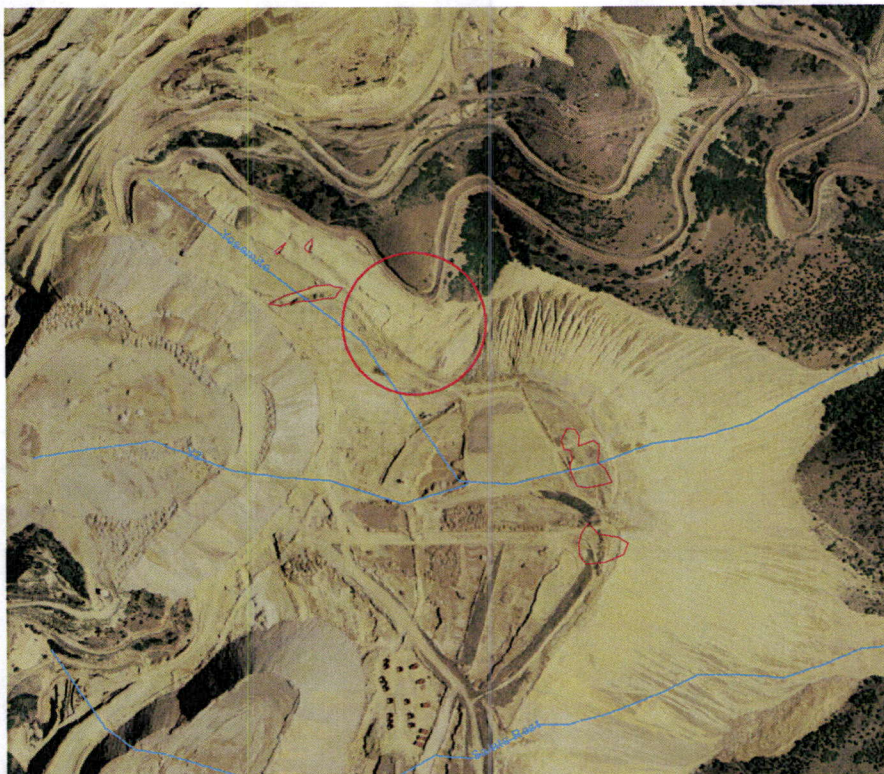
Figure A-12 - 2006 Yosemite Aerial
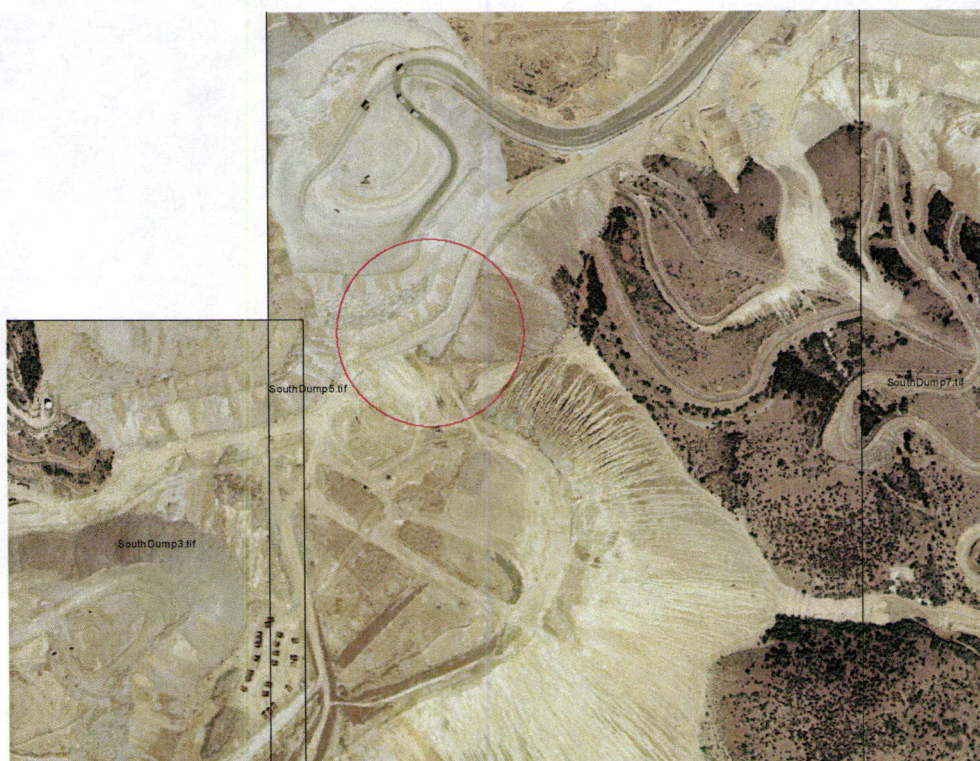
Figure A-13 - 2008 Yosemite Aerial – note how new material has been placed above the large erosional gully that was formerly located within the red circle. This material may have altered the surface drainage on the dump.

Photographs beginning with Figure A-14 show a similar sequence for the Saints Rest dump:
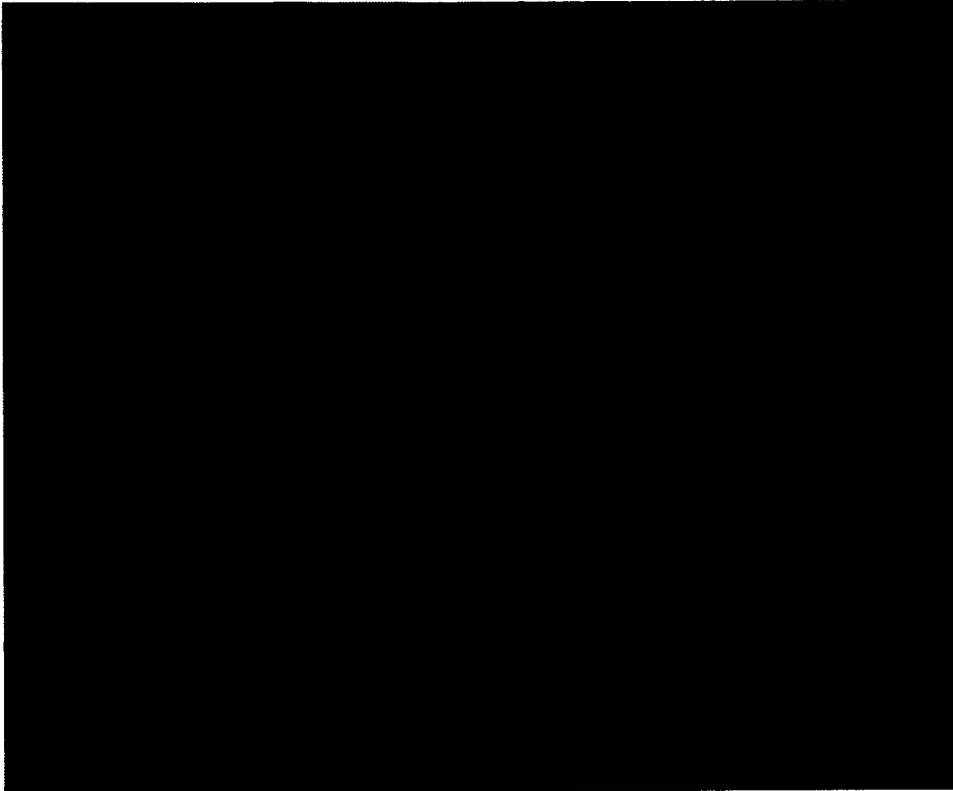
Figure A-14 - Footprint below the future Saint's rest dump in 1977. This is the area prior to the 1979 failure.
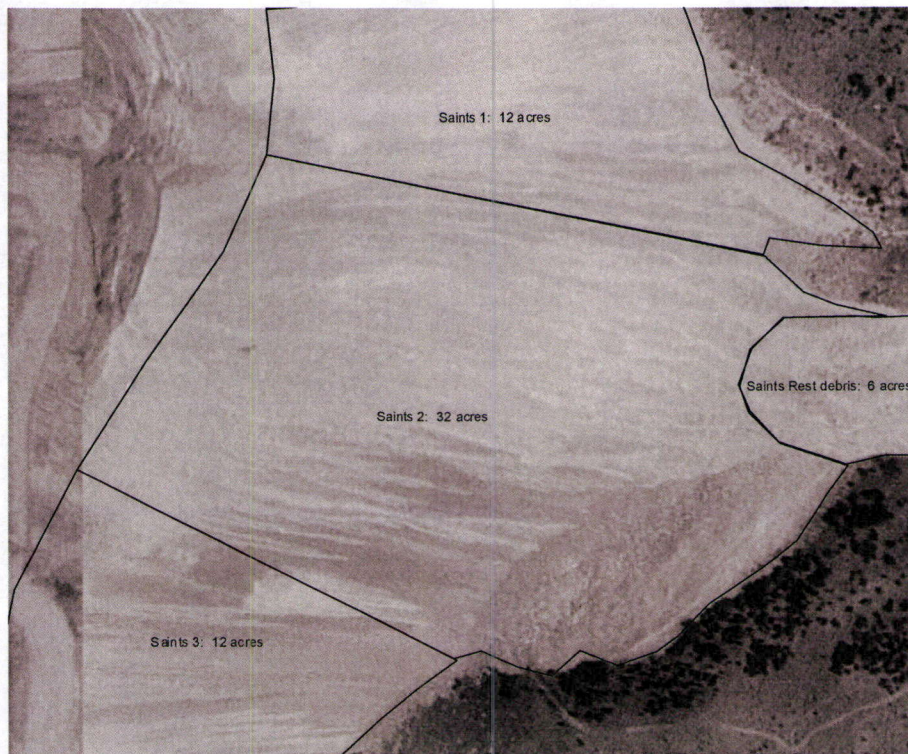
Figure A-15 - The same dump area in 1983. The granular material in the lower (southeast) is the 1979 failure debris. Note that minor erosion has begun.
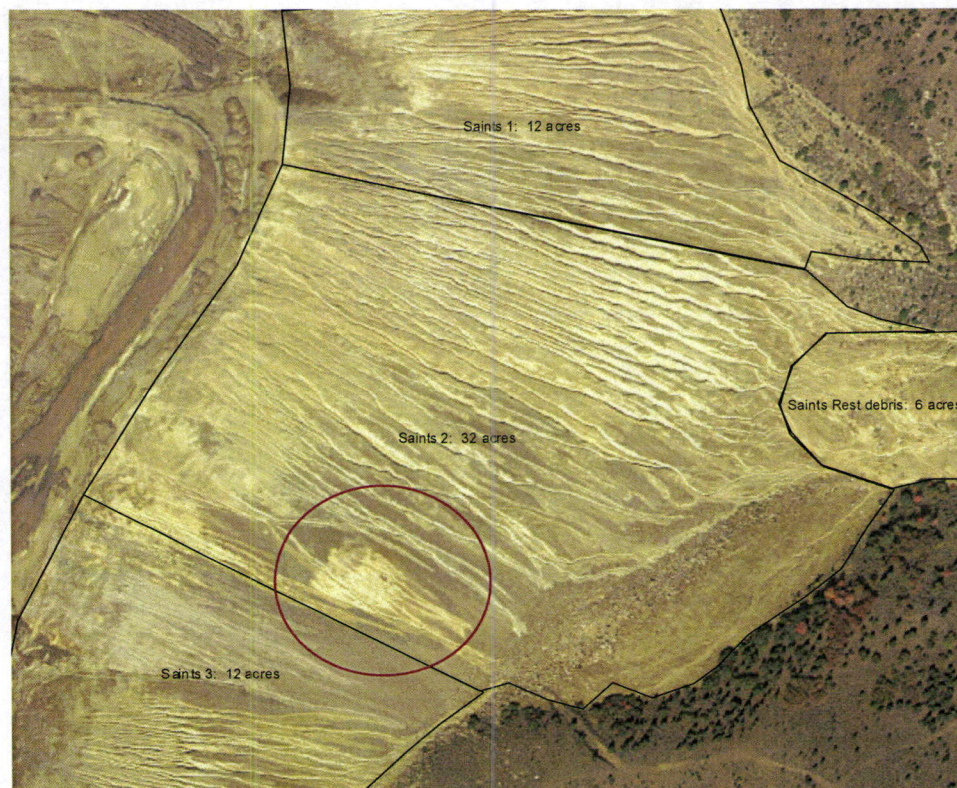
Figure A-16 - Severe erosion and rilling is shown on the 2003 aerial photograph. The red circled area may be indicating seepage from the previous base of the 1979 failure and has been stable since being back filled in 1979. The 2006 aerial photograph is not shown because of quality (albedo) issues.
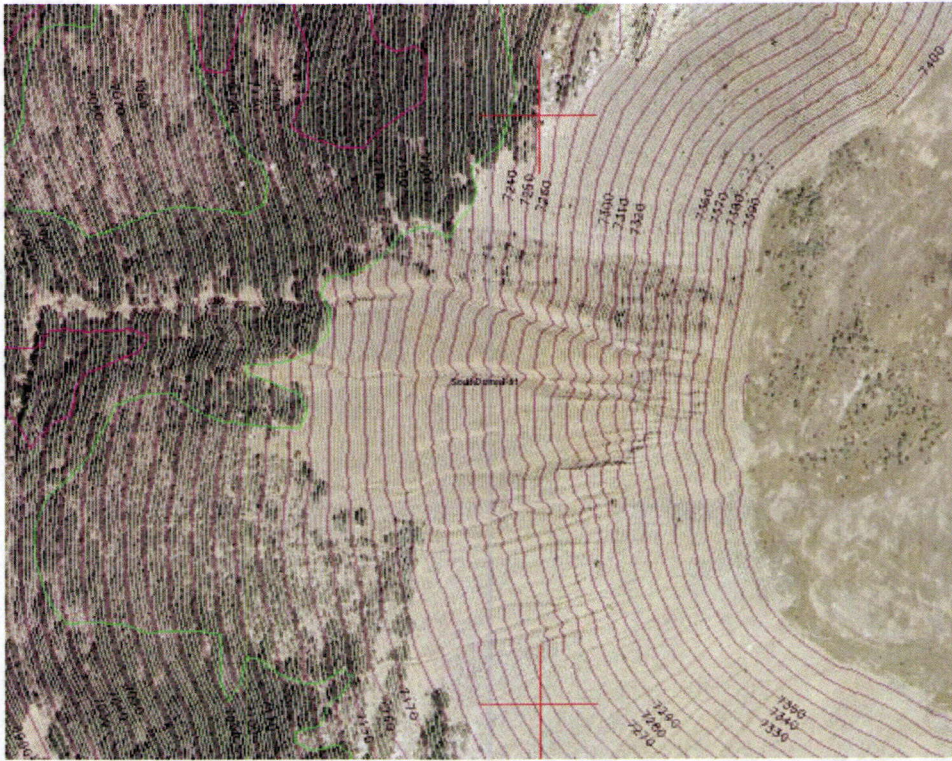
Figure A-17 - Saint's Rest dumps showing areas of concentrated erosion and scarring.

Dump Cross Sections

Cross sections were developed along the primary South dump drainages, as shown on Figure A-18. The average cross section used for the Dan-W analysis is also depicted by the heavy red line shown on this figure.
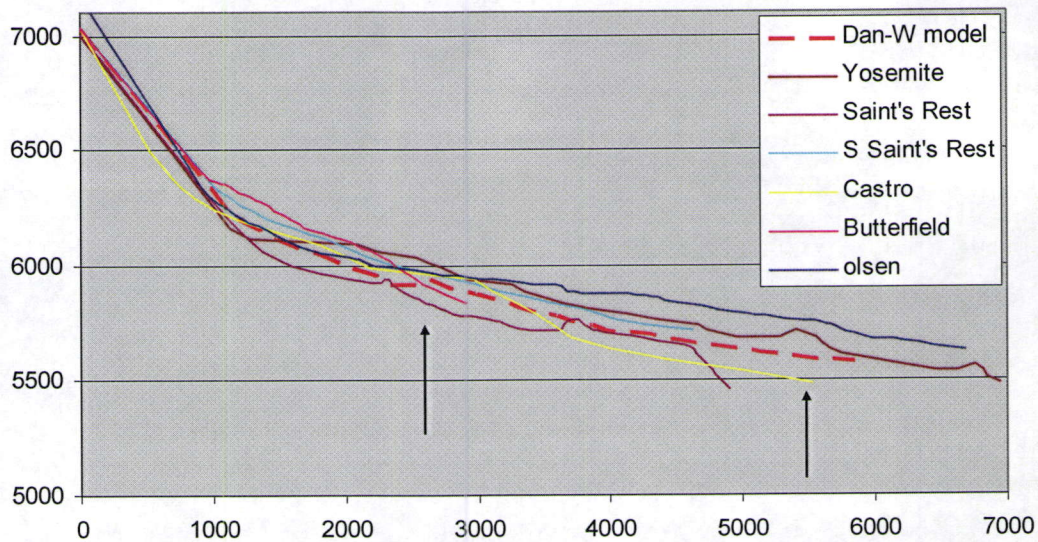
Figure A-18 - Comparison of South End drainage dump profiles

1. Calibration of Run-out Distance and Pore Pressure Parameter

The Yosemite and the "average" profile shown on Figure A-18 were used in combination with varying the pore pressure parameter, R_u. It was found that pore pressure parameter between 0.2 and 0.6 provided the only realistic runout distances that matched the case history observations. At pore pressure parameters below 0.2, the debris flows just travelled down the dump face. This condition is observed at numerous locations along the dump face. At R_u values greater than about 0.6, the debris flows became airborne after crossing the debris catch basins, a situation which has not been observed. Analyses indicate that the best calibration appears to occur in the narrow range between 0.4 and 0.45. A summary of the run out distance and R_u parameter is provided on Figure A-19.

Runout Distance Versus Ru
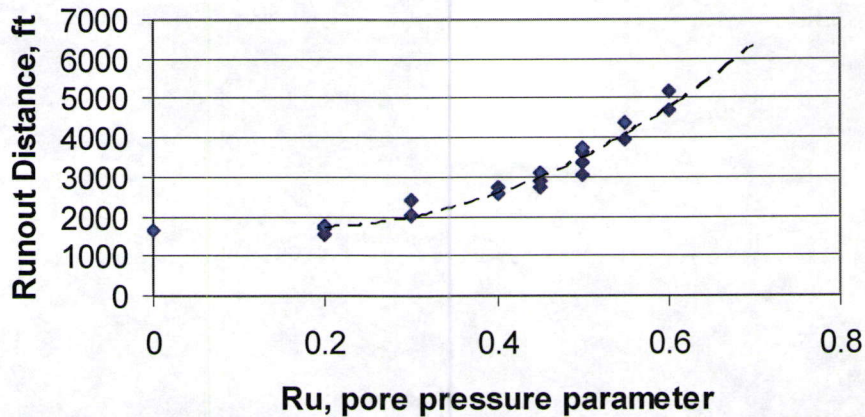
Figure A-19 - Run out distance versus pore pressure parameter, R_u

2. Gully Volumes

Following review of the above and other aerial photographs, estimates of the gully volumes were made from 2003 aerial photography. The 2003 photographs were used because of the clarity and availability of Cadd drawings as overlays. Volume estimates were made as follows:

- Cadd drawings and aerial imagery were georeferenced within ArcGIS (as shown on previous figures),

- The geometry of the gullies was estimated from the "V" shape of the contours, which reveal both the width and depth of the gully. The actual gully depth was corrected from the horizontal contour shape assuming a 37 degree dump slope.

- It was assumed that the cross section area of the gully was triangular in shape (as evidenced from the contours) and that the volume was the triangular cross section of the gully times its (incremental) length.

- These estimates were biased towards the "larger" visible gullies since accurate estimates of the smaller gullies could not be made from the available gullies.

Figure A-20 summarizes the gully volumes.

Gully volume versus location
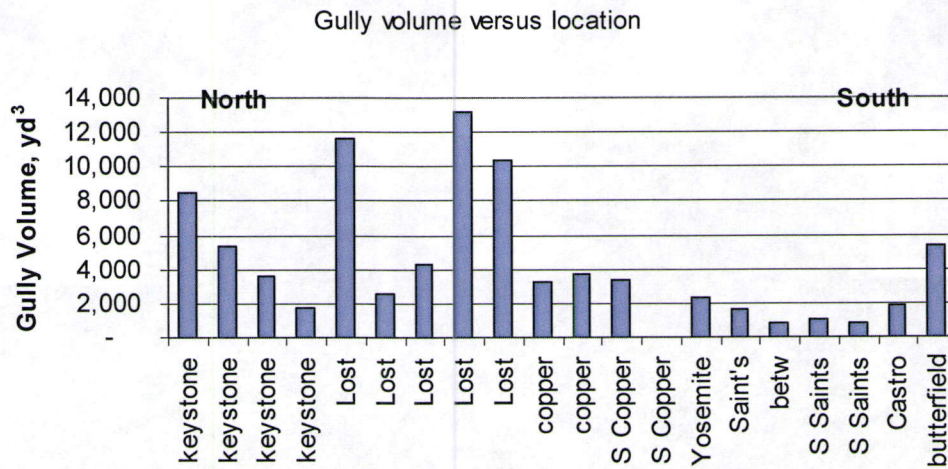
Figure A-20 - Gully volumes

It is apparent that the gully sizes appear to be larger in the higher Keystone, Lost Gulch and Copper drainages than in the south dumps. The gully volume versus dump heights is shown on the following figure A-21.

Gully Volume Versus Total Dump height

Note: At 50 ft bench heights; there are few gullies
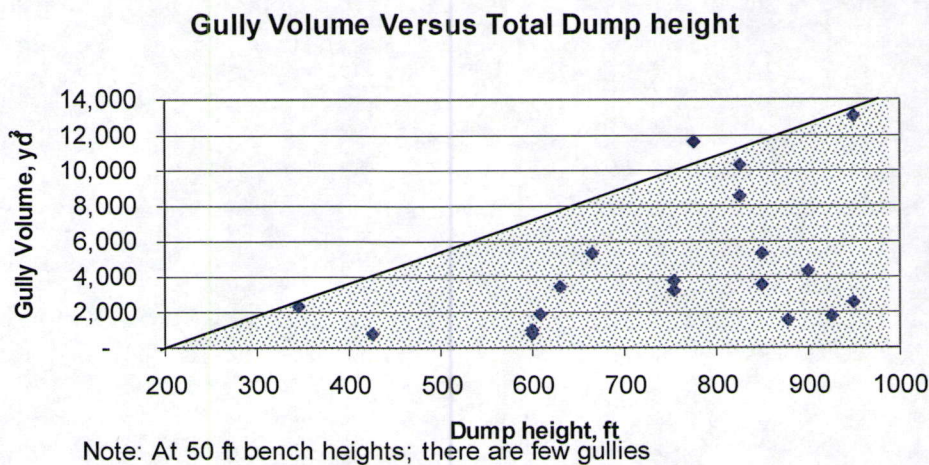
Figure A-21 - Relationship between dump height and maximum volume of gullies measured from aerial photography

Geometrically, it would be expected that larger gullies can result from higher dump heights. The inventory of the larger, recognizable gullies on the aerial photography indicates that this does appear to be the case. The following graph also indicates that the gully distribution is not a normal distribution, but has a number of larger gullies that extend beyond the mean gully size. The approximate normal distribution of the gullies is shown on figure A-22.

Distribution of Gully Volume
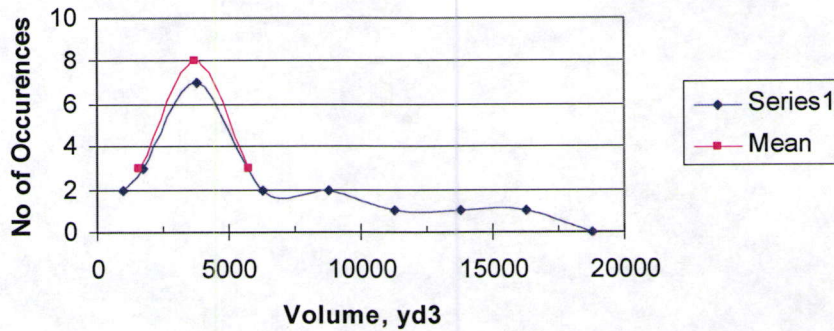
Figure A-22 - Distribution of gully sizes. The mean values shown are the mean and standard deviation of the gullies less than 7500 yd^3 in volume.

To evaluate the size of a typical medium to large size gully, the cross-sectional area and resulting cumulative volume of several typical gullies was calculated. It is observed that large gullies do not appear to form within the initial 400 feet of gully length. Thereafter, small to medium sized gullies tend to merge and become relatively large "scars." Figure A-23 shows the relationship between the length of the gully, the cross-sectional area (assumed to be triangular in shape) and the gully volume.

Individual Gully Area & Volume Vs Distance
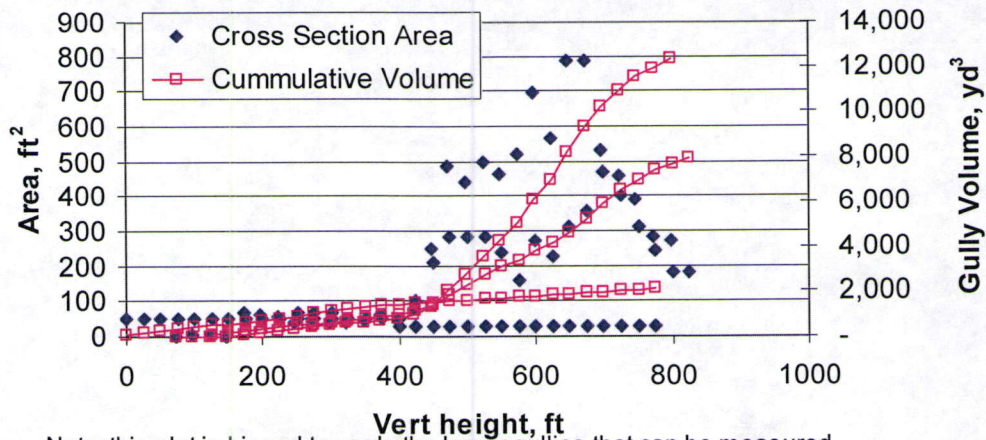
Note: this plot is biased towards the larger gullies that can be measured

Figure A-23 - Gully cross-sectional area and cumulative volume

It is noted that smaller gullies may not increase significantly in cross-sectional area or volume as they erode down the dump face.

To estimate the volume of material that is being eroded down the dump face over time, the typical small, medium and large erosion geometries calculated above were used. The method used to make this calculation involves a number of simplifying assumptions, as follows:

- The dump slope was divided into various areas within visually similar erosion features on the 2003 aerial photograph. A significant increase in the size and number of erosion gullies was observed on the 2003 aerial photographs as compared to prior photographs. However, it must be noted that the quality of the images and the resulting image resolution did vary.

- The dump face was divided into areas designated by orientation and drainage. The numbers of small, medium and large gullies identified on the aerial photographs were then counted. Based on measuring select gullies, the assumptions regarding the gully volume were as follows:
  - Small gully – 800 yd^3
  - Medium gully – 3200 yd^3
  - Large gully - 12,000 yd^3

- Based on the number of small, medium and large gullies counted within a specific area, the total volume of material that has eroded down from the dump face was estimated.

- Given the observation that very few gullies were observed in the 1983 aerial and a large number of gullies was observed in the 2003 aerial, the total volume of material eroded in gullies was divided by 20 years to calculate an annual erosion rate (based on gullies alone). The 20 year assumption is a critical assumption because it occurs in the divisor; however, it is the best estimate that we have available.

It was found that an average of 2.3 +/- 1.2 feet of material had been eroded down the dump face within a 20 year period. This translates to an average erosion rate of 0.11 +/- 0.06 ft/yr erosion. The resulting distribution of erosion rates is shown on Figure A-24.

Erosion Rate Vs Dump
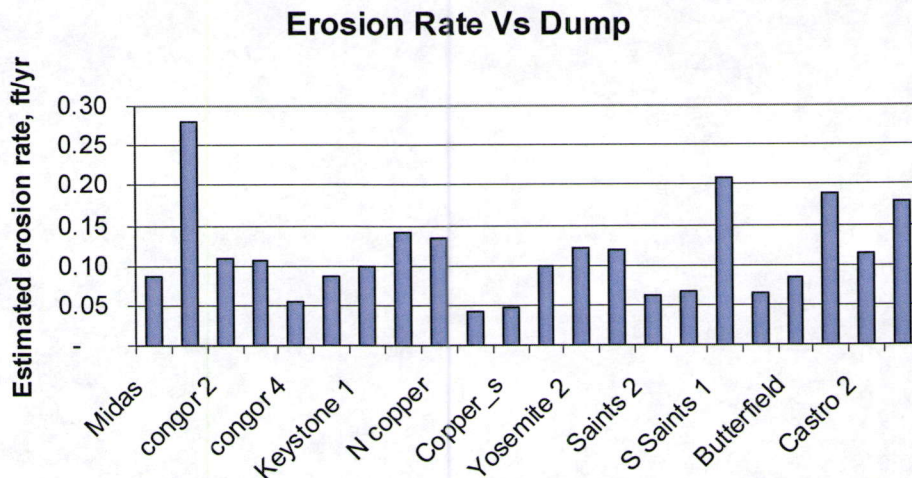
Figure A-24 - Approximate erosion rates by dump area

The anomalous, high erosion rate for one of the Midas dump areas is probably due to this being a continuous channel for surface water flowing down the dump face. Erosion rates for the predominantly quartzite rock north dumps average about 0.11 ft/yr and erosion rates for the southern dumps are only slightly higher at 0.12 ft/yr.

The erosion rate based on dump exposure or orientation was also calculated. It was found that the erosion rate for the east and northeast facing dumps averages about 0.12 ft/yr and the erosion rate for the southeast facing dumps averages about 0.09 ft/yr. This would be expected given the varying micro-climatic conditions between the north facing slopes and the south facing slopes. It is therefore likely that slope orientation is more important than dump composition in the actual erosion rate.

Attachment B – July 27th Debris Flow Observations

(Previous memorandum re-printed with revised figure numbers)

Date: August 2, 2007   **Project:** 12094

To: Kelly Payne, Vicky Peacey, Brian Vinton, Jack Bloom, Zip Zavodni

From: J. Pilz

Subject: July 27, 2007 debris flow observations

Dear Kelly,

The following documents observations made on August 1 in regards to the July 27 debris flow and thoughts regarding a path forward in evaluating the dump erosion and gullying issue.

Observations regarding the July 27 debris flow
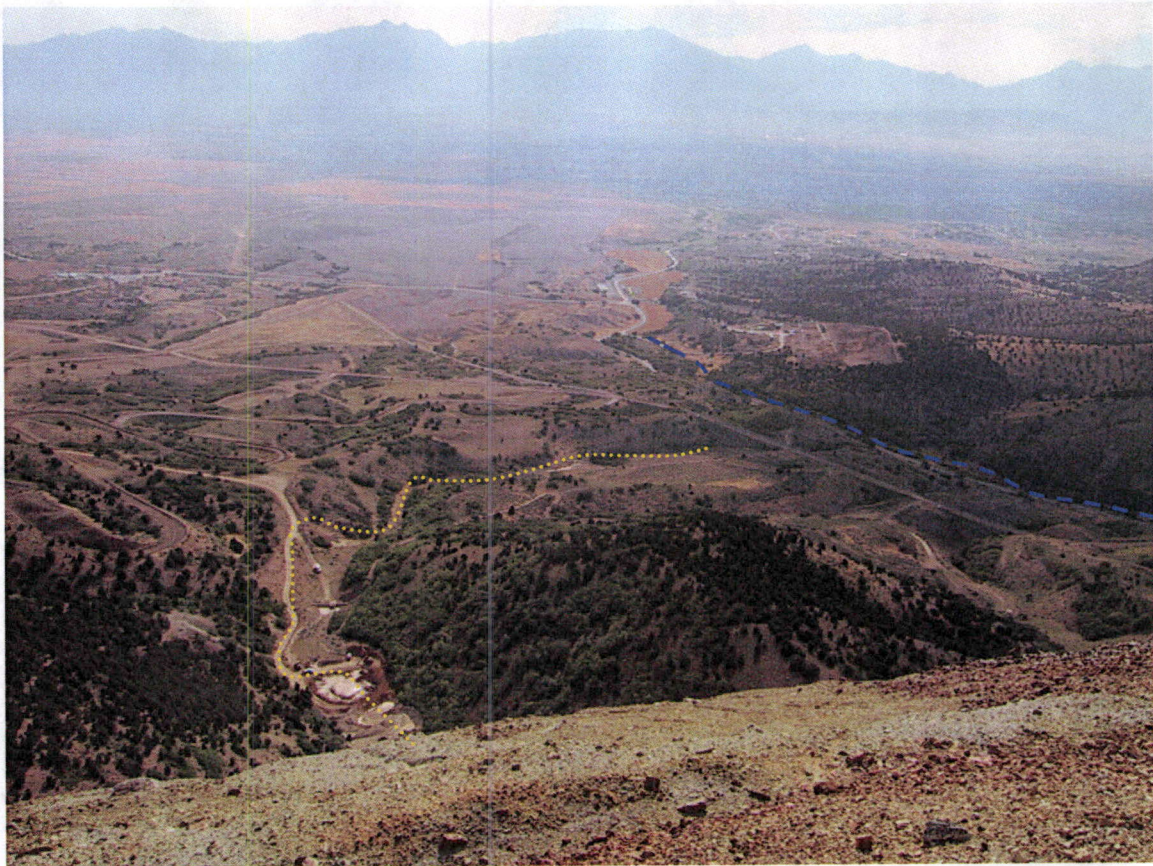
Figure B-25 - View eastward and downward from the Yosemite dump crest. The approximate path of the debris flow is indicated in yellow, along with location of Butterfield Creek by the blue line.

The July 27 debris flow is attributed to a concentrated thunderstorm event. The debris eroded down the numerous rills and gullies on the dump. There was no evidence that surface water overtopped the dump edge, causing concentrated flow from the crest. However, it was reported that the dump crest was very "spongy" immediately following the debris flow, indicating near saturation.

Figure B-26 - View of settlement cracks / surficial movement at crest of dump. There is abundant evidence that shallow slips of the surface continue to occur. Tension cracks are sometimes observed as far back as 500 feet from crest. Cracks tend to "heal" themselves over time (close up). Survey monuments situated up slope of these cracks settled 3 ½ to 4 ½ inches from Oct 2005 to April 2007. This is less than the 6 inches of average settlement during the period. Displacement along these scarps is obviously much greater and on the order of feet. It is also possible that this terraced topography is reducing over-land flow velocities so that gullying and erosion does not occur at the dump crest.

Figure B-26 shows the dump crest on August 1. The dump crest features are indicative of an "infinite slope" slip surface where the factor of safety of the slope is equal to the tangent of the angle of repose divided by the tangent of the friction angle. When the material becomes saturated, this factor of safety reduces by the ratio of the buoyant to saturated unit weight, as shown on the following equations. The measured slope angles at the top of Yosemite varied from about 29 to 33 degrees, which is less than the typical 34 to 37 degree friction angle for these materials. This suggests that movement due to saturation has occurred.

$$FS = \frac{Tan\phi}{Tan\beta}$$

where,

ϕ = the angle of internal friction for the soil

β = the slope angle relative to the horizontal

$$FS = \left(\frac{\gamma_b}{\gamma_s}\right)\frac{Tan\phi}{Tan\beta}$$

where,

γ_b = the buoyant unit weight of the soil

γ_s = the saturated unit weight of the soil

Also, it is known that perched water table conditions exist within both the Yosemite and Castro dump, as shallow as 10 – 15 feet below the dump surface. If these perched water table conditions were to day light or come close to the slope face, this could partly explain the surface movements.

Figure B-27 - Debris flow material in basin up slope of the east side collection cut off wall. Material is a classic debris flow, consisting of viscous gravel, sand, silt and clay. The majority of the coarse particles were contained within the basin.

Figure B-28 - View from embankment supporting the east side collection pipeline. At this point, the debris flow only transported the finer grain size sand, silt and clay. Some of this material was transported through a culvert at the base of the embankment toward Butterfield Creek.

Figure B-29 - Erosion gullies and rills extending down the face of the gulch. The gullies and rills generally do not extend to the dump crest, rather begin about 10 to 20 percent down the face of the dump.

As shown in Figures B-27 and B-28, the debris flow material consists of angular, fully saturated gravel, sand, silt and clay particles. The actual erosion gully which transported the July 27 debris down the dump face could not be identified (see Figure B-29). A typical debris flow "scar" from which the majority of the material was transported is not visible in this particular area. The crest of the dump gives the "appearance" of having a higher moisture content (greenish hue on photo), but this is not certain. The very dark colored areas on the photo are coarse rock (this is not a change in moisture).

Attachment C – Dan-W Manual

DAN-W RELEASE 4
DYNAMIC ANALYSIS OF LANDSLIDES

O. Hungr Geotechnical Research Inc., January 25, 2004

4195 Almondel Rd., West Vancouver, B.C., Canada, V7V 3L6

USER'S MANUAL

DAN-W

DYNAMIC ANALYSIS OF LANDSLIDES

O. Hungr Geotechnical Research Inc.
4195 Almondel Rd., West Vancouver
B.C., Canada, V7V 3L6
Tel. (604) 926-9129

TABLE OF CONTENTS

A   INTRODUCTION

A.1 Purpose and Limitations

DAN-W is a windows-based program used to model the post-failure motion of rapid landslides. It implements a Lagrangian solution of the equations of motion for a mass of earth material which starts from a prescribed static configuration and flows according to one of several rheological relationships.

IMPORTANT NOTICE: DAN-W is a tool suitable for estimating the runout behaviour of landslides on the basis of specific data on geometry and material properties, supplied by the program user. The results of the calculations are entirely dependent upon the data provided by the user. Therefore, persons using the program to make runout estimates should be geoscience professionals thoroughly familiar with landslides, soil and rock material behaviour and rheology, who have also studied the relevant references as listed on page 48 of this manual. The properties entered into the program should always be checked by back-analysis of real landslide case histories similar to the existing or potential landslide being studied. The results of the analysis should never be relied on exclusively, but should be interpreted carefully by a qualified person in the light of field observations, other analyses and appropriate judgment and experience.

DAN-W is based on shallow flow assumptions. The solution may be unstable in certain cases where the flow is deep, or where abrupt changes of slope occur. If the solution shows signs of instability such as the appearance of irregular or translatory waves, the results should not be trusted. In many cases, such problems can be overcome by using a smaller number of reference blocks, shorther time interval or switching between vertical and normal geometry. (The normal geometry is usually considered superior).

NOTE: While operating DAN-W on certain computers outside North America, please do not forget to set your system to recognize dot, rather than comma, as the decimal symbol. To do this, please go to Control Panel, Regional Settings.

A.2 Theory

The following paragraphs are a summary of the theory described in Hungr (1995). It is strongly recommended that the user read these references to obtain a more detailed understanding of DAN-W.

The dynamic model DAN-W is based on the Lagrangian solution of St. Venant's equation. This equation can be derived by applying conservation of momentum to thin slices of flowing mass that are perpendicular to the base of the flow. These "boundary blocks" divide the slide mass into n "mass elements" of constant volume. The resulting formula for the net driving force acting on each boundary block i is:

$$F = \rho \, g \, H_i \, ds \, B_i \, sin\theta - T - P \qquad\qquad [1]$$

where: F = net driving force = $\rho \, H \, ds \, B \, dv \, / \, dt$

3

ρ = bulk density of the flow material
H = flow depth normal to base
B = channel width
ds = infinitesimal length of boundary block
θ = angle of base from horizontal
T = resisting shear force on base
P = tangential internal pressure
v = mean flow velocity

Eq. 1 can be solved for successive time steps after the initial at-rest condition of the slide mass. For a single time step of Δt and a unit length for ds, the change in velocity of each boundary block is:

$$\Delta v = g \, (F \, \Delta t - M) \, / \, (\gamma \, H_i \, B_i) \qquad [2]$$

where: γ = unit weight of the boundary block = $\rho \, g$

F is the net force as defined in eq. 1. M is a momentum flux term caused by erosion or entrainment of material, as discussed below. The velocity change can be represented by the difference between the new velocity at the end of time step Δt and the old velocity.

Now, integrating eq. 2 over the same time step Δt, gives the curvilinear displacement S of each boundary block:

$$S_i = S_{i, \, old} + \Delta t \, / \, 2 \, (v_i + v_{i, \, old}) \qquad [3]$$

This result can be used in conjunction with the constant volume constraint to find the new height of each boundary block, defined by the mean depth h of adjacent mass elements j - 1 and i:

$$H_{i, \, new} = (h_{j-1} + h_j) \, / \, 2 \qquad [4]$$

where: $h_j = 2 \, V_j \, / \, [(S_{i+1} - S_i) \, (B_{i+1} + B_i)]$
V_j = constant volume of boundary element j

Note that DAN-W uses triangular end elements, therefore, the height of the first and last boundary blocks, respectively, is $h_1 \, / \, 2$ and $h_{n-1} \, / \, 2$.

The flow resistance term, T

The basal flow resistance term, T, in eq. 1, is governed by the rheology of the material. Eight rheologies are available in DAN-W. They are outlined below along with their appropriate equations for T. A more detailed discussion can be found in Hungr (1995).

1. *Plastic flow*: Flow controlled by a constant shear strength c:

4

$$T = cA_i$$

where: A_i = boundary block base area = $ds \, B_i$

2. *Friction flow*: Flow controlled by the effective normal stress on the base of the boundary block:

$$T = A_i \, \gamma \, H_i \, (cos\theta + a_c / g) \, (1 - r_u) \, tan \, \varphi$$

where: a_c = centrifugal acceleration = v_i^2 / R
R = vertical curvature radius of path
r_u = pore-pressure coefficient = ratio of pore pressure to total normal stress at base of boundary block
φ = friction angle

3. *Newtonian flow*: Viscous flow where T is a linear function of velocity:

$$T = 3 \, A_i \, v_i \, \mu / H_i$$

where: μ = dynamic viscosity of fluid

4. *Turbulent flow*: Flow where T is a function of velocity squared:

$$T = A_i \, \gamma \, v_i^2 \, n^2 \, H^{1/3}$$

where: n = roughness coefficient

5. *Bingham flow*: Flow where T is a function of flow depth, velocity, constant yield strength and Bingham viscosity:

$$v_i = 1/6 \, H_i / \mu \, (2T / A_i - 3\tau + \tau^3 \, A_i^2 / T^2)$$

where: μ = Bingham viscosity
τ = constant yield strength

6. *Coulomb viscous flow*: Bingham flow with a yield strength dependent on the normal stress:

$$\tau = \gamma \, H_i \, (cos\theta + a_c / g) \, (1 - r_u) \, tan \, \varphi$$

where: parameters are the same as for a friction flow

7. *Power Law*: Based on Fread (1988):

$$T = A_i \, H_i \, \mu \, [(R + 2) \, v_i / H_i^{(R+1)} + (R + 2) \, (\tau / \mu)^R / (2 \, H_i^R)]^{1/R}$$

where: $R = 1 / R_b$
R_b = power law exponent
μ = viscosity

8. *Voellmy fluid*: Flow where T contains a friction term and a turbulent term:

$$T = A_i \left[\gamma \, H_i \, (cos\theta + a_c / g) \, tan \, \varphi + \gamma \, v_i^2 / \xi \right]$$

where: ξ = turbulence coefficient
other parameters are the same as for a friction flow

The internal pressure term, P

The internal pressure term, P, in eq. 1, is determined by assuming that the flow lines are parallel to the slide path and that the pressure increases linearly with depth:

$$P = -k \, \gamma \, (dh / ds) \, (1 + a_c / g) \, H_i \, B_i \, cos\theta \, ds$$

where: a_c = centrifugal acceleration = v_i^2 / R
$k_i \, (dh / ds) = 1 / 2 \left[k_j \, (h_j - H_i) / (s_j - S_i) + k_{j-1} \, (H_i - h_{j-1}) / (S_i - s_{j-1}) \right]$
s_j = curvilinear displacement of each mass element centre
k_j = lateral pressure coefficient (= 1 under hydrostatic conditions)
$= k_{j, \, old} + S_c \, \Delta\varepsilon_j$
S_c = stiffness coefficient
$= (k_p - k_a) / 0.05$ (for compression)
$= (k_p - k_a) / 0.025$ (for unloading)
$\Delta\varepsilon_j$ = incremental tangential strain in each mass element
$= \left[(S_{i+1} - S_i) - (S_{i+1, \, old} - S_{i, \, old}) \right] / (S_{i+1, \, old} - S_{i, \, old})$

The passive and active tangential pressure coefficients, k_p and k_a are determined based on the internal frictional strength of the sliding body (Savage and Hutter, 1989).

The momentum flux term, M

The momentum flux term is based on how much material is deposited or entrained by the slide mass. A total erosion / deposition depth is specified, and as each mass element passes over a single point on the path profile, a fraction of this depth (and hence, volume) is eroded or deposited by the slide. The total erosion depth is only reached once the whole slide mass has passed over the point. As the path is deposited or entrained, the volume of each mass element is increased or decreased by the volume of material eroded or deposited, respectively. A the same time, the momentum flux term is set to:

$$M = \Delta m \, v$$

where: Δm = is the increment of mass picked up during each time step

$$v = \text{mean velocity}$$

Note that this momentum term is zero for deposition of material (see Hungr, 1995, page 616).

A.3 Precautions

- DAN-W is a shallow-flow solution. Highly curved slopes are not recommended for analysis with deep slide masses. DAN-W has the option of using slices that are either vertical or normal to the path profile. If the walls of the boundary blocks are drawn normal to the slope profile, a highly curved slope will cause the top surface to loop on itself if it is too deep, creating an incorrect geometry, as shown in Figure 1 (a) and (b). Vertical slices do not have this problem, however, it is not recommended that they be used on steep slopes because their geometry becomes very stretched as shown in Figure 1 (c).

- Large time steps are more prone to instability caused by numerical divergence of the solver. It is recommended that while testing a problem, a larger time step be used, however a smaller time step should be used for the final analysis.

- In order to prevent instability, a smaller time step should be used when a large number of mass elements are chosen. If instability cannot be prevented, the user should try to draw a smoother path. Seriously unstable analyses should not be trusted.

- DAN-W graphics do not implicitly show the decoupling of a slide mass when the peak of a hill is reached and one part of the mass flows down one side while the other flows down the opposite side. Note that the model accounts for this decoupling, however the graphics do not, so there is a straight line drawn between the two material accumulations.

- Running the front of a slide mass past the extents of the path geometry can result in solution instability. It is recommended that a sufficient runout be included in the path profile to prevent flow beyond the extents.

- CAUTION: Please ensure that the copy you are using is Release 4 or later. Previous releases contained an error which would lead to overestimation of runout in cases where strong entrainment of material is specified, together with frictional rheology.

A.4 Problem Size Limits

- Maximum number of materials: 20
- Maximum number of boundary blocks: 59
- Maximum number of geometry input points: 100

(a)

Vertical slices   Normal slices (same data)

(b)

Vertical slices   Normal slices (same data)

(c)

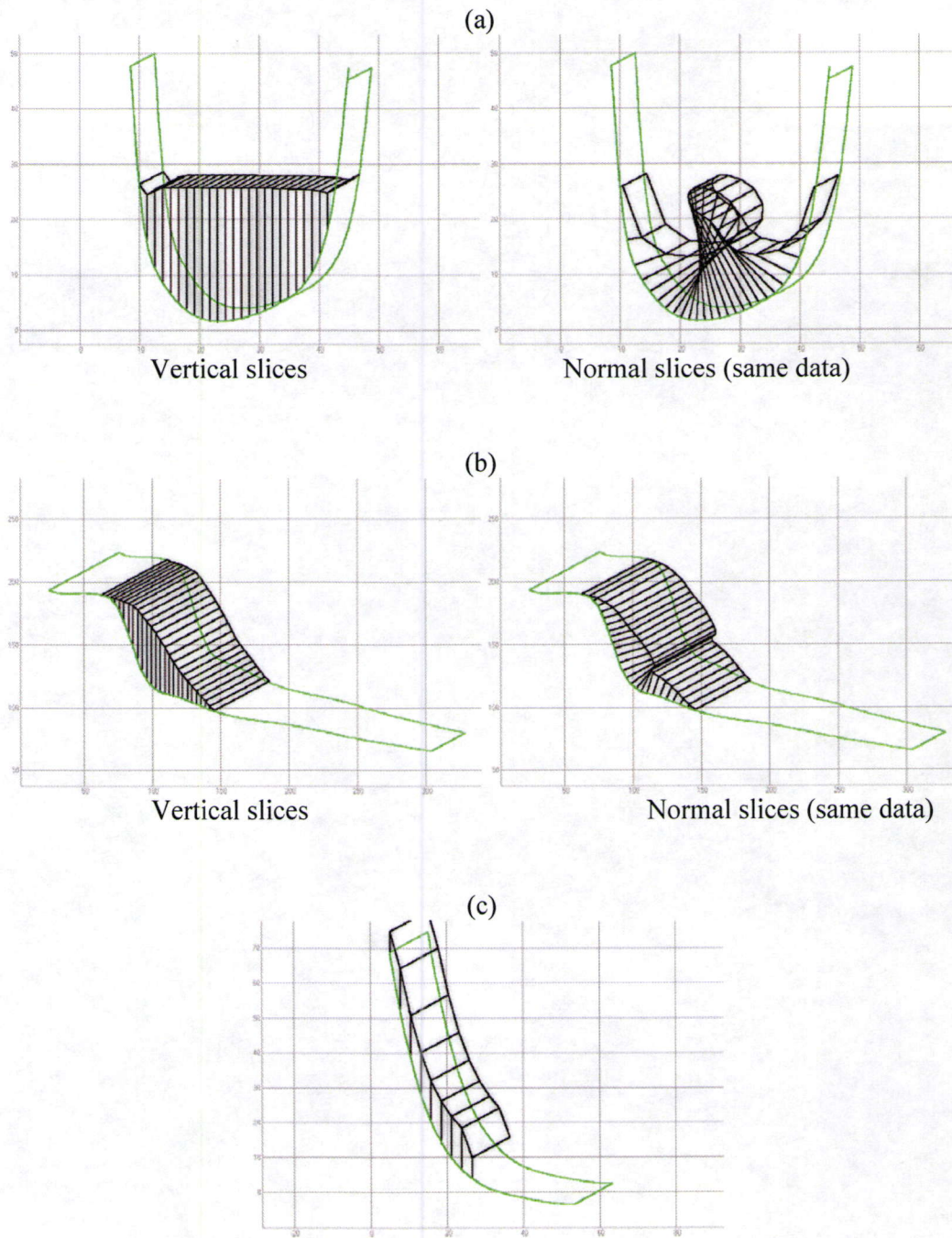*Figure 1*: *Examples of the kinds of geometrical discrepancies and errors caused by deep slide masses or steep slopes. (a) An exaggerated example showing how the use of normal slices in a highly curved slope can cause the slide mass to loop on itself. (b) A more practical example of the above. (c) An example of how the mass elements become stretched in a steep-slope problem that uses vertical slices.*

B   PROGRAM ORGANIZATION

B.1 Program Layout

DAN-W is split into three main components: data input, analysis, and data output. The data input component allows the user to define the problem geometry, material properties, and analysis options. Once the problem is defined, the user can run an analysis. Data is collected during the analysis and can be output in various ways after the run is complete.

B.2 Coordinate System

The coordinate system used in DAN-W varies throughout the program. The main screen shows an isometric view of the slope profile and flowing mass. Horizontal distance, in metres, is shown from left to right, while elevation, also in metres, is shown from bottom to top. In the three-dimensional configuration, the width of the channel is drawn in an isometric view defined by a projection angle (see Section C.9).

During data input, the screen's coordinate system changes depending on the data being input. When inputting the slope and flowing mass's profiles, the horizontal axis shows horizontal distance from left to right, while the vertical axis shows elevation. When inputting the channel width, the vertical axis changes to width, in metres.

SLIDING DIRECTION:
It is important to note that the program was designed primarily for a sliding direction of left to right. Therefore, a mass flowing from left to right will result in positive velocities while a mass sliding from right to left will result in negative velocities. It is recommended that the problem be designed such that the sliding mass begins on the left side and flows to the right of the screen.

B.3 2D / 3D Configurations

DAN-W has a two-dimensional as well as a three-dimensional configuration. The two dimensional configuration consists of a unit channel width. The three-dimensional configuration allows for a varying channel width along the length of the slope. To read about how to change configurations, please refer to the Section C.4. For details on how channel width is defined, refer to Section C.8, Section C.1, and Section D.1.

B.4 Opening and Saving Data Files

Problems created in DAN-W can be saved under the file extension *.DNW. An ASCII character file is saved containing all the input data, including problem geometry, material properties, and material locations. Files created in the DOS version of DAN (file

extension *.DAN) can be opened by DAN-W. However, some data may be incomplete and all data should be checked.

To save a *.DNW file, choose the *File-Save* or *File-Save As* menu selection in the main menu. To open a *.DNW file, choose the *File-Open* menu selection. To open a *.DAN file, choose the *File-Open .DAN* menu selection.

B.5 The Main Menu

The program is controlled primarily through the Main Menu, which allows the user to access the data input/edit screens, run an analysis, and control the output of data during analysis. The Main Menu returns at the conclusion of each function. The following is a list of all the options found in the Main Menu with a short description of each:

- *File*: The items under this menu deal with file manipulation.
  - *File-New*: Opens a new file with all the data either empty or set to a default value. Also initializes the New-File Sequence (see Section C.3) that guides the user through all the necessary data input screens. Shortcut key: Ctrl+N.
  - *File-Open*: Allows the user to open a previously saved *.DNW file. Shortcut key: Ctrl+O.
  - *File-Open .DAN*: Allows the user to open a *.DAN file previously created and saved in the DOS version of DAN.
  - *File-Save*: Saves the current problem in the current directory and under the current *.DNW file name. Shortcut key: Ctrl+S.
  - *File-Save As*: Allows the user to save the current problem in any available directory as a *.DNW file.
  - *File-Exit*: Ends and closes DAN-W.
- *Edit*: The items under this menu allow the user to access the various data input/edit screens as well as the options screen. This menu is enabled only when a file is loaded.
  - *Edit-Control Parameters*: Opens the Control Parameters Screen (see Section C.4) which allows the user to input and modify the current file's identifying labels and problem boundaries, define the number of materials and boundary blocks, and choose a cross-section shape factor, a 2D or 3D configuration, end conditions and the uniform thickness option.
  - *Edit-Material Properties*: Opens the Material Properties Screen (see Section C.5) which allows the user to choose the rheology of each material and input/edit each material's relevant properties. This screen also allows the user to add and delete materials.
  - *Edit-Material Locations*: Opens the Material Locations Screen (see Section C.6) which allows the user to define where the various materials are located along the slope profile.
  - *Edit-Path*: Opens the Edit Path Screen (see Section C.7) which allows the user to input/edit the slope profile.

- *Edit-Top*: Opens the Edit Top Screen (see Section C.7) which allows the user to input/edit the initial flowing mass profile.
- *Edit-Width*: Opens the Edit Width Screen (see Section C.8) which allows the user to edit the width of the channel. This item is only available in the three-dimensional configuration.
- *Edit-Options*: Opens the Options Screen (see Section C.9) which allows the user to change various boundary, display, and analysis options.

- *Solve*: This menu accesses the analysis component of the program. It is enabled only when a file is loaded.
    - *Solve-Calculate*: Activates the Run Control Box (see Section D.3) which allows the user to run an analysis of the problem. Shortcut key: Ctrl+R.

- *Output*: The items under this menu deal with data output. This menu is enabled only when a file is loaded.
    - *Output-Report*: Displays a report (see Section E.1) summarizing the most recent analysis.
    - *Output-Export ASCII Graph Files*: Allows the user to choose at what time intervals data is to be collected and placed into ASCII files (see Section E.3).
    - *Output-Observation Point-View Data*: Displays plots of the velocity and the thickness of the sliding mass at a pre-specified location along the path, as functions of time. This item is only available when the Observation Point (see Section E.5) option is chosen in the Options Screen.
    - *Output-Observation Point-Export Data*: Allows the user to export the velocity and thickness data collected at the Observation Point to an ASCII data file. This item is only available when the Observation Point option is chosen in the Options Screen (see Section C.9).
    - *Output-Copy to Clipboard*: Copies the current image on the main screen to the clipboard. In the *Depth-Profile* mode, the two graphs shown are separate images. To copy either of these graphs, click on the desired graph and then select this menu option. Shortcut key: Ctrl+C.

- *View*: The items under this menu allow the user to change the main-screen view from a three-dimensional isometric view of the problem to a two-dimensional depth profile.
    - *View-Isometry*: Displays in the main screen a three-dimensional isometric view of the problem, as described in Section D.1.
    - *View-Depth Profile (2D)*: Displays in the main screen a two-dimensional depth profile showing the sliding mass's current velocity and thickness distributions, as described in Section D.1.
    - *View-View Options*: Gives rapid access to the 'display' portion of the Options Screen (see Section C.9).

- *Help*: Provides access to the DAN-W Help system, as well as copyright information.

C.1 Data Preparation

Before creating a data file for analysis in DAN-W, the user should be aware of the following assumptions used by the model:

- All geometry is two-dimensional. The slope and top surface profiles do not vary along the width of the channel.
- The direction of flow of the slide mass is parallel to the two-dimensional plane used to define the slope profile (i.e. from left to right of the screen).
- The top surface geometry has a rectangular lateral cross-section defined by the hydraulic depth of the slide mass and the channel width at that location along the slope.
- The slide mass is assumed to be a homogeneous "apparent fluid" with consistent rheology throughout.

For more detailed assumptions used in this model, please refer to Hungr (1995).

Given these assumptions, the geometry of the problem can be prepared. To create the slope profile, an elevation versus horizontal distance coordinate system should be setup with its origin just to the left of the up-slope extremity of the initial slide mass and just below the lowest point of the slope. In this way, the origin will appear in the lower left corner of the screen with the slope profile in the centre of the screen, as shown in Figure 2. A reasonable number of data points containing elevation vs. horizontal distance along the slope from the source to beyond the expected runout should then be chosen.

IMPORTANT NOTE: The input profile should be made reasonably smooth to avoid instability. Do not use too many points and avoid details such as minor steps in the profile. Round out abrupt slope changes. The user should test the influence of such simplification (usually it has relatively small effect on the results).
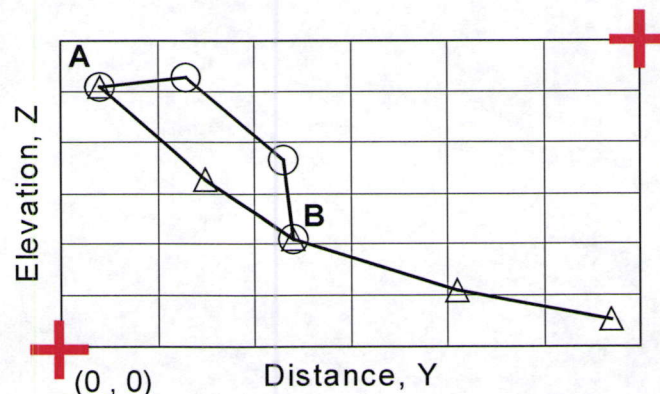

Figure 2: Vertical cross-section of a simple profile showing the layout of the coordinate system and the position of the origin. Triangular data points represent the slope profile and circular data points represent the slide mass profile. Note that point A is the initial time zero rear of the slide mass, while point B is the initial time zero front of the slide mass.

To create the top profile, the same coordinate system is used as defined for the slope profile. Once again, elevation versus horizontal distance data points should be chosen in the same way as described above. Note that the elevation values will represent the hydraulic depth of the slide mass.

> NOTE:
> The user should choose the central or deepest profile of the initial slide mass to define its geometry with. The cross-section shape factor can then be used to compensate for the actual cross-sectional shape of the channel, resulting in a reasonable approximation of the hydraulic depth, as illustrated in Figure 3. Please refer to Section C.4 for more details.
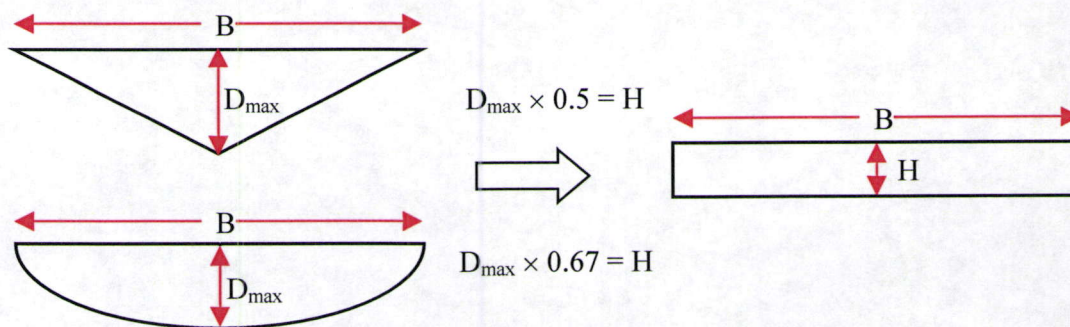
Figure 3: Illustration of how DAN-W uses the cross-section shape factor to convert the maximum depth of a non-rectangular channel (D_{max}) to the corresponding hydraulic depth (H). B is the channel width.

It is recommended that the front and the rear of the initial slide mass coincide with data points on the slope profile (see Figure 2).

For the three-dimensional configuration, width data is defined by the top-surface width of the channel as a function of the same horizontal distance axis as described above. Enough data points should be taken to sufficiently approximate the width profile of the channel.

Next, data on the properties of the various materials encountered on the slope must be prepared. Each material must be approximated by one of the provided rheologies, as described in the Section A.2 and Section C.5. The beginning and ending locations of each material along the profile of the slope must also be determined. These locations must correspond to data points on the slope profile.

C.2 Problem Geometry Setup

Once the data input is complete, DAN-W constructs the problem's geometry by interpolation. A smooth slope profile is created by interpolating between data points using the spline function. The top surface profile, on the other hand, is created by linear interpolation between the data points. This surface is then split into the chosen number of equally-spaced boundary blocks.

WARNING:
DAN-W is a shallow-flow solution. Highly curved slopes are not recommended for analysis with deep slide masses. DAN-W has the option of using slices that are either vertical or normal to the path profile. If the walls of the boundary blocks are drawn normal to the slope profile, a highly curved slope will cause the top surface to loop on itself if it is too deep, creating an incorrect geometry. Vertical slices do not have this problem, however, it is not recommended that they be used on steep slopes because their geometry becomes very stretched. Refer to Figure 1 for details.

C.3 New File Sequence

The New File Sequence, accessed through *File-New* in the main menu, or from the startup screen, is a sequence of screens that guides the user through all the data input steps that are required to create a new file. Once the sequence is complete and the user is returned to the main screen, the problem is sufficiently defined to allow for proper analysis. The sequence of screens is as follows:

1. Control Parameters screen.
2. Material Properties screen.
3. Edit Path/Top screen.
4. Edit Width screen (this screen is skipped if the 2D configuration was chosen in the Control Parameters screen).
5. Material Locations screen (this screen is skipped if only one material was chosen in the Control Parameters or Material Properties screens).

These screens can be visited individually after the sequence is finished. Note that the Edit Path/Top screen cannot be exited until sufficient geometry data points are entered for both the slope profile and the top surface. Also note that if the *Cancel* option is chosen from the menus in the Control Parameters and Material Properties screens during the New File Sequence, then the new file will be closed and exited without being saved.

C.4 Control Parameters Screen

The Control Parameters screen, shown in Figure 4, is accessed through the *Edit-Control Parameters* option in the main menu. It is also the first input screen in the New File Sequence. This screen is used to input or edit the problem's identifying labels, geometry extents, and other fundamental parameters.

Figure 4: Control Parameters screen.

The following is a list of the input labels found on this screen and a description of each:

- PROJECT: Optional. Any alphanumeric string of any length representing the name of the project.
- DATA SET: Optional. Any alphanumeric string of any length representing the data set used in the project.
- INPUT BY: Optional. Any alphanumeric string of any length representing the user's name.
- DATE: Automatically updated to the system's calendar. Can be changed to any string.
- UNIT WEIGHT OF WATER: Initially set to 9.81 kN/m^3. All units are henceforth in SI metric units, including: metres (m), kilonewtons (kN) and kilopascals (kPa). The Imperial units option is disabled in this version of DAN-W.

- **NUMBER OF MATERIALS:** The number of materials or rheologies used in the problem. There must be at least one material. The maximum number of materials is 20.

- **NUMBER OF ELEMENTS:** The number of constant-volume mass elements that the slide mass is split into for analysis. There must be at least one element. The maximum number of elements is 59. Note that to prevent instability due to numerical divergence and to increase precision, the more mass elements used, the smaller the time step should be during analysis.

- **CROSS-SECTION SHAPE FACTOR:** A factor that accounts for the shape of the channel cross-section. It is defined as the ratio between the hydraulic (average) depth and the maximum depth of the channel cross-section. For example, a triangular channel has a factor of 0.5 and an elliptical channel has a ratio of 0.67, as illustrated in Figure 3. A rectangular channel has a factor of 1. This factor allows the user to input the geometry of the slide mass based on the maximum channel depth. DAN-W then uses the factor to convert the data to the required hydraulic depth. For more details, please refer to Section C.1 and Hungr (1995). The factor must be greater than zero.

- **SET PROBLEM EXTENTS:** The problem extents, described in Section C.1, are defined by the coordinates of the bottom left and upper right corners of the problem, as indicated by the graphic on this screen.

- **UNIFORM THICKNESS:** Optional. Allows the user to enter a uniform thickness (in metres) for the top surface geometry. If chosen, DAN-W will create a top surface that will have the defined uniform thickness everywhere above the slope. Note that this thickness is measured parallel to the type of slices used (normal or vertical). Please refer to Section C.7 for further details.

- **CONFIGURATION:** Allows the user to choose between the two-dimensional configuration and the 3-dimensional configuration. A problem with a 2D configuration has a unit channel width. A problem with a 3D configuration has a channel width that varies along the length of the slope, as defined by the user. For details on how to define the channel width, please refer to Section C.8.

- **END CONDITIONS:** Allows the user to fix the front or the rear of the slide mass in their initial position. A fixed end will not flow during analysis and will be drawn in blue.

The *Continue* option in the menu will accept all the input data and either return to the main menu or continue to the next input screen in the New File Sequence. The *Cancel* option will ignore any changes made in this screen and return to the main menu. Note that choosing Cancel during the New File Sequence will cancel the new file completely.

C.5 Material Properties Screen

The Material Properties screen, shown in Figure 5, is accessed through the *Edit-Material Properties* option in the main menu. It is also the second input screen in the New File Sequence. This screen is used to input or edit the problem's material rheologies and properties. It also allows the user to add and delete materials. The user has a choice of eight rheologies, including:

- Frictional
- Plastic
- Newtonian
- Turbulent
- Bingham
- Coulomb Frictional
- Power Law
- Voellmy

These rheologies are described in Section A.2, and in Hungr (1995) and Hungr and Evans (1996). Each rheology requires input of specific material properties, as listed in the leftmost column of the table. Properties that are not associated to the type of rheology chosen are disabled.

Figure 5: Material Properties screen.

The following is a list of all the material properties shown in this screen and a brief description of each:

- MATERIAL: Optional. Any alphanumeric string of any length representing the name of the material.
- UNIT WEIGHT: Unit weight of the material in kN/m^3. Must be greater than 0.
- SHEAR STRENGTH: Constant shear strength of the material, such as the steady state undrained strength of liquefied material.
- FRICTION ANGLE: Friction angle of the material, in degrees.
- PORE-PRESSURE COEFFICIENT: Ratio of the pore pressure to the total normal stress at the base of the sliding mass.
- VISCOSITY: Dynamic viscosity of the fluid (kPa *s).
- FRICTION COEFFICIENT: Coefficient used in the Voellmy model (dimensionless).
- TURBULENCE COEFFICIENT: In the turbulent rheology: number that represents the squared roughness coefficient in the Manning equation. In the Voellmy rheology: coefficient that defines the turbulent term of the basal flow resistance equation (m/s^2).
- POWER LAW EXPONENT: Exponent that defines the Power Law rheology, as shown in Section A.2.
- EROSION DEPTH: Depth to which the material is eroded or deposited after the whole slide mass passes over it (in metres). A positive value indicates material erosion, while a negative value indicates material deposition.
- INTERNAL FRICTION ANGLE: Angle that defines the amount of internal friction in a material. This is used to derive the tangential stress coefficients k_a and k_p using a formula developed by Savage and Hutter (1987). DAN-W assumes that all materials are frictional when they deform internally. In other words, for each boundary block, its resistance to shear deformation is proportional to the normal stress experienced by it (0 for fluid; degrees).

  NOTE: A default value of the internal friction angle is set to 35°, which is appropriate for dry fragmented rock. The user should experiment with other values, although generally, the model is not strongly sensitive to it.
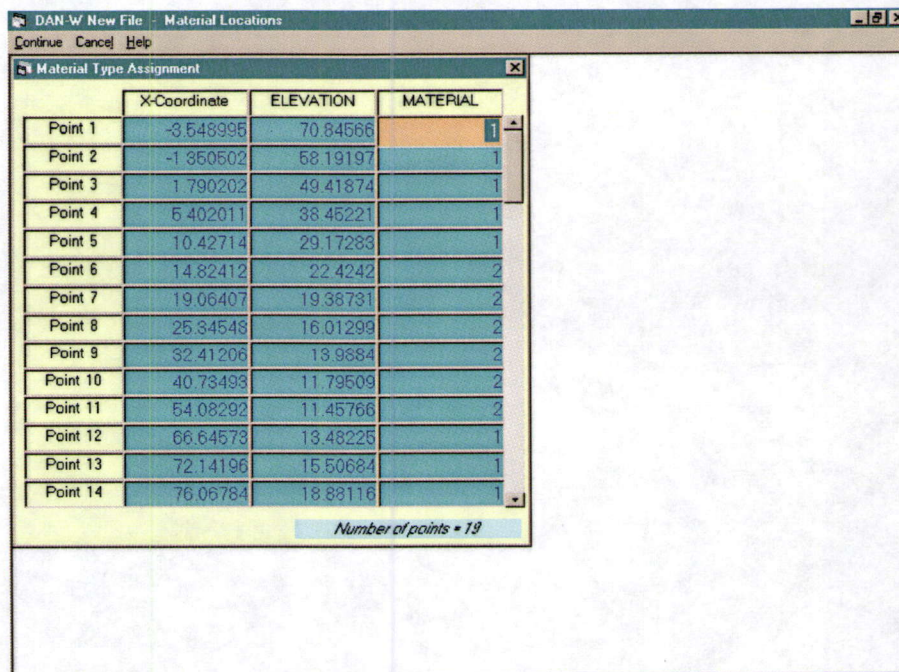
Each material is assigned a colour, shown in the top row of the table. These colours are used to draw the materials in the isometric view of the problem. To add a material, place the cursor in the next available column in the table. To insert a material in front of another material, place the cursor on the column where the new material is to be inserted. Then select the *Insert Material* option from the menu. To delete a material, place the cursor on the column to be deleted and select the *Delete Material* option from the menu.

The *Continue* option in the menu will accept all the input data and either return to the main menu or continue to the next input screen in the New File Sequence. The *Cancel* option will ignore any changes made in this screen and return to the main menu. Note that choosing Cancel during the New File Sequence will cancel the new file completely.

C.6 Material Locations Screen

The Material Locations screen, shown in Figure 6, is accessed through the *Edit-Material Locations* option in the main menu, or as the final screen in the New File Sequence. This screen allows the user to determine the location of each material along the length of the slope profile. The coordinates of all the points input in the Edit Path screen are shown on the left of the table. The user can set what material is located at which path segment(s) by inputting the appropriate material's code number in the MATERIAL column. If no or the wrong material code is given, then DAN-W automatically assumes the first material.

The *Continue* option in the menu will accept all the input data and return to the main menu. The *Cancel* option will ignore any changes made in this screen and return to the main menu.

Figure 6: Material Locations screen.

C.7 Edit Path/Top Screen

The Edit Path/Top screen, shown in Figure 7, is accessed through the *Edit-Path* or the *Edit-Top* options in the main menu, or as the third screen in the New File Sequence. This screen allows the user to input and edit the problem's slope (path) and sliding mass (top) profiles. The coordinate system used in this screen is described in Section B.2.

The data prepared as described in Section C.1, can be input graphically by clicking the mouse in the appropriate positions on the screen. Alternatively, data can be input numerically in the provided table. Points can only be input from left to right.

Data can also be imported from an existing tab or comma delimited *.TXT or *.DAT file by selecting the *Data-Import Data* option in the menu. The format of the file must be as follows:

```
n
y1      z1
y2      z2
...
yn      zn
```

where n is the number of data points in the file, y is the horizontal distance and z is the elevation. Remember that the number of data points accepted by DAN-W is limited to 100. It is also important that the user sets the appropriate Problem Extents, as specified in Section C.4, to ensure that the imported data is within the screen's range.

Points can be inserted between two existing points by selecting the *Points-Insert Point* option from the menu and clicking either on the screen or in the table in the desired position. Points can be deleted by selecting the *Points-Delete Point* option from the menu and clicking the point to be deleted on the screen or in the table. All the points in the selected line can be deleted by selecting the *Points-Delete Line* option from the menu.

The user can toggle between inputting the path profile and inputting the top profile by selecting the appropriate option in the menu. The current profile being edited is drawn in red, while the other profile is drawn in blue. If the user selected a uniform thickness top surface in the Control Parameters screen, then only the first and last data points entered for the top surface will be read by DAN-W. These two points will determine the front and the rear of the slide mass, while the slide mass in between these points will follow the path profile at the uniform thickness specified. The thickness will be measured parallel to the type of boundary block geometry chosen in the Options screen (either normal or vertical). It is recommended that normal slices be used in conjunction with the uniform thickness option.

The *Spline* option in the menu displays a pink line that fits the spline-interpolation that DAN-W will use during analysis, given the current path data points. This option is simply for the user's reference, to make sure that the right amount of data points have been input. It is not required that this option be selected before exiting this screen.

NOTE:
The front and the rear of the slide mass (first and last points in the top profile) should coincide with points on the path profile. To simplify this process, this screen has a built-in "snap" function that automatically snaps points together when they are close together.
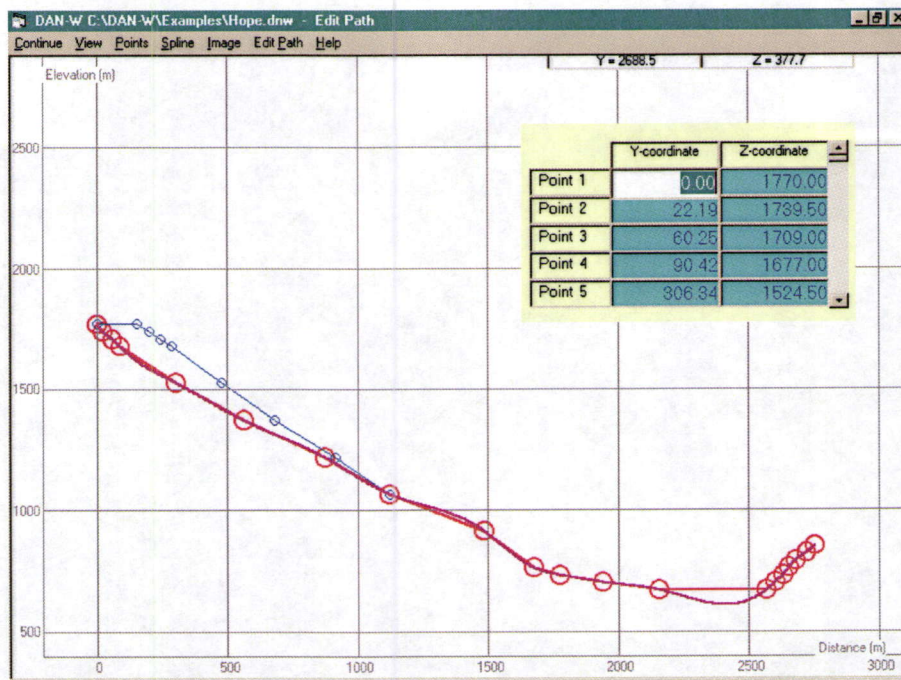
Figure 7: Edit Path/Top screen. In this figure, the path is selected in red, while the spline interpolation is drawn over it in pink. The top profile is drawn in the background in blue.

TIP:
To prevent obstruction of screen graphics, the table can be dragged to any position on the screen. It can also be made invisible by right-clicking the mouse.

A background image can be loaded and scaled to the screen coordinates to allow the user to trace a pre-drawn cross-section with high accuracy. Loading and scaling an image can be done by choosing the *Image-Load Image* option in the menu. Once an image is loaded, the user is asked to input the coordinates of two known points on the image. These two points must be located on the bottom left and the top right of the picture, as shown in Figure 8. The user is then asked to locate these two points on the image shown on the screen. Note that the more precisely these points are located on the image, the better the image scaling will correlate with the screen coordinate system. The image should then scale itself to the screen. The image can be unloaded or rescaled by selecting the appropriate option under the *Image* menu. The image will remain in the background of this screen as long as the current file remains loaded in DAN-W or until the *Unload* option in the menu is chosen.
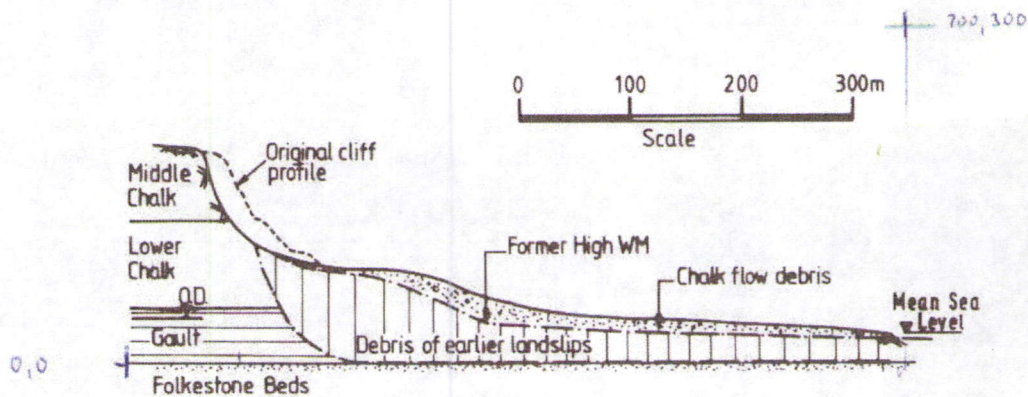
Figure 8: Example of a scanned image with known coordinates marked in blue at the bottom left and upper right corners of the image.

The screen can be zoomed in or out to help with the graphical input of points. To zoom in, select the *View-Zoom In* option in the menu and click the centre of the desired region. To zoom in on a specific rectangular region, select the *View-Zoom Box* option then click and drag across the region to be zoomed. Click the Zoom button in the bottom left of the screen to zoom in on the red extents drawn on the screen. To zoom out, select the *View-Zoom Out* option in the menu. The *View-Fit to Screen* option will return the screen to its original zoom position.

TIP:
Pessing and holding the SHIFT key and the left mouse button together, allows the user to drag the graphics across the screen. This is useful when tracing images at higher zoom levels.

The *Continue* option in the menu will accept all the path and top geometry data and will return to the main menu or to the next screen in the New File Sequence. Alternatively, the user can continue to the Edit Width Screen by choosing *Edit-Edit Width* from the menu. In either case, the user will be warned if the path or top geometry has been input incorrectly or is incomplete and will not be allowed to continue.

C.8 Edit Width Screen

The Edit Width screen, shown in Figure 9, is accessed through the *Edit-Width* option in the main menu or as the fourth screen in the New File Sequence. This screen is used to input or edit the channel width and is not accessible in the two-dimensional configuration. The data should be input as described in Section C.1. This screen functions exactly like the Edit Path/Top screen (see previous section), except that the vertical axis represents the channel width (in metres). The two vertical purple lines display the first and last points of the path profile. The width of the problem should be completely defined by the user between these two lines.

Figure 9: Edit Width screen.

C.9 Options Screen

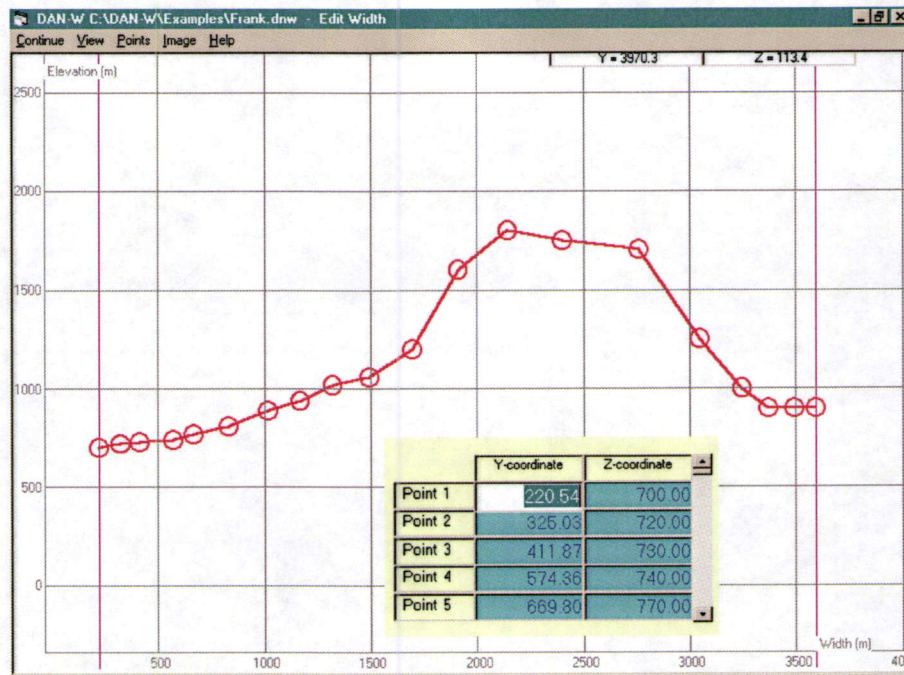The Options screen, shown in Figure 10, is accessed through the *Edit-Options* or the *View-View Options* selections in the main menu. This screen allows the user to edit various boundary, display, and analysis options.
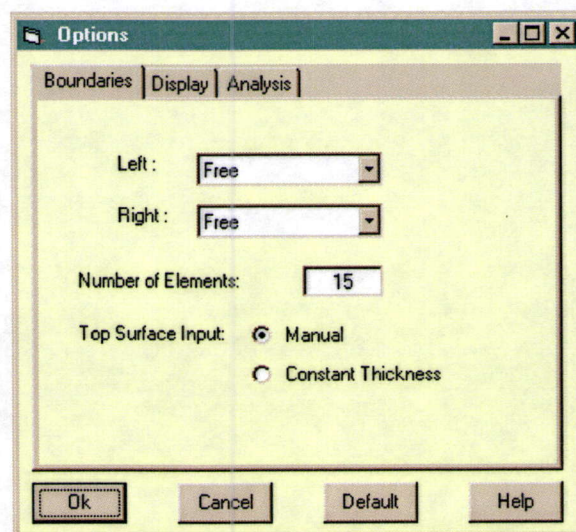
Figure 10: Options screen.

The following is a list of all the options with a brief description of each:

- LEFT AND RIGHT BOUNDARIES: These options allow the user to fix the rear (left) or front (right) of the slide mass during analysis. For further details, please refer to Section C.4. Default = *Free*.
- NUMBER OF ELEMENTS: This option allows the user to specify the number of mass elements that the slide mass is to be split into. Minimum = 1, maximum = 59. For further details, please refer to Section C.4. Default = 15.
- TOP SURFACE INPUT: This option allows the user to choose the type of data input used to define the top surface. The *Manual* option requires that the user input data points through the Edit-Top screen. The *Uniform Thickness* option allows the user to input a slide mass of uniform thickness above the path profile, as described in Section C.4. Note that the thickness must be defined in the Control Parameters screen otherwise it is defaulted to 1 metre. Default = *Manual*.
- PROJECTION ANGLE: This option allows the user to choose a projection angle in degrees for the three-dimensional isometric plot displayed in the main screen. This angle must be between -90 and 90 degrees. Default = 30.
- VERTICAL ENLARGEMENT: This option allows the user to input a vertical exaggeration ratio to help exaggerate the top surface for viewing purposes. A value of 1 means no exaggeration. Default = 1.
- PLOTTING MODE: This option allows the user to choose the type of plot shown in the main screen. If *Isometry* is chosen, an isometric view of the problem is shown in the main screen and is defined by the projection angle described above. If *Depth Profile (2D)* is chosen, the sliding mass's velocity and thickness profiles are plotted on the screen. These plotting modes are described in greater detail in Section D.1. Default = *Isometry*.
- VELOCITY EXTENTS: This option allows the user to specify the extents of the vertical axis of the velocity graph displayed in the main screen when the plotting mode is set to *Depth Profile (2D)*. This option essentially allows the user to zoom in or zoom out on the velocity profile. It is only available when the Depth Profile option is chosen. Default = *0 - 50 m/s*.
- OBSERVATION POINT: This option allows the user to place an observation point anywhere along the length of the path profile, as described in Section E.5. Default = *Off*.
- LOCATION ALONG X-AXIS: This option allows the user to specify the location of the observation point along the x-axis. It is only available when the Observation Point option is turned on. Default = 0.
- ANIMATION SPEED: UPDATE GRAPHICS EVERY ... TIME STEPS: This option allows the user to specify how often the screen graphics are updated during analysis. A larger number causes the graphics to be redrawn fewer times during the run and hence increases the speed of the analysis. The animation, however, becomes less smooth. Note that this option affects the screen graphics only. Background analysis calculations still occur for every time step regardless of the animation speed. Default = 10.

- TIP RATIO: This option allows the user to define the shape of the first and last mass elements on the slide mass. A ratio of 0.5 represents triangular end elements, while a ratio of 1 represents rectangular end elements. Default = 0.5.
- STIFFNESS COEFFICIENT: This option allows the user to modify the stiffness coefficient, which is described in Hungr (1995). Default = 0.05.
- STIFFNESS RATIO: This option allows the user to modify the stiffness ratio, which is described in Hungr (1995). Default = 5.
- CENTRIFUGAL FORCES: This option allows the user to turn the centrifugal forces caused by the curvature of the slope profile, on or off. Default = *On.*
- BOUNDARY BLOCK GEOMETRY: This option allows the user to choose between boundary blocks created by vertical slices or slices that are normal to the path. Vertical slices should be used if the rupture surface in the source area is highly curved. If normal slices were to be used in this situation, the geometry of the sliding mass would be distorted, as explained in Section C.2. Default = *Normal.*

D.1 Graphics

Once all the data input is complete, two types of plots can be drawn in the main screen, as listed under the *View* option in the main menu. The default plot shows an isometric view of the slope and sliding mass profiles. An example is shown in Figure 11. This view shows one half of the entire channel from the central cross-section out to the left margin of the flow path. The grid lines on the screen relate to the central cross-section. The projection angle and vertical exaggeration of the profile can be defined in the Options screen. The sliding mass is drawn in black, while the slope profile is drawn in the appropriate material colours, as defined in the Material Locations screen. The boundary blocks within the sliding mass are shown in black, or if they are under compression, in red.
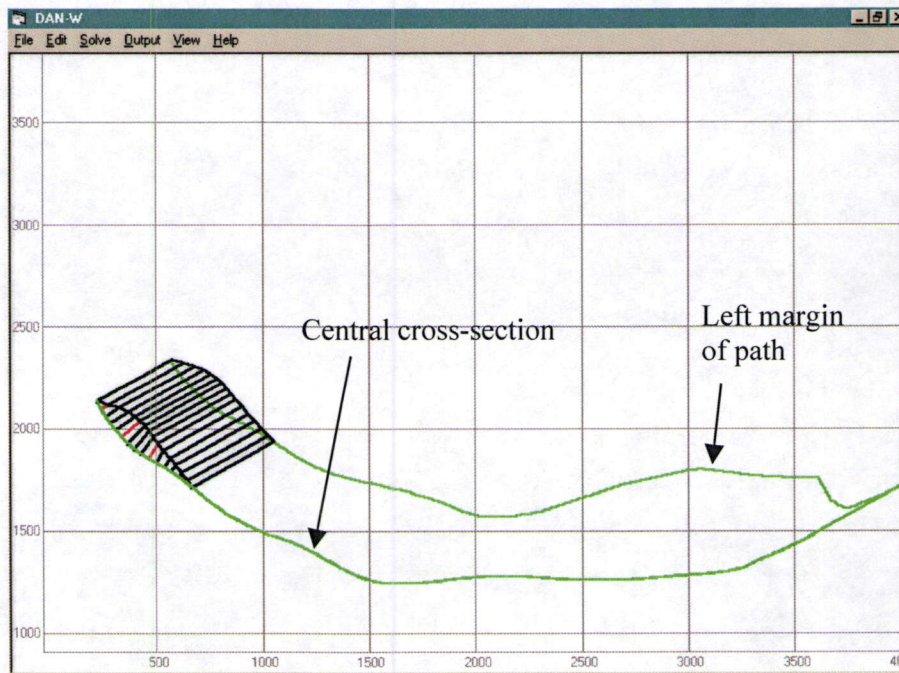
Figure 11: Three-dimensional isometric view.

The second type of plot shows a two-dimensional depth profile of the sliding mass. It consists of two graphs, one above the other, as shown in Figure 12. The upper graph shows the current velocity profile of the sliding mass (drawn in black), as well as the front velocity (drawn in blue) and rear velocity (drawn in pink) for each time step. The lower plot shows the thickness profile of the sliding mass, including the current location of all the boundary blocks (black normally and red if under compression). It also shows the current erosion or deposition profile in the appropriate material colours. The various materials throughout the profile are also drawn for reference along the length of the x-axis, in their corresponding colours. During an analysis, if the velocity profile runs

beyond the current extents of the graph, it automatically rescales itself. The extents of the velocity plot can also be set manually, as described in Section C.9.
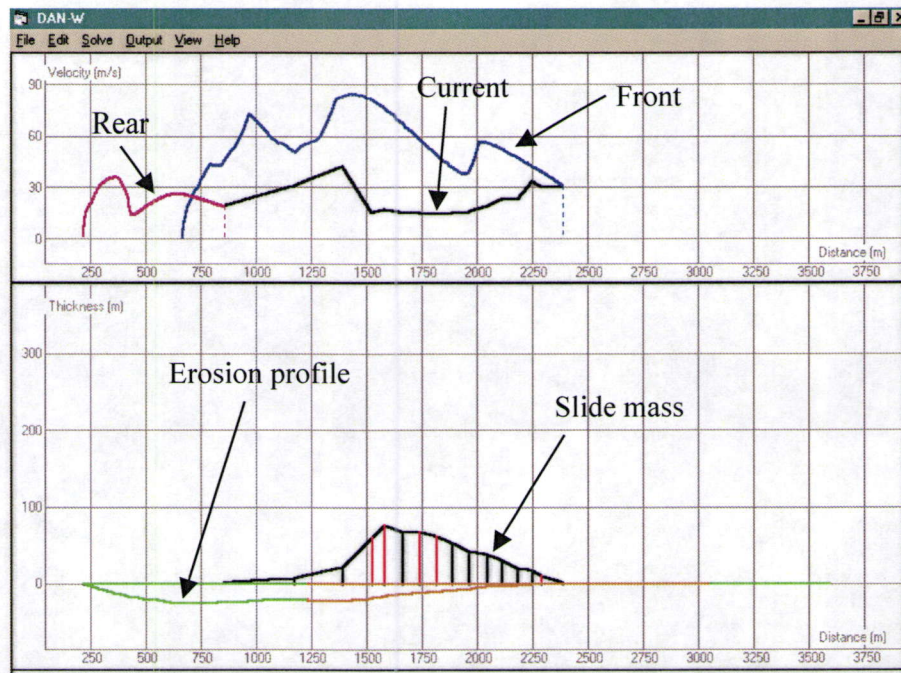
Figure 12: Two-dimensional depth profile view.

The user can switch between these two plotting modes during an analysis. The run must first be paused and then the plotting mode can be chosen either through the *View* menu or through the *Display* tab in the Options screen (which can also be accessed through the *View* menu by selecting *View-View Options*).

D.2 How to Run an Analysis

To run an analysis on a problem, select the *Solve-Calculate* option from the main menu or press Ctrl+R on the keyboard. This opens the Run Control Box which controls the analysis run. The analysis always begins with the sliding mass in its initial static condition, as drawn in the main screen. An appropriate time step should be chosen in the Run Control Box before the run is started. Once the run begins, the sliding mass is animated with each time step in the main screen. The speed of the animation can be set in the Options screen under the Display tab (see Section C.9).

D.3 Run Control Box

The Run Control Box, shown in Figure 13, is activated when the *Solve-Calculate* option is selected from the main menu. This box controls the analysis run of the problem. Before starting the run, it is important that an appropriate time step is chosen to prevent numerical divergence problems caused by an excessively large time step (see Section D.4). Remember that the larger the number of mass elements used in the slide mass, the smaller the time step should be. Typically, an appropriate time step ranges between 0.05 and 0.1 seconds.
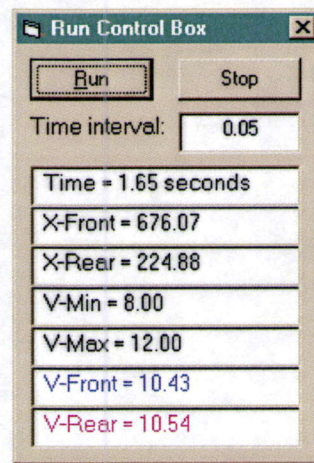
Figure 13: Run Control Box.

To begin the run, click the *Run* button or press Enter on the keyboard. The run can be paused by pressing the *Pause* button. Pressing *Run* again will continue the analysis from where it left off. Pressing *Stop* will finish and exit the run. Note that both the time step and the plotting mode (as described in Section D.1) can be changed in the Pause mode.

As the problem is running, data calculated at each time step is displayed. The following is a list of the displayed output along with a brief description of each:

- TIME: The total time elapsed from the beginning of the run (seconds).
- X-FRONT: The current position of the front of the sliding mass along the horizontal axis (metres).
- X-REAR: The current position of the rear of the sliding mass along the horizontal axis (metres).
- V-MIN: The velocity of the slowest boundary block in the slide mass at the current time (m/s).
- V-MAX: The velocity of the fastest boundary block in the slide mass at the current time (m/s).
- V-FRONT: The current velocity of the front of the sliding mass (m/s).
- V-REAR: The current velocity of the rear of the sliding mass (m/s).

More detailed output can be accessed during the Pause mode by selecting the *Output-Report* option in the main menu. Please refer to Section E.1 for a description of this screen.

When the run is stopped and exited, ASCII graph files are created if the user requested it prior to the beginning of the run. Before completely exiting the run mode, the user is given the chance to view the final Report for the problem as well as Observation Point data if it exists.

D.4 Model Instability

In some instances, the model may become unstable due to divergence of the numerical solver used during analysis of the equations of motion. This typically occurs when the problem encounters conditions that cause a drastic change in the strain of a mass element. DAN-W attempts to correct the situation by automatically reducing the time step, but this does not always prevent increasing instability. Examples of such conditions include large time steps, sudden and pronounced changes in geometry, and sudden changes of flow direction due to reverse slopes. It is recommended that a time step of about 0.05 to 0.1 seconds be chosen initially. If this time step results in instability, decrease it and run the analysis again. If it is not possible to stabilize an analysis by reducing the time steps, try using a smaller number of elements (10 recommended). This may reduce the accuracy of the solution, but will usually prevent instability.

When the slide mass reaches the right-most point of the slope profile, the run is paused and the user is asked if they want to continue. DAN-W extrapolates the geometry data beyond the end of the profile by continuing the slope at the same radius of curvature as that of the last profile point. This may eventually cause a reverse in the slope which in turn causes the sliding mass to change flow directions. As mentioned above, this usually results in instability. It is not recommended that the user continue the analysis beyond the last profile point. The length of the profile should be extended instead.

E DATA OUTPUT

E.1 Report

The Report screen, shown in Figure 14, can be accessed by selecting the *Output-Report* option in the main menu. This screen displays all the calculated values output during problem analysis. The screen can be opened when a run is paused, as described in Section D.3, or after the full completion of the run. The screen can also be printed by selecting the *Print* button. The data displayed in this screen is described in the next section. To export this data along with a list of materials and their properties into a text file, select the *Export* button. This opens a screen where an appropriate folder can be chosen to save the data in. Clicking *Export* in this screen creates a file called OUTPUT.TXT. In this file, all numerical values are tab delimited from their corresponding text descriptions. This allows the user to open the file in a spreadsheet program.

Final Report

File: C:\DAN-W\Examples\Example1.dnw

No of Blocks = 15

Time step = 0.10 seconds

End at time = 29.00 seconds

Configuration = 3-dimensional

Shape factor = 1.00

Maximum velocity = 99.00 at X = 1583.06

Maximum front velocity = 98.66 at X =1583.06

CENTRE OF GRAVITY: X-Source = 388.14

Z-Source = 1973.38

X-Depos. = 1702.86

Z-Depos. = 1305.58

CG Ratio = 0.51

Travel angle = 26.93

FAHRBOSCHUNG = 23.65

FRONT DISPLACEMENT: Horiz. Location = 2166.11

Curvilinear Displ. = 1621.36

Horiz. Displ. = 1496.51

REAR DISPLACEMENT: Horiz. Location= 767.25

Curvilinear Displ. = 751.81

Horiz. Displ. = 546.69

SLIDE VOLUME: Initial = 32186480.00

Final = 46061000.00

AREA IN PLAN: Initial = 328451.90

Final = 1642014.00

Runout uncompleted, V-MAX = 61.00
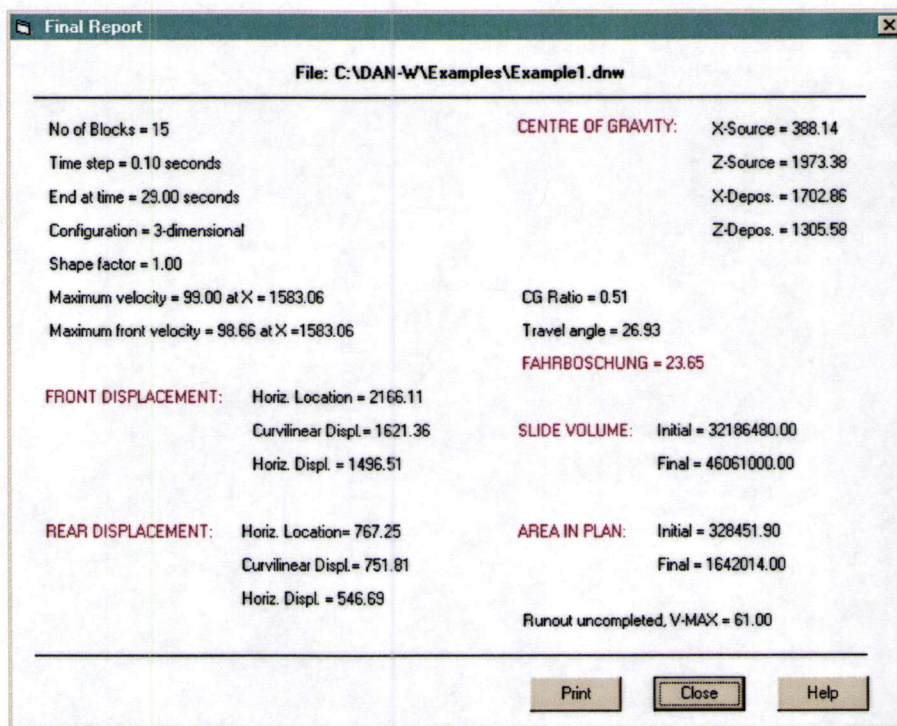
Print   Close   Help

Figure 14: Sample Report screen.

E.2 Output Data

The following is a list of the output values displayed in the Report screen along with a brief description of each:

- NUMBER OF ELEMENTS: The number of mass elements in the slide mass.
- TIME STEP: The time step used during analysis (seconds).
- END AT TIME: The total time elapsed since the beginning of the run (seconds).
- CONFIGURATION: Two-dimensional or three-dimensional configuration.
- SHAPE FACTOR: The cross-section shape factor used to define the shape of the channel cross-section.
- MAXIMUM VELOCITY: The maximum velocity reached by any boundary block during the whole run (m/s), occurring at the given horizontal distance (metres).
- MAXIMUM FRONT VELOCITY: The maximum velocity reached by the front of the slide mass during the whole run (m/s), occurring at the given horizontal distance (metres).
- FRONT DISPLACEMENT:
    - HORIZONTAL LOCATION: The final location of the front of the slide mass along the horizontal axis (metres).
    - CURVILINEAR DISPLACEMENT: The total displacement of the front of the slide mass along the path profile (metres).
    - HORIZONTAL DISPLACEMENT: The total horizontal displacement of the front of the slide mass (metres).
- REAR DISPLACEMENT:
- Same as for Front Displacement except for the rear of the slide mass.
- CENTRE OF GRAVITY:
    - X-SOURCE / Z-SOURCE: The coordinates of the centre of gravity of the initial, time zero position of the slide mass (metres).
    - X-DEPOSIT / Z-DEPOSIT: The coordinates of the centre of gravity of the slide mass at the end of the run (metres).
- CG RATIO: The ratio between the total vertical displacement of the centre of gravity and the total horizontal displacement of the centre of gravity of the slide mass (dimensionless).
- TRAVEL ANGLE: The horizontal angle between the original centre of gravity and the final centre of gravity (degrees).
- FAHRBOSCHUNG: The horizontal angle between the original rear of the sliding mass and the final front of the sliding mass (degrees).
- INITIAL / FINAL SLIDE VOLUME: The initial and final volumes of the slide mass (m^3).
- INITIAL / FINAL AREA IN PLAN: The initial and final area in plan of the slide mass (m^2).
- RUNOUT UNCOMPLETED, V-MAX: The problem was not allowed to settle. The maximum velocity for the total run is displayed (m/s).
- RUNOUT TIME: The time it took the slide mass to completely settle (seconds).

E.3 How to Create ASCII Graph Files

DAN-W can produce *.DAT data files in text (ASCII) format, which can be used to plot profiles using GRAPHER (TM, Golden Software Inc.) or any other graphing software, including most spreadsheets programs. The types of profiles created and their format are described in Section E.4.

To create ASCII graph files, select the *Output-Export ASCII Graph Files* option in the main menu and then select the *Create ASCII Graph Files* option on the form that appears. This enables the rest of the labels on the form, as shown in Figure 15. Choose a time interval at which you want data to be collected for the profile plot and for the velocity plot. It is recommended that the velocity plot have a smaller time interval than the profile plot. Note, if you choose a time interval of zero, no files will be created. Next, choose a folder in which to save the graph files in. Be careful not to choose a folder that already contains other graph files of the same name, because they will be overwritten. Choose OK to accept the information entered on the form. Now, to create the graph files, the problem must be analyzed, as described in Section D.2. Once the run is stopped, a message will be displayed notifying the user that the files have been created in the chosen folder. Note that the vertical enlargement ratio, described in Section C.9, can be used to make the data files more clear.
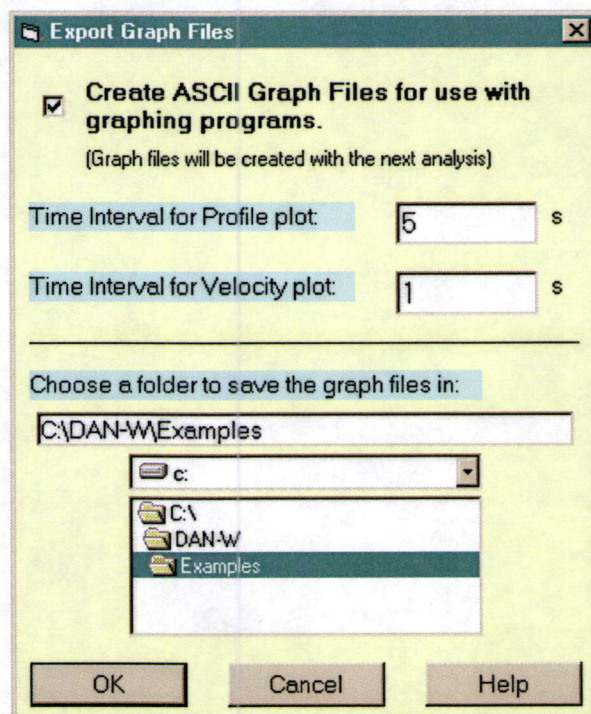

Figure 15: Export Graph Files screen.

E.4 ASCII Graph File Types

ASCII graph files containing profile data can be created by DAN-W, as described above. The following is a list of the eight types of *.DAT graph files created. Note that the column headings do not appear in the file, each column is tab delimited, and that the "a" characters are read as empty cells.

- PR.DAT: Records at first the path profiles (original and modified by erosion or deposition), then the slide mass profiles at the specified time intervals. An example of the format of the file is shown below. A sample plot created from this data file is shown in Figure 16.

X-Path	Y-Path	Width	X-Dep	Y-Dep	Y-Top$_1$	Y-Top$_2$
0.00	10.00	2.00	0.00	10.00		
0.10	9.95	2.00	0.10	9.95		
0.20	9.90	2.00	0.20	9.89		
0.30	9.85	2.00	0.29	9.84		
etc...						
0.03	"a"	"a"	"a"	"a"	10.05	
0.50	"a"	"a"	"a"	"a"	10.00	
1.00	"a"	"a"	"a"	"a"	10.00	
1.48	"a"	"a"	"a"	"a"	9.96	
1.83	"a"	"a"	"a"	"a"	9.67	
2.08	"a"	"a"	"a"	"a"	9.16	
0.04	"a"	"a"	"a"	"a"	"a"	10.05
0.50	"a"	"a"	"a"	"a"	"a"	10.00
0.99	"a"	"a"	"a"	"a"	"a"	9.91
1.60	"a"	"a"	"a"	"a"	"a"	9.66
2.44	"a"	"a"	"a"	"a"	"a"	9.21
etc...						

X-Path: X-coordinate of a point on the path.
Y-Path: Y-coordinate (elevation) of a point on the path.
Width: Path width.
X-Dep.: X-coordinate of a point on the path, modified by erosion or deposition.
Y-Dep.: Y-coordinate (elevation) of a point on the path, modified by erosion or deposition.
Y-Top$_1$: Y-coordinate of the top of each boundary block during the first profile time interval.
Y-Top$_2$: Y-coordinate of the top of each boundary block during the second profile time interval.
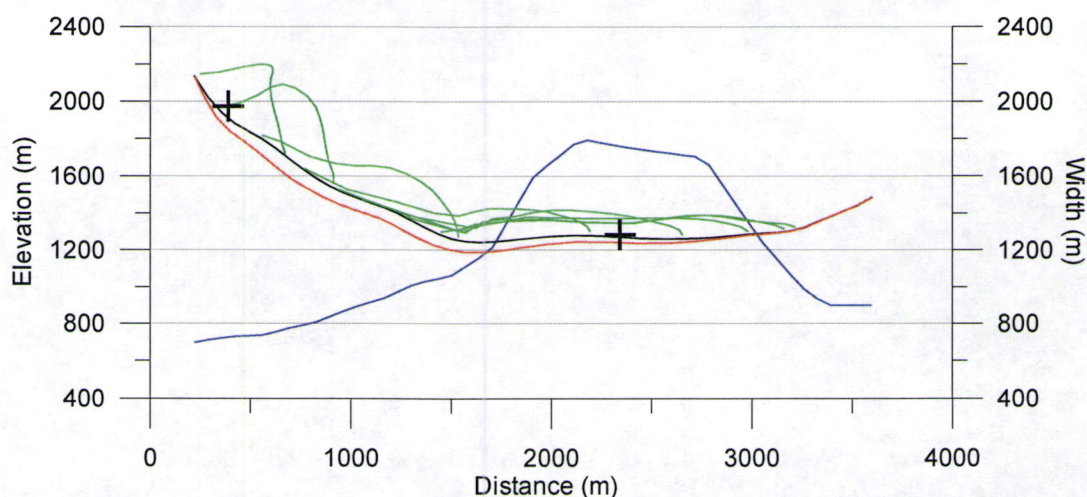
Figure 16: Sample profile plot created from PR.DAT, using GRAPHER (TM, Golden Software Inc.). Black is the path profile; green is the top profile; orange is the erosion profile; blue is the channel width; crosses indicate initial and final centres of gravity of the slide mass, taken from CG.DAT.

- TR.DAT: Records velocities and positions of the front and rear of the mass, vs. time. A sample plot created from this data file is shown in Figure 17.

Time	X-Rear	V-Rear	X-Front	V-Front	V-Max	V-Min	X-CG
0.00	0.00	0.00	2.00	0.00	0.00	0.00	1.16
0.10	0.00	0.08	2.04	0.82	0.82	0.00	1.18
0.20	0.01	0.07	2.14	1.58	1.58	0.00	1.22
0.30	0.01	0.00	2.32	2.31	2.31	0.00	1.28
0.40	0.01	0.00	2.55	2.96	2.96	0.00	1.37
0.50	0.01	0.00	2.85	3.53	3.53	0.00	1.49
0.60	0.01	0.00	3.18	4.03	4.03	0.00	1.63
etc…							

Time: Time in seconds, depending on the specified interval.
X-Rear: X coordinate of the rear of the sliding mass.
V-Rear: Velocity of the rear of the sliding mass.
X-Front: X coordinate of the front of the sliding mass.
V-Front: Velocity of the front of the sliding mass.
V-Max.: Maximum velocity at the current time.
V-Min.: Minimum velocity at the current time.
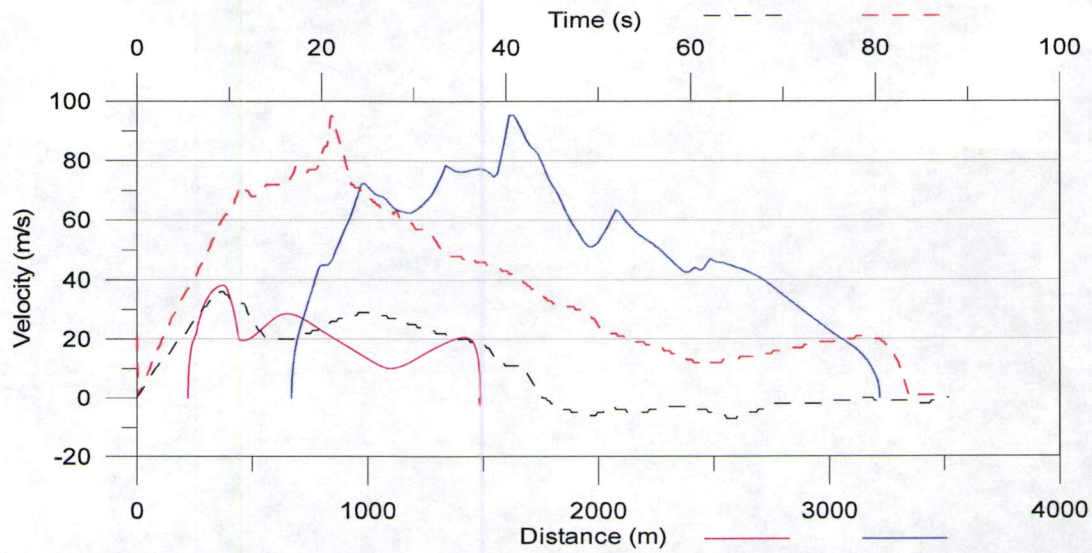*X-CG*: X-coordinate of the centre of gravity of the flowing mass.

Figure 17: Sample velocity plot created from TR.DAT, using GRAPHER (TM, Golden Software Inc.). Blue is the front velocity vs. distance; pink is the rear velocity vs. distance; red is the maximum velocity vs. time; black is the minimum velocity vs. time.

- CG.DAT: Records the X and Z coordinates of the centre of gravity before the slide and at the end of runout. This data can be plotted in the profile plot, as shown in Figure 16.

X-CG	Z-CG
11.53	52.39
64.72	17.82

X-CG: X-coordinate of the centre of gravity of the flowing mass.
Z-CG: Z-coordinate of the centre of gravity of the flowing mass.

- VE.DAT: Records the velocity distribution at each profile time interval, as a function of the X-coordinate. A sample plot created from this data file is shown in Figure 18.

X-Slide	V-Slide$_1$	V-Slide$_2$	V-Slide$_3$
-1.461	0.00		
0.285	0.00		
2.07	0.00		
3.857	0.00		
5.647	0.00		
etc...			
-1.455	"a"	0.346	
0.291	"a"	0.334	
2.075	"a"	0.332	
3.863	"a"	0.33	
5.652	"a"	0.328	
etc...			
0.823	"a"	"a"	6.509
2.507	"a"	"a"	6.272
4.317	"a"	"a"	6.23
6.144	"a"	"a"	6.19
7.983	"a"	"a"	6.154
etc...			

X-Slide: X-coordinate of each boundary block in the slide mass during each profile time interval.
V-Slide$_1$: Velocity of each boundary block in the slide mass during the first time interval.
V-Slide$_2$: Velocity of each boundary block in the slide mass during the second time interval.
V-Slide$_3$: Velocity of each boundary block in the slide mass during the third time interval.
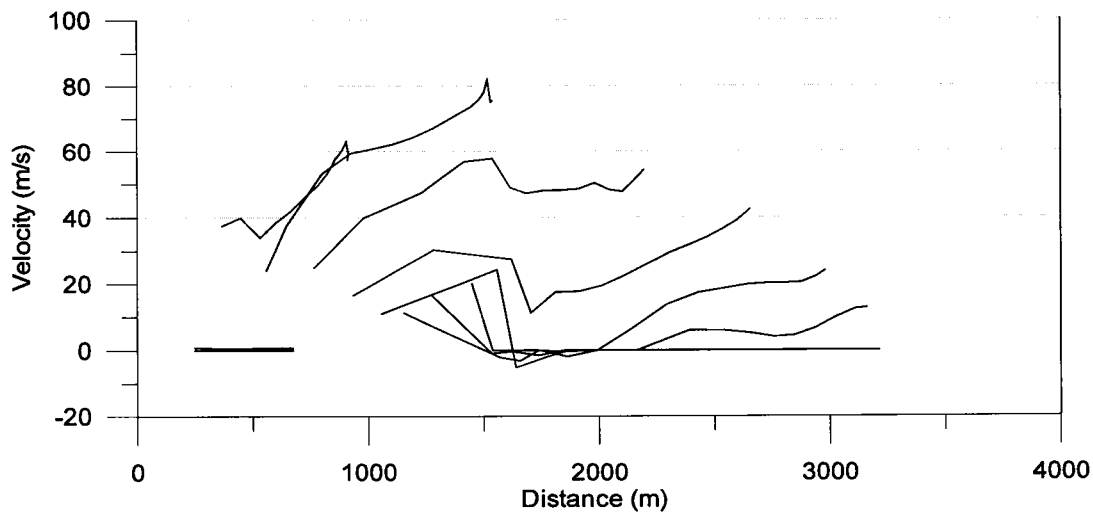
Figure 18: Sample velocity profile plot created from VE.DAT, using GRAPHER (TM, Golden Software Inc.). Each line represents the velocity profile across the slide mass at the same time intervals used in PR.DAT.

- DE.DAT: Records the erosion or deposition depth distribution at each profile time interval, as a function of the X-coordinate. The format is the same as for VE.DAT.
- HT.DAT: Does the same for flow depths.
- K0.DAT: Does the same for the lateral earth pressure coefficient.
- DIS.DAT: Does the same for discharge.

E.5 Observation Point

An Observation Point can be placed anywhere along the path profile to allow the user to monitor the velocity and the thickness of the sliding mass at that point through time. To set an Observation Point, choose the appropriate *On* option in the Options screen. The location of the point can then be specified in the same screen. Once an Observation Point is created, its location is shown in the isometric view by a short blue line on the front cross-section, and in the depth profile by a vertical blue line extending down the screen.
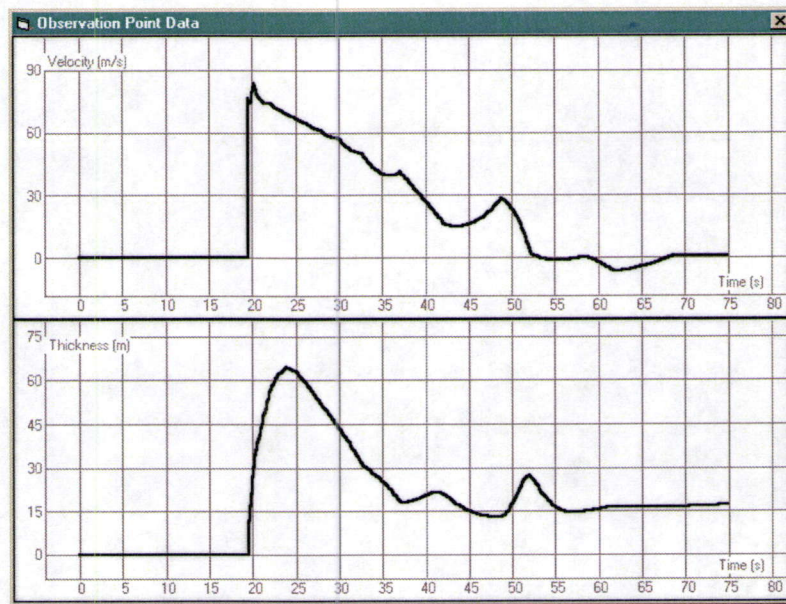
Figure 19: Example of a plot created by DAN-W, showing the velocity and thickness of the slide mass at a specified observation point location.
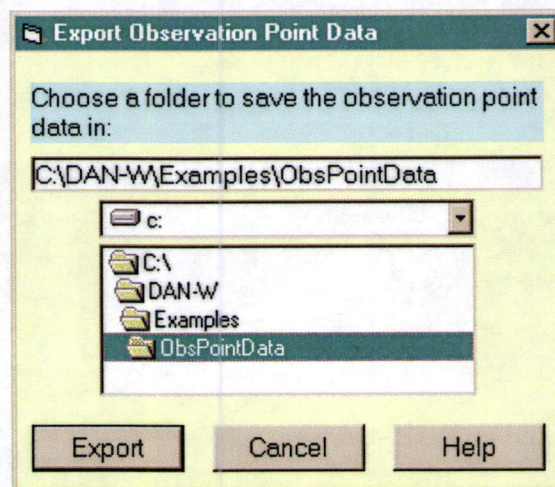
Figure 20: Export Observation Point screen.

After a run has been completed, the user can view a plot of the data collected, by selecting the *Output-Observation Point-View Data* option in the main menu. An example of the plot can be seen in Figure 19. The data can also be exported into a ASCII data file, similar to those described in Section E.4. To export the data, choose the *Output-Observation Point-Export Data* option in the main menu. A form, shown in Figure 20, appears in which the user can choose the appropriate folder to save the file in. When the *Export* button is chosen, the data is saved in the chosen folder under the name OBS.DAT. The first column in this file is time (in seconds) depending on the time interval chosen for

the analysis. The second column is the thickness of the slide mass (in metres) at this location for each time interval. The third column is the velocity of the slide mass (in metres per second) at this location for each time interval.

Note that with each subsequent analysis, all the previous Observation Point data stored by DAN-W is replaced by the latest data.

F   LIST OF WARNINGS AND ERROR MESSAGES

ARE YOU SURE YOU WANT TO DELETE ALL THE POINTS IN THE SELECTED LINE?

All the points in the profile currently being edited will be permanently deleted.

ARE YOU SURE YOU WANT TO REVERT TO DEFAULT VALUES?

All values in the Options screen will be changed back to their default values.

CANNOT OPEN FILE ....

There is a formatting error in the file being opened.

CHOICE OF POINTS IS INCORRECT!

The first scale point must be located to the left and below the second scale point.

CROSS-SECTION SHAPE FACTOR MUST BE GREATER THAN 0.

The cross-section shape factor must be positive and non-zero.

FILE NOT FOUND. PLEASE TRY AGAIN.

The chosen image file is not found in the chosen directory. Check spelling or check another directory.

FRICTION ANGLE OF MATERIAL # ... MUST BE BETWEEN 0 AND 45 DEGREES.

Friction angle must be within the specified bounds.

FRICTION COEFFICIENT OF MATERIAL # ... MUST BE BETWEEN 0 AND 1.

Friction coefficient must be within the specified bounds.

GEOMETRY ERROR. PLEASE CHECK GEOMETRY POINTS.

The solver encountered an error when setting up the problem geometry. Check that all the data in the edit geometry screens corresponds to the rules described in Section C.1, Section C.7, and Section C.8. Common reasons for the appearance of this error are that the spline is very wavy or that all the top data points are below the interpolated path data points.

GRAPH FILES: PATH ... ACCESS ERROR.

The folder chosen to save the ASCII graph files in is read only. Please choose a different folder.

IF YOU CHANGE TO A 2-DIMENSIONAL CONFIGURATION, YOU WILL LOSE ALL OF YOUR WIDTH DATA. ARE YOU SURE YOU WANT TO CONTINUE?

Changing from a three-dimensional configuration to a two-dimensional configuration will permanently replace all existing width data to unity.

LHS Y-COORDINATE MUST BE SMALLER THAN RHS Y-COORDINATE.

Problem extents must be defined by the lower left and the upper right coordinates of the problem.

LHS Z-COORDINATE MUST BE SMALLER THAN RHS Z-COORDINATE.
> Problem extents must be defined by the lower left and the upper right coordinates of the problem.

MAXIMUM ... ELEMENTS.
> The number of mass elements must not exceed the specified amount.

MAXIMUM ... MATERIALS ALLOWED.
> The number of materials must not exceed the specified amount.

MUST HAVE AT LEAST ONE MASS ELEMENT.
> The minimum number of mass elements is 1.

MUST HAVE AT LEAST ONE MATERIAL.
> The minimum number of materials is 1.

NO OBSERVATION POINT DATA LOADED. YOU MUST RUN AN ANALYSIS TO LOAD DATA.
> Observation Point data is stored during an analysis and can be exported only after the analysis is completed.

ONLY ... POINTS ALLOWED.
> Can't add any more geometry points. The maximum has been reached.

PATH NOT FOUND. PLEASE TRY AGAIN.
> The chosen path is incorrect. Try another directory.

PLOTTING ERROR. PLEASE CHECK GEOMETRY POINTS.
> The solver encountered an error when plotting the three-dimensional problem geometry. Check that all the data in the edit geometry screens corresponds to the rules described in Section C.1, Section C.7, and Section C.8. Common reasons for the appearance of this error are that the spline is very wavy or that all the top data points are below the interpolated path data points.

POINT ... MUST BE TO THE RIGHT OF POINT ....
> Points in the edit geometry screens must go from left to right and must not overlap.

PROJECTION ANGLE MUST BE BETWEEN -90 AND 90 DEGREES.
> The projection angle for the isometric view in the main screen must be within the specified bounds.

RUNOUT COMPLETE.
> The slide mass has fully settled. The run is complete.

SLPINE ERROR. PLEASE CHECK GEOMETRY POINTS.

   The solver encountered an error when spline-interpolating between the path data points. Check that all the data in the edit geometry screens corresponds to the rules described in Section C.1, Section C.7, and Section C.8. Common reasons for the appearance of this error are that the spline is very wavy or that all the top data points are below the interpolated path data points.

STIFFNESS COEFFICIENT MUST BE GREATER THAN 0.

   The stiffness coefficient must be positive and non-zero.

THE PROBLEM HAS REACHED THE PROFILE EXTENTS. DO YOU WISH TO CONTINUE?

   The front of the sliding mass has reached the right-most extent of the slope profile. Continuing beyond this point may result in instability.

THICKNESS MUST BE GREATER THAN 0.

   The uniform thickness of the top above the path must be positive and non-zero.

TIP RATIO MUST NOT BE ZERO.

   The tip ratio must be positive and non-zero.

UNIDENTIFIED ERROR # ... OCCURRED: ....

   An unidentified error, as described, has occurred when loading the image.

WARNING: POINTS ... AND ... HAVE EQUAL Y-COORDINATES AND WILL MAKE THE SPLINE FUNCTION UNSTABLE. PLEASE MODIFY THE POINTS.

   Path points with equal y-coordinates will cause the spline function to become dramatically unstable. Make sure these coordinates are not the same and then test the spline to make sure it gives the desired path profile.

WARNING, WIDTH ARRAY NOT DEFINED.

   Must have at least two data points to completely define the channel width.

WEIGHT OF MATERIAL # ... MUST BE GREATER THAN 0.

   All materials must have a positive and non-zero unit weight.

WIDTH MUST BE GREATER THAN 0.

   Must have at least two data points to completely define the channel width.

YOU MUST ENTER AT LEAST ... POINTS IN ORDER TO PROPERLY DEFINE THE ... GEOMETRY.

   Must have at least the minimum number of data points specified to completely define the path, top, and width profiles.

ZOOM BOX EXTENTS ARE TOO SMALL

   The chosen zoom box is too small. Please try again.

G REFERENCES

***Note: References 1 and 2 are included with the program in pdf format.

1. Hungr, O., 1995. A model for the runout analysis of rapid flow slides, debris flows and avalanches. Canadian Geotechnical Journal, 32(4):610-623.

2. Hungr, O. and Evans, S.G., 1996. Rock avalanche runout prediction using a dynamic model. Procs., 7th. International Symposium on Landslides, Trondheim, Norway, 1:233-238.

3. Savage, S.B. and Hutter, K., 1989. The motion of a finite mass of granular material down a rough incline. Journal of Fluid Mechanics, 199: 177-215.

4. Revellino, P., Hungr, O., Guadagno, F.M. And Evans, S.G., 2002 Velocity and runout prediction of destructive debris flows and debris avalanches in pyroclastic deposits, Campania Region, Italy. Accepted by Environmental Geology, March, 2003.

5. Hungr, O., Dawson, R., Kent, A., Campbell, D. and Morgenstern, N.R., 2002. Rapid flow slides of coal mine waste in British Columbia, Canada. In "Catastrophic Landslides" Geological Society of America Reviews in Engineering Geology 15, pp. 191-208.

6. Evans, S.G., Hungr, O., and Clague, 2001. The 1984 rock avalanche from the western flank of Mt. Cayley, Garibaldi Volcanic Belt, British Columbia: description and dynamic analysis. Engineering Geology, 61:29-51.

7. Ayotte, D. and Hungr, O., 2000. Calibration of a runout prediction model for debris flows and avalanches. Procs., 2nd. International Conference on Debris Flows, Taipei, Wieczorek, G.F. and Naeser, N.D., Eds., 505-514, Balkema, Rotterdam.

8. Ayotte, D., Evans, N. and Hungr, O., 1999. Runout analysis of debris flows and avalanches in Hong Kong. Proceedings, Slope Stability and Landslides, Vancouver Geotechnical Society Symposium May, 1999, 39-46.

9. Tse, C.M., Chu, T., Wu, R., Hungr, O. and Li, F.H., 1999. A risk-based approach to landslide hazard mitigation design. Procs., Hong Kong Institution of Engineers, Geotechnical Division Annual Seminar, May 1999, 35-42.

Appendix G – South Dump Stability

There are two considerations to be evaluated in waste dump stability:

o Evaluation of shallow, infinite slope stability conditions along the dump surface.

o Evaluation of deep seated, circular and semi-circular slip surfaces that generally intercept the foundation.

The WR dumps have been constructed by end dumping at the angle of repose, as a result the factor of safety of the infinite slope condition will be low. The infinite slope is presently positively affected by settlement and cementation and negatively affected by water flowing down the dump face due to direct precipitation, run off or seepage. The factor of safety of deep seated slip surfaces are governed by the shear strength of the waste materials, the foundation shear strength and to a minor extent by seepage along the waste / foundation interface. These considerations are discussed in greater detail in the following sections.

Infinite Slope Conditions

Due to the end dump method of construction, the waste dumps are initially placed at an angle of repose in a loose surface condition. Therefore, the dumps are initially at a factor of safety of 1.0, defined as:

$$FS = \tan \phi / \tan i$$

Where:

ϕ = angle of internal friction, degrees

i = slope angle, degrees

Conversely, by measuring the slope angle of the dump, the angle of internal friction of the dump materials in a loose condition can be estimated[1]. Possible seepage parallel to the slope reduces the factor of safety, thereby causing potential mass movement. As additional materials are placed on the dumps, with time the dumps settle and transition from a loose to dense state, thereby increasing the angle of internal friction.

Due to particle segregation during dumping, fine grain size dump material tends to remain near the dump crest while the larger particle sizes roll and *saltate down* the dump slope. This process causes internal dump stratification, as described in Appendix B. The fine grain size material remaining at the dump crest may posses "apparent cohesion" due to capillary forces under partly saturated conditions. This apparent cohesion tends to over-steepen the crest of the dumps initially. As time passes, periodic saturation causes these materials to slump or fail in an infinite slope condition, flattening the dump crest over time (see Appendix F for further description). Secondly, as additional materials are placed on the dump, settlement occurs due to the materials assuming a more dense condition. Weathering and geochemical reactions may add a degree of surface cementation, therefore the angle of internal friction increases during both this settlement and weathering process. A photograph of infinite slope slippage is depicted on Figure B-26, included as Attachment B to Appendix F.

If local areas of the dump face become saturated, a "scar" typically occurs. A scar is considered to be an infinite slope failure, which may result in a debris flow. Although an infinite slope failure could conceivably be quite large, empirical evidence suggests that such scars are of limited extent. This phenomenon is discussed in detail in Appendix F and Figure A-8 in the attachment to Appendix F shows a typical dump scar.

General Slope Stability

General slope stability analysis consists of evaluating potential "deep seated" slip surfaces. Such surfaces may intersect the foundation materials, particularly if the foundation materials are weaker (have a lower shear strength) than the dump materials. When performing such analyses, the shallow infinite slope condition described above is usually ignored. Such analyses are usually performed using limit equilibrium method (LEM) slope stability analysis, although more sophisticated methods are available (finite element or difference analysis using a stress reduction method to calculate the factor of safety).

Screening level stability analyses were completed to assess the probable range in factors of safety for deep seated slip surfaces. By screening level, it was meant that conservative, bounding assumptions were made on the shear strength of the waste rock, foundation soil, water table and stratigraphy to develop a range in factors of safety of the dumps in their current condition. A conservative assumption was also

---

[1]   The infinite slope analysis simplistically ignores apparent cohesion. Derivations for evaluating the infinite slope condition with cohesion are available and can be used to parametrically assess cohesion and friction angle ranges.

Deleted: Oct-20-09

made that the soil underlying the dumps has a uniform thickness. In all likelihood, bedrock outcrops are present below specific dump cross sections, thereby increasing stability.

Limit equilibrium method (LEM) stability analyses were completed using the program SLIDE5.0 by Rocscience®. LEM analyses define a factor of safety as the summation of resisting forces divided by the summation of driving forces. A factor of safety of one (1.0) indicates that the resisting forces are equal to the driving forces and the slope is essentially at incipient failure. For mining engineering purposes, acceptable static factors of safety are generally considered to be greater than or equal to 1.2. The more rigorous LEM methods include the Spencer and Morgenstern-Price methods, which base the factor of safety on both summation of forces and moments (about a point defining the slip surface). The Spencer method of analysis was used in the calculations presented herein.

The stability analyses assumed the following:

- The foundation shear strength is based on testing a limited number of samples obtained from beyond the toe of the dumps, described in Appendix A and summarized in Figure G-1. The foundation was characterized as either having a silty clay foundation or a silty gravel foundation. For screening level analysis, it was conservatively assumed that the foundation soils were at least 10 ft thick below the entire footprint of the dump.

- Shear strength of waste rock materials is reasonably modeled by the non-linear shear strength envelope developed in Appendix B. The non-linear shear strength envelope takes into consideration that at high stresses, breakage of the asperities contributing to friction occurs and there is a reduction in friction angle with increasing confining (overburden stress). The waste rock strength was characterized by an upper bound, lower bound and average range. The average value was set to coincide with the Leps (1970) values for mine waste. Strength properties for the primarily quartzite materials represent the upper bound envelope, while the lower bound estimate is represented by the intrusive units. The non-linear envelope is shown on Figure G-2.

- For most dumps, it is assumed that the dumps are relatively well drained and do not support a high phreatic surface. This input assumption is based on monitoring of seepage flows from dump leaching, which shows that the dumps drained quickly following leaching operations. Secondly, the particle segregation within the dumps indicates that larger, more permeable materials are present at the dump toe. Lastly, available permeability data of the dumps (Appendix B, Table B-3) indicate drained conditions with values in the range of 10^{-1} to 10^{-3} cm/sec at depth. The stability analyses assume the base of the dump is saturated, and that the phreatic surface extends 5 feet uniformly above the dump / foundation interface. This should be a reasonably conservative assumption given the coarse nature of materials at the dump

Deleted: Oct-20-09

toe. The exception to this assumption is the Yosemite / Castro dumps, where analyses were completed using an elevated phreatic surface.
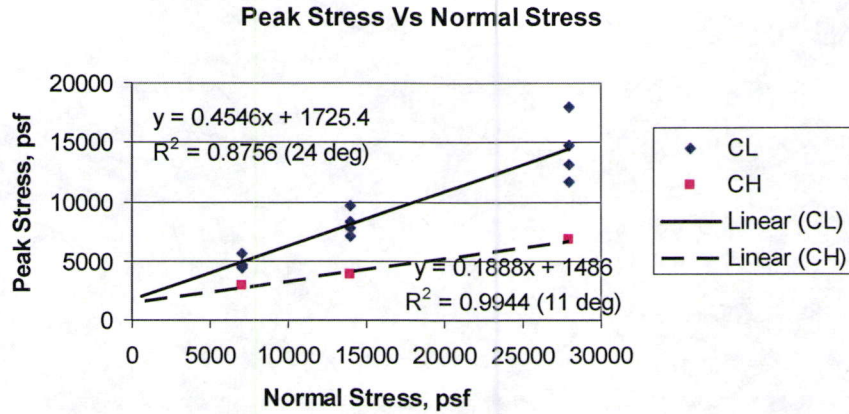
Peak Stress Vs Normal Stress

$y = 0.4546x + 1725.4$
$R^2 = 0.8756$ (24 deg)

$y = 0.1888x + 1486$
$R^2 = 0.9944$ (11 deg)

Figure G-1 - Foundation Clay shear strength test data (see discussion in Appendix A)
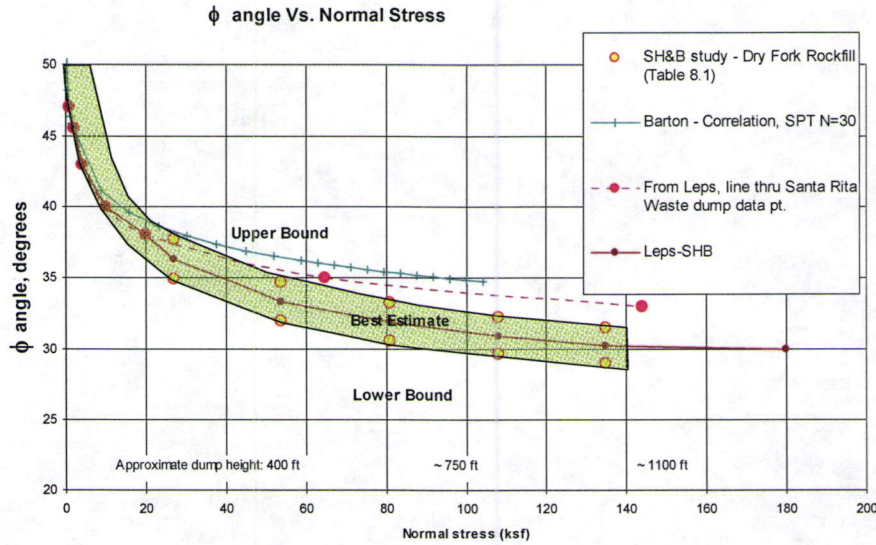
φ angle Vs. Normal Stress

Figure G-2 - Waste rock shear strength envelopes (see discussion in Appendix B).

The following matrix of assumptions was used to complete a probabilistic, screening level stability assessment of the waste dumps. In comparison to traditional deterministic stability assessment, this approach should be considered a non-traditional method where the best estimate values only are presented. The benefit of this approach is that uncertainty in input parameters is captured.

Deleted: Oct-20-09

Table G-1 - Matrix of Waste Rock and Foundation shear strength parameters

Dump	Foundation Conditions / Strength Parameters	Upper bound Waste Rock Strength	Average Waste Rock Strength	Lower Bound Waste rock strength
South Dumps				
Yosemite and Saint's Rest	Lean Clay ϕ = 20 deg Coh = 1400 psf	X	X	X
	Clayey, Sandy Gravel w/ ϕ = 35 deg Coh = 500 psf	X	X	X

The above WR and foundation material properties required six stability calculations per cross section. Assuming that the upper and lower bound estimates for the WR and foundation soils represented values one standard deviation above and below the mean (actual) value for the WR dumps, one can statistically calculate the probability of failure using a "point estimate method" (Harr)[2]. The point estimate method assumes that the Lower WR/Lower foundation, Lower WR/Upper foundation, Upper WR/Upper foundation, Upper WR/upper foundation, average WR/Lower foundation and average WR/upper foundation calculations statistically identify the range (assuming +/- one standard deviation) of possible factors of safety for the dump. The probability that the factor of safety lies within a given range can then be calculated. These calculations are then used to screen which areas warrant further field investigation to confirm the actual factors of safety. The stability analyses themselves also provide the critical slip surface location to identify where understanding of the foundation conditions are most critical. In most cases this location is near the toe of the dumps. Likewise, where the statistical range in factor of safety meets or exceeds accepted criteria for WR dump stability, no further investigations or analyses are warranted. This last statement is supported by the observed stable conditions of the dumps over the last 30 to over 80 years.

Stability analyses for Yosemite and Saint's Rest dumps are presented in Table G-2, on the attached Figures and legend at the end of this Appendix. It is observed that the best estimate factors of safety (i.e. traditional factors of safety estimates) for both the Yosemite and Saint's Rest dump are acceptable, exceeding generally acceptable

---

[2]   The range in shear strengths were initially selected to reasonably represent one standard deviation range in typical geotechnical materials having similar gradation and particle constituent characteristics. Cohesion and cementation were ignored for the waste dump materials.

Report number12094   Page 5 of 6

Date Mar-9-10   ©2008 Technological Resources Pty Limited

Deleted: Oct-20-09

criteria for mining engineering applications. For the best estimate and upper bound assumptions the factors of safety are also acceptable for both geometries evaluated. Under the lower bound assumptions, however, the calculated factors of safety are marginal, reflecting uncertainty in our knowledge of foundation conditions. For example, at Yosemite it is observed that if a uniform clay material underlies the entire drainage, then the calculated factor of safety is near one. The observed stability of the Yosemite dump indicates that the assumption of a weak silty clay soil uniformly underlying the dump is overly conservative. To evaluate a more realistic case for Yosemite, two sensitivity cases were run: (1) the silty clay was assumed to be present only in along the reach of the foundation where volcanic bedrock is mapped and (2) the perched phreatic surface was omitted and an assumption that the water table extends 5 feet above the foundation was made. For these cases, the minimum factor of safety was found to be 1.2, which is considered to more realistically reflect the lower bound site conditions. Traditional factors of safety for Yosemite and Saints Rest dumps are 1.4 and 1.45.